POLITECNICO
MILANO 1863

POLITECNICO DI MILANO
DEPARTMENT OF ELECTRONICS, INFORMATION AND BIOENGINEERING
DOCTORAL PROGRAMME IN SYSTEMS AND CONTROL

DESIGN OF COLLABORATIVE ECO-DRIVE CONTROL ALGORITHMS FOR TRAIN NETWORKS

Doctoral Dissertation of:
Hafsa Farooqi

Supervisor:
Prof. Patrizio Colaneri

Tutor:
Prof. Paolo Bolzern

The Chair of the Doctoral Program:
Prof. Barbara Pernici

2018 – XXXI

Two there are who are never satisfied – the lover of the world and the lover of knowledge.
(Jalalud-Din Rumi)

Acknowledgement

To my teacher, Prof.Patrizio Colaneri. This journey would have been impossible without your support. It is quite difficult to come across such extraordinary men as you who try to be so ordinary.
To my parents, I cannot even comprehend the sacrifices you have made to see my dreams turn into reality. To my brother, your laughter has always filled my life with joy.
To my friends and colleagues in the office Aida, Alessandro, Basak, Daniele, Marco, Ricky, Riccardo and Stefano for their support and smiles always.
Special mention to Lorenzo Fagiano and Gian Paolo Incremona, for helping me through many hurdles and constantly supporting me throughout my thesis.
Thanks to Prof.Christopher Kelett and Philipp Braun for being extremely kind hosts while for my period aboard at University of Newcastle, Australia.

Abstract

In today's age, green transportation remains one of the most important topics of research. The main goal is to promote vehicle technologies and driving styles which are energy efficient and environment friendly. In this thesis, the main focus is on the Energy Efficient Train Control (EETC) or eco-driving strategies of railways. For this purpose, two main research paths have been explored. The first research direction is associated with a single train control problem, where the control problem is to find the best driving strategy for the train to go from one stop to another, given an optimal timetable. EETC strategies can be either fully automated (ATO) or serve as an advisory system to the driver (DAS) for the purpose of assisting drivers in following an energy efficient driving style. For this purpose, three control strategies using Model Predictive Control (MPC) have been presented. In the first two strategies, shrinking horizon techniques have been combined with input parametrization approaches to reduce the computational burden of the control problem and to realize the nonlinear integer programming control problem which arises in the DAS scenario, while the third strategy is based on switching MPC with receding horizon. All the strategies have been tested on the official simulation tool CITHEL of our industrial partner Alstom, and the obtained results in comparison with the existing techniques have proven to be more energy efficient. The second research direction falls under the paradigm of collaborative eco-drive control strategies, involving multiple trains belonging to a substation network. The main aim is to use the energy regenerated by the braking trains through collaboration among the trains connected and active in the network. In this case, three strategies

to decide the collaborative law have been presented along with the extensions from the single train control strategies presented in the first part of the thesis. For the design of collaborative laws, techniques such as manual supervision, substation modeling and dissension based adaptive laws with concept similar to Markov chains have been used. The strategies have been validated with simulation examples. Finally, comparisons of energy efficiency with and without collaboration have been presented, which show the advantage of using the developed collaborated laws as compared to no collaboration.

Contents

CHAPTER 1

Introduction

1.1 Motivation and Objectives

The risk of global warming threatening to destroy our planet is continuously increasing. Global warming is a consequence of the Green House Effect, which in turns results from an increase in the release of heat trapping gases known as the green house gases (GHGs). GHGs consist of water vapor, carbon dioxide (CO_2), methane, nitrous oxide, and ozone and have always been present in the earth's atmosphere. They are essentially important in order to maintain the earth's temperature due to their tendency to absorb and trap heat and hence support life. Without these gases, the average temperature of earth's surface would be about -18°C (0 °F), rather than the present average of 15 °C (59 °F). Human activities since the beginning of the industrial revolution (around 1750) have produced a 40% increase in the atmospheric concentration of CO_2, from 280 ppm (parts per million) in 1750 to 406 ppm in early 2017. This increase has occurred despite the uptake of more than half of the emissions by various natural "sinks" involved in the carbon cycle. The vast majority of anthropogenic carbon dioxide emissions (i.e., emissions produced by human activities) come from combustion of fossil fuels, principally coal, oil, and natural gas, with comparatively mod-

est additional contributions coming from deforestation, changes in land use, soil erosion, and agriculture. Presently, the level of these gases are alarmingly higher than have been in the last 650,000 years [2]. The result is a constant increase in the earth's temperature, which in turn has resulted in melting glaciers, increased sea levels, dying cloud forests and scrambling wildlife. If the greenhouse gas emissions continue at their present rate, earth's surface temperature could exceed historical values as early as 2047, with potentially harmful effects on ecosystems, biodiversity and the livelihoods of people worldwide. Recent estimates also suggest that at current emission rates, the earth's temperature could pass a threshold of 2°C global warming, which the United Nations Intergovernmental Panel on Climate Change (IPCC) designated as the upper limit to avoid dangerous global warming by 2036.

On the other hand, in the recent past, electropollution or electromagnetic pollution has been a source of open discussion and has been referred to as 21st century catastrophe [40]. It usually refers to the introduction of biologically toxic electrical frequencies into the earth's environment by electromagnetic frequencies (EMFs). These radiations have been shown to cause serious health issues ranging from diabetes to cancer. Some scientists believe it to be a greater threat than global warming, as Robert Becker, nominated twice for the nobel price said, "The greatest polluting element in the earth's environment is the proliferation of electromagnetic fields. I consider that to be a far greater threat on a global scale than warming, or the increase of chemical elements in the environment." An expert in electromagnetic pollution, Camilla Rees has been working continuously to bring awareness about this issue and has been quoted as saying, "This is a species issue. There is early evidence there may be a link between EMF exposures and autism. We know radiation is affecting our DNA and jeopardizing the health of future generations. There is research from many countries now showing dramatic decline in sperm count from exposure to cell phone radiation. I really don't think it's possible, when you know the disturbing truth, to stop caring, to stop wanting to support life."

Though in general, transportation remains one of the major contributers of CO_2 emissions and hence global warming, railway remains by far the most efficient means of transportation from the point of view of energy consumption and therefore a strategic sector in today's society. Keeping in mind the present risks and dangers associated with global warming, the European Union (EU) has set up certain restrictions to deal with it. For railway sector, these targets are set together by the International Union of Railways (UIC) and Community of European Railway and Infrastructure

Figure 1.1: *Loss of natural habitat of animals as an effect of global warming: A polar bear stands sentinel on Rudolf Island in Russias Franz Josef Land archipelago, where the perennial ice is melting, National Geographic.*

Companies (CER). Their short term target is to decrease the CO_2 emissions by 30 % over the period from 1990 to 2020, while the long term goal is to firstly further decrease these emissions by 50 % towards the end of 2030 and secondly to decrease the overall energy consumption of railways by 30% towards the end of 2030 as compared to 1990 [1].

In order to fulfill these goals, a lot of European railway companies have started research on opportunities to decrease energy consumption in order to be sustainable and more profitable in the future. The proposed methods differ on the basis of certain factors. Some of these methods are operator based, which at time requires upgrade in the vehicle technology, while others are control based. For example, in order to reduce energy, an operator can deploy rolling stock that is more energy efficient by using more energy efficient engines or streamlining. Also, the operator may work to better match the capacities of the trains with the demand, so that fewer seats are moved around and/or deploy measures concerning heating, cooling, lightning, etc. of parked trains during night in order to save energy. On the

other hand, the control based methods are mostly focused on development of techniques aimed at reducing fuel consumption and emissions which are affected by the behavior of the driver, without necessarily upgrading the vehicle technology. In the literature, they are commonly referred to as Energy Efficient Train Control (EETC) or eco-driving strategies. In other words, given the timetable, a train is driven with the least amount of traction energy. The timetable may be constructed in such a way that it allows EETC most effectively, resulting in Energy Efficient Train Timetabling (EETT). In case of electrical trains, which can regenerate energy during braking, the control based techniques need to be further enhanced to be able to use this regenerated energy effectively.

For this thesis, the main focus is to investigate two main research questions for electrical trains as also required by our industrial partner Alstom.

1. Firstly, given an optimal timetable, what is the best driving strategy for the train to go from stop A to stop B? This research question falls under the paradigm of EETC or eco-driving techniques.

2. Secondly, in case of available regenerative energy in a network substation consisting of more than one train, what is the best way to use this regenerated energy for overall networked energy minimization? Can the trains connected to the same substation collaborate with each other and share this regenerated energy among themselves? This research question falls under the paradigm of collaborative EETC or collaborative eco-driving techniques.

1.2 Proposed Approach

The system dynamics of a single train involved in the EETC are studied. Two main models have been used for the developed control strategies, which will be presented. The control strategies developed are based on Model Predictive Control (MPC). Robustness analysis in case of disturbances/uncertainties on the system model have also been carried out. Then these strategies are extended to include regenerative braking and energy sharing among trains connected to the same substation network. For this purpose, specifically new control strategies are proposed, where the energy regenerated by the braking train is exploited effectively by other trains which are connected to the same substation network.

1.3 Thesis Outline

The thesis is divided into four main parts. The first part contains Chapter 1, which explains the motivation behind this work and the main research questions which have been explored in this thesis.

The second part of thesis consists of five chapters, providing answers to the first research question, that is the EETC problem of a single train. While Chapter 2 provides a historical overview of the single train EETC problem along with a review of the previous control strategies developed in the literature to deal with it and finally our motivation behind the application of MPC to deal with this problem, Chapter 3 provides preliminaries needed to better explain the EETC problem. Finally, Chapter 4, Chapter 5 and Chapter 6 present the different system models and the associated control strategies developed in this thesis work. Each chapter concludes with simulations tested on real train data kindly provided by our industrial partner Alstom.

The third part of this thesis explores the second research question, which is based on developing strategies involving a substation network consisting of more than one train. The main reason, which gives significance to this research question is the case of electrical trains. For these trains, there is a possibility of energy regeneration when they brake, resulting in a portion of the braking energy being regenerated rather than being completely lost to the environment. This makes electrical trains among the most efficient trains from the point of view of energy consumption. This part consists of two chapters. Chapter 7 provides a historical perspective on the first use of regeneration energy and a review of the different strategies developed to effectively use this regenerated energy along with two developed supervisor control strategies via collaboration among trains connected to the same substation, while Chapter 8 presents another collaborative strategy developed using Dissension strategy based on Markov chains.

The final part of this thesis consist of Chapter 9, where we present some concluding remarks on the work presented in this thesis.

CHAPTER 2

Historical Perspective: Single Train EETC Problem

Historically speaking, the research on EETC/ eco-driving started as early as 1968 in Japan [47] and has ever since been an interesting topic in the literature. As already mentioned in Chapter 1, it usually refers to the application of techniques aimed at reducing energy consumption and carbon emissions effected by the driver behavior/ driving style, without necessarily upgrading the vehicle technology. These techniques can be categorized into two main branches: The Driver Advisary Systems (DAS) and the Automatic Train Operation (ATO). DAS are developed to advice the train drivers on the driving strategy to implement for energy efficient operation, while in ATO the energy efficient operation is completely automated with the driver being removed from the loop.

The earliest solutions involving EETC have been developed by the application of the Pontryagin's Maximum Principle (PMP), as in general, the EETC problems fall under the category of optimal control problems (OCPs). The next sections will describe in detail the basic train control problem along with its system dynamics, constraints, the earliest solutions present in the literature and a general review of the techniques developed

till date as a solution to the EETC problem.

2.1 Basic Optimal Train Control Problem

This section will describe in detail the basic train OCP starting from its system dynamics, the constraints the train is subjected to, performance index to reduce the energy consumption, the need to represent the train model with respect to space (distance) and finally the solutions previously presented to solve this problem. The basic OCP solved through EETC is based on selecting the optimal driving style for the train to go from one station to another within a given allowable time, such that energy is minimized.

2.1.1 Basic Train Model

In continuous time domain representation, the simplified model of a single train can be presented as a differential motion equation, described as

$$M\frac{dv}{dt} = F_T(v, u(t)) - F_B(v, u(t)) - F_R(v, s) \tag{2.1}$$

where

Table 2.1: *Train Parameter Symbols and their Definitions*

M	total mass of the train;
v	velocity of the train;
F_T	traction force;
F_B	braking force;
F_R	resistance force;
u	input handle of the train.
s	space(distance) of the train.

The resistance force F_R is given as a combination of frictional effects due to velocity, described by the Davis equation [20], and the frictional effects due to slopes and radius of the track, i.e.,

$$\begin{aligned} F_R(v, s) &= R_v(v) + R_g(s) \\ R_v(v) &= A + Bv + Cv^2 \\ R_g(s) &= M_s\left(g\tan(\alpha(s)) + \frac{\lambda_t}{r_c(s)}\right) \end{aligned} \tag{2.2}$$

Table 2.2: *Train Resistance Parameter Symbols and their Definitions*

R_v	frictional forces due to velocity;
A, B, C	Davis equation parameters;
R_g	frictional forces due to slope of the track and gravity;
M_s	static mass of the train;
r_c	radius of the curve of the track;
α	slope of the track;
λ_t	train dependent parameter;
g	acceleration due to gravity.

Remark 2.1.1. *Notice that the resistance force is hardly known in practice and only nominal values of Davis parameters are known in advance. Hence, identification of the adherence status of the railways is an important issue for braking and traction performances. Recent contribution can be found in [16]. In the following, these parameters are considered to be known. Also, since the considered EETC problem is in between two stops, as such the mass M of the train is considered constant in the train models used throughout this work.*

As for the traction and braking forces, they are functions of the handle and velocity (see Fig. 2.1) and for a particular value of the velocity, their models can be captured by the following formulas

$$F_T = F_{T_{\max}}(v)u(t) \tag{2.3}$$
$$F_B = F_{B_{\max}}(v)u(t)\ , \tag{2.4}$$

with $F_{T_{\max}}$ and $F_{B_{\max}}$ being the maximum allowable traction and braking forces, respectively.

Furthermore, the train is subject to velocity constraints (which are functions of the space s) and maximum allowable journey time. For $s \in [0, s_f]$, where s_f is the final point of the track, the space dependent velocity constraints are given by

$$0 \leq v(s) \leq v_{\max}(s)\ , \tag{2.5}$$

with $v_{\max}(s)$ being the maximum allowed velocity value at space s. Furthermore, the journey time limits are described as:

$$T(s_f) \leq t_f\ . \tag{2.6}$$

Note that, the velocity constraints (2.5) and the slopes and radius (see (2.2)) are functions of space. Hence, in order to account for these constraints and

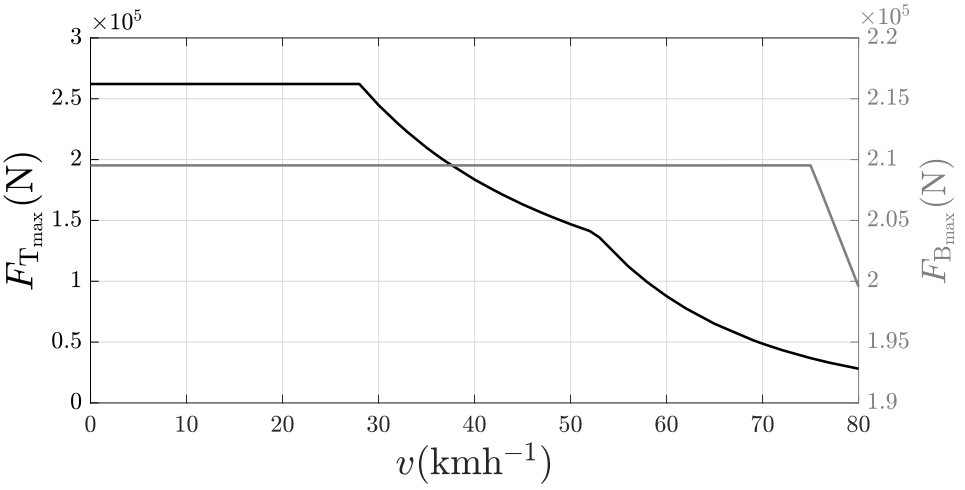

Figure 2.1: *Maximum traction (black line) and braking (gray line) forces as functions of velocity. The force characteristics of one of the trains used in the simulations with real data provided by Alstom.*

dynamics, another way is to represent the train model with respect to space rather than time. The representation of the train model in space domain is given as

$$\frac{dv}{ds} = \frac{F_T(v, u(s)) - F_B(v, u(s)) - F_R(v, s)}{Mv} \,. \tag{2.7}$$

Remark 2.1.2. *The input handle $u \in [1, -1]$ represents the normalized allowed traction (positive) and braking (negative) force, that the train can use at a particular time instant. Since this work focuses on electrical trains, the input handle is continuous and can assume any value belonging to the above mentioned finite interval. Also, with a slight abuse of notation, the same notations have been used throughout the thesis to denote the system dynamics of the models with respect to time and space.*

2.1.2 Optimal Train Control Problem in Time Domain

Having defined the basic train model and the constraints the train operation is subjected to, the basic OCP involving the EETC essentially consists of minimizing the energy consumption of the train used in traction. In the literature, the time domain model (2.1) has been reformulated a bit differently by normalizing the right hand side of the equation with the mass M of the train and introducing some new variables. The first variable $h(t)$, which is the input and also the optimization variable is given by $h(t) = \frac{F_T - F_B}{M}$. The

second variable $r(v) = \frac{F_R}{M}$ represents the normalized resistance force, originally given by (2.2). The input $h(t)$ is constrained by the maximum and minimum forces such that $h(t) \in \overline{H} = [-h_{\min}, h_{\max}(v(t))]$ for $t \in [0, t_f]$, where $h_{\max}(v) = \frac{F_{T_{\max}}(v)}{M} > 0$ and $h_{\min}(v) = \frac{F_{B_{\max}}(v)}{M} < 0$. Finally, the performance index is given by the energy consumption, which is the work done by the traction power $P(t) = F_T(t)v(t)$ over time and can be further simplified as $\int_0^{t_f} h^+(t)v(t)dt$ such that $h^+(t) = \max(h(t), 0)$. Mathematically, it can be expressed as:

$$\begin{aligned} & J = \min_h \int_0^{t_f} h^+(t)v(t)dt \\ & \text{subject to} \\ & \dot{s}(t) = v(t) \\ & \dot{v}(t) = h(t) - r(v(t)) \\ & s(0) = 0, s(t_f) = s_f, v(0) = 0, v(t_f) = 0 \\ & v(t) \geq 0, h \in [-h_{\min}, h_{\max}(v(t))] \end{aligned} \tag{2.8}$$

where $s(t)$ is the distance traveled over time. The variables (s, v) are the state variables and h is the control variable.

Remark 2.1.3. *For OCP* (2.8)*, certain simplifications were made due to the modeling in time domain. Firstly, it was assumed that the resistance component R_g due to the gradients and curvature was zero, such that only the resistance component R_v due to the velocity of the train was considered (see* (2.2)*). Secondly, the velocity limits* (2.5)*, which are a function of distance were not considered, as can be observed from the OCP* (2.8)*. Finally, it was also assumed that $h_{\min} = \frac{F_{B_{\max}}}{M} < 0$, such that the braking force does not depend on the velocity.*

Pontryagin's Maximum Principle for Time Domain OCP

The Pontryagin's Maximum Principle [63] states that the optimal control state trajectory $\hat{x}$, optimal control $\hat{h}$, and the corresponding Lagrange multiplier vector $\hat{\lambda}$ must maximize the Hamiltonian H so that:

$$H(\hat{x}(t), \hat{h}(t), \hat{\lambda}(t), t) \geq H(\hat{x}(t), h, \hat{\lambda}(t), t), \quad \forall h \in \overline{H}, t \in [0, T] \tag{2.9}$$

where the Hamiltonian H associated with the maximum principle is defined for all $t \in [0, T]$ by:

$$H(x(t), h(t), \boldsymbol{\lambda}(t), t) = L(x(t), h(t)) + \boldsymbol{\lambda}^T(t) f(x(t), h(t)). \tag{2.10}$$

The notation $\cdot^T$ will denote the matrix transpose operator throughout this work. The constraints on the system dynamics can be adjoined to the Lagrangian L by introducing time-varying Lagrange multiplier vector $\boldsymbol{\lambda}$, whose elements are called the co-states of the system.

If we analyze the OCP (2.8), it can be noted that it has a standard form of the OCPs for which the necessary conditions are given by the PMP. In particular, it minimizes an objective function $\min_h \int_0^T L(s, v, h)dt$, where $T = t_f$ and $L(s, v, h) = h^+(t)v(t)$ subject to the system dynamics described by the ordinary differential equations (ODE) $\dot{s}(t) = f_1(s, v, h)$ and $\dot{v}(t) = f_2(s, v, h)$ with boundary conditions on s and v and path constraints $g_i(s, v, h) \geq 0, i = 1, \ldots, n$. The Lagrange multiplier is given by $\boldsymbol{\lambda} = [\phi,\ \lambda]^T$, whereas $f_1(s, v, h) = v(t)$, $f_2(s, v, h) = h(t) - r(v(t))$ and $x(t) = [s(t),\ v(t)]^T$.

The control is also upper and lower bounded depending on the maximum and minimum available force to the train. The general Hamiltonian can be given by:

$$H(s, v, \phi, \lambda, h) = -L(s, v, h) + \phi f_1(s, v, h) + \lambda f_2(s, v, h) \tag{2.11}$$

without the boundary conditions and the augmented Hamiltonian (or Lagrangian) is given by

$$\tilde{H}(s, v, \phi, \lambda, \mu, h) = H(s, v, \phi, \lambda, h) + \sum_{i=1}^{n} \mu_i g_i(s, v, h) \tag{2.12}$$

where (ϕ, λ) are the co-state (or adjoint) variables which satisfy the differential equations

$$\dot{\phi}(t) = -\frac{\delta \tilde{H}}{\delta s}(s, v, \phi, \lambda, \mu, h) \ \text{ and } \ \dot{\lambda}(t) = -\frac{\delta \tilde{H}}{\delta v}(s, v, \phi, \lambda, \mu, h) \tag{2.13}$$

with respect to the additional path constraints $g_i(s, v, h) \geq 0$, where μ_i are Lagrange multipliers satisfying the complementary slackness conditions $\mu_i \geq 0$ and $\mu_i g_i(x, v, h) = 0$. Moreover, the Karush-Kuhn-Tucker (KKT) necessary condition $\frac{\delta \tilde{H}}{\delta h} = 0$ must be satisfied by the optimal solution.

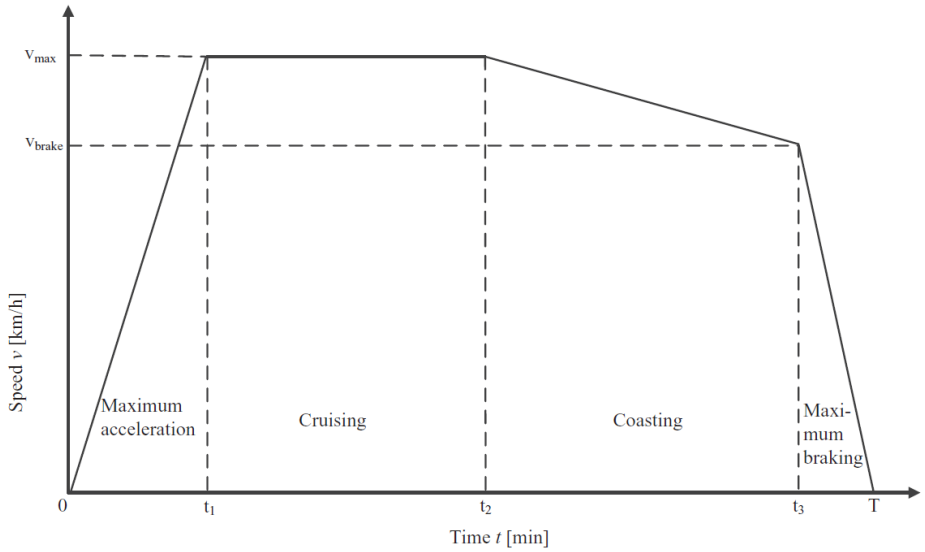

Figure 2.2: *Graphical representation of optimal driving regimes for energy efficient driving on flat track as function of time with switching points at t_1, t_2 and t_3 where time is in minutes (min).*

According to PMP, the candidate optimal control variable $\hat{h}$ should be selected from the admissible control variables that maximize the augmented Hamiltonian $\tilde{H}$ and the candidate optimal control is given by:

$$\hat{h} = \arg\max_{h \in \overline{H}} \tilde{H}(\hat{s}(t), \hat{v}(t), \hat{\phi}(t), \hat{\lambda}(t), h) \tag{2.14}$$

where $(\hat{s}, \hat{v})$ and $(\hat{\phi}, \hat{\lambda})$ are the state and the co-state trajectories associated to the control trajectory $\hat{h}$.

Typical for an optimal train control problem is that the Hamiltonian is (piecewise) linear in the control variable h, by which the optimal control may not be uniquely defined from the necessary conditions on some non-trivial interval. For the example problem, the Hamiltonian can be split around $h = 0$. Taking the control constraints into account, the optimal control is characterized as

$$\hat{h} = \begin{cases} h_{\max}(v(t)) & \text{if } \lambda(t) > v(t) \text{ (MA)} \\ h \in [0, h_{\max}] & \text{if } \lambda(t) = v(t) \text{ (CR)} \\ 0 & \text{if } 0 < \lambda(t) < v(t) \text{ (CO)} \\ -h_{\min} & \text{if } \lambda(t) \leq 0 \text{ (MB)} \end{cases} \tag{2.15}$$

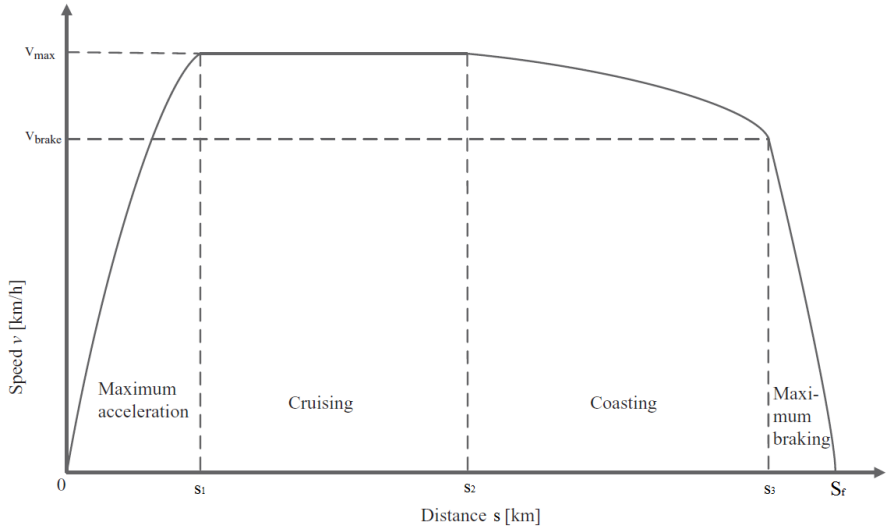

Figure 2.3: *Graphical representation of the optimal driving regimes for energy efficient driving with switching points at s_1, s_2 and s_3.*

The optimal control is illustrated in Fig.2.2. The maximum control $\hat{h} = h_{\max}$ implies maximum acceleration (MA), zero control $\hat{h} = 0$ implies coasting (CO) i.e., rolling with the engine turned off, and the minimum control $\hat{h} = -h_{\min}$ implies maximum braking (MB). The singular solution defined by $\lambda(t) = v(t)$ corresponds to speed-holding or cruising (CR), i.e. driving at a constant optimal speed using partial tractive effort $\hat{h} \in [0, h_{\max}]$.

2.1.3 Optimal Train Control Problem in Space Domain

Referring to Remark 2.1.3, in order to deal with gradients, track curvature and speed limits which are functions of distance, the model (2.7) was used but with the same reformulation as in Subsection 2.1.2. This change of coordinates was first proposed in [43, 64]. It should be noted here that now resistance component R_g due to the gradients and curvature is no longer considered zero.

In space domain, energy consumption is the work done by the traction power $P(t) = F_T(s)$ over space and can be written as:

$$\begin{aligned} J &= \min_h \int_0^{s_f} h^+(s)ds \\ &\text{subject to} \\ \dot{t}(s) &= \frac{1}{v(t)} \\ \dot{v}(s) &= \frac{h(s) - r(v(s))}{v(s)} \\ t(0) &= 0, t(s_f) = t_f, v(0) = 0, v(s_f) = 0 \\ v(s) &\geq 0, v(s) \leq v_{\max}(s), h \in [-h_{\min}, h_{\max}(v(s))] \end{aligned} \tag{2.16}$$

where $t(s)$ is the travel time over the distance. The variables (t, v) are the state variables and h is the control variable.

Remark 2.1.4. *In general, $h(t) \neq u(t)$ due to the reformulation presented above. For the purpose of our work, we will use $u(t)$ as our input to the train and also our optimization variable. More details can be found in the next chapter. The reformulation leading to OCPs* (2.8) *and* (2.16)*, where $h(t)$ is the optimization variable has just been introduced to explain the previous methods used in the literature.*

Pontryagin's Maximum Principle for Space Domain OCP

The necessary conditions, Hamiltonian, state and co-state equations are expressed in the same way as in Subsection 2.1.2. Then according to the PMP, the candidate optimal control for varying gradients in space domain is given by:

$$\hat{h} = \begin{cases} h_{\max}(v(s)) & \text{if } \lambda(s) > v(s) \text{ (MA)} \\ h \in [0, h_{\max}] & \text{if } \lambda(s) = v(s) \text{ (CR1)} \\ 0 & \text{if } 0 < \lambda(s) < v(s) \text{ (C0)} \\ h \in [-h_{\min}, 0] & \text{if } \lambda(s) = 0 \text{ (CR2)} \\ -h_{\min} & \text{if } \lambda(s) \leq 0 \text{ (MB)} \end{cases} \tag{2.17}$$

The speed profile in this case is shown in Fig. 2.3.

2.2 Literature Review for a Single Train Problem

EETC problems can be classified on the basis of many considerations. One way to classify them is based on the methodologies involved in solving them. Based on this criteria, EETC problems have been solved using either exact methods or heuristic methods. Another criteria is on the basis of traction control. Usually, traction force model can be continuous or discrete based on whether we are dealing with electric traction or diesel-electric traction. The main difference lies in the presence of an on-board prime mover. A prime mover is an engine that converts fuel to useful work. The electric traction trains usually do not have any on-board prime mover and hence rely on an external power station for power, while diesel-electric traction trains have an on-board prime mover in the form of a diesel engine or a gas turbine which acts as a power source for these kinds of trains. A recent review can be found in [71]. The focus of our work is on exact methods and electrical traction trains. In electrical trains, the force can be considered as continuous. They were also the earliest problems to be considered in the literature. The first study was carried out in Japan [47] in 1968. The model used was very similar to the one described in Section 2.1, but in this case the resistance force was simplified to be simply the velocity rather than a quadratic function of the velocity and track was considered to be flat and straight, making the differential equations describing the model behavior linear. The analytical expressions for the various regimes were derived by using the PMP principle and include all four driving regimes on level tracks:

1. Maximum acceleration (MA)
2. Cruising by partial traction force (CR)
3. Coasting (CO),
4. Maximum braking (MB),

as well as resulting optimal control rules. This work was further extended by including the resistance force due to velocity as a quadratic function of the velocity and also taking into account the resistance due to the slopes and the curvature [74]. However, they then linearized the resistance function and thus could derive analytical expressions for all driving regimes using the PMP as well. As a result of the possible negative slopes partial braking to maintain cruising was found to maintain cruising during descent, and the driving regime consisted of:

1. Maximum acceleration (MA)

2. Cruising by partial traction force (CR1)
3. Coasting (CO),
4. Cruising by partial braking force (CR2)
5. Maximum braking (MB),

It is significant to point out here that the approach in [74] was implemented in the form of a computer aided train operation and formed the basis of the first DAS implemented in board computers of the Berlin S-Bahn (suburban trains) in Germany at the beginning of the 1980s. However, in this case the computations were made offline due to the limited computational power available at that time. This research was again revisited by [8], where solutions were calculated backwards from the target station using simulink. The algorithm numerically calculated the switching curves that could be used to calculate the switching points in the optimal trajectory and was applied in a DAS on the train driving simulator at Dresden University of Technology (TU Dresden), and in real-time passenger operation of the suburban railway line S1 in Dresden.

Around the same time, starting from 1982, train control research has also been carried out actively by the University of South Australia (UniSA). The research was initiated with the Ph.D thesis of Milroy on continuous train control. Milroy's research [57] was focused on urban railway transport and he also applied the PMP principle to solve the optimal train control problem. His research conclusions were based on the assumptions that the track is flat with fixed speed limit and there are three driving regimes (see Fig. 2.4) in the optimal driving strategy:

1. Maximum acceleration (MA)
2. Coasting (CO),
3. Maximum braking (MB),

However, in [44] it was mathematically proven based on the PMP that the general optimal driving strategy for level track and a fixed speed limit consists of four driving regimes including cruising, which confirmed the results provided before in [74]. All these ideas were implemented by UniSA in a commercial system named Metromiser. The DAS part of the Metromiser advised the train driver when to coast and when to brake in order to minimize energy consumption using light and sound indications. However, the Metromiser considered a constant effective gradient during coasting and braking phases. The first successful runs with the system were done on the (sub)urban trains in Adelaide (Australia) in 1984, and later in Toronto (Canada), Melbourne (Australia). The achieved energy savings

were more than 15% compared to the trains running without Metromiser, and also punctuality increased. In case of suburban trains to which Metromiser was applied, the coasting phase was found out to be the most important driving regime due to short stop distances [13, 43].

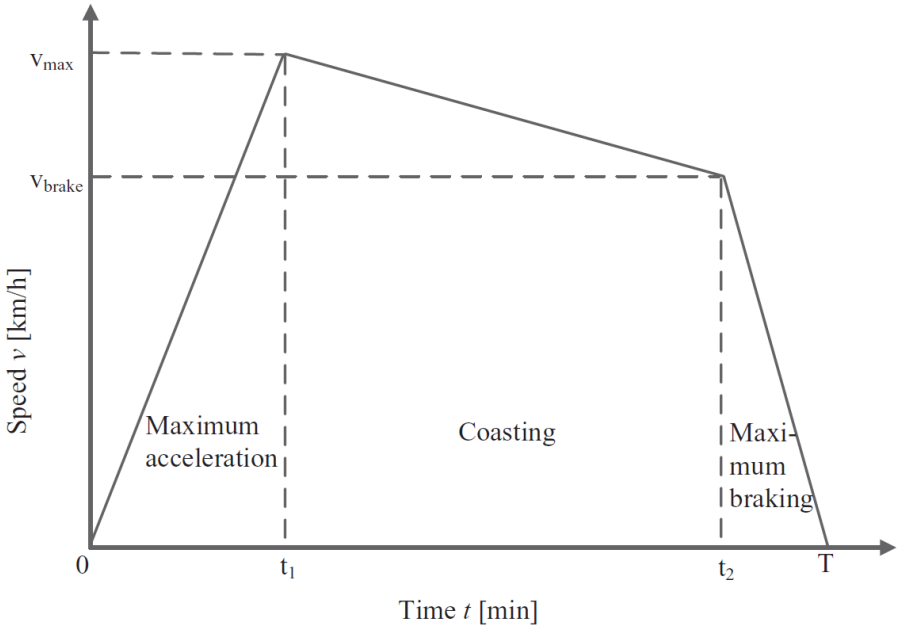

Figure 2.4: *Graphical representation of optimal driving regimes for energy-efficient driving on flat track without cruising as function of time with switching points at t_1 and t_2.*

As the EETC research gained momentum, around 1990 Netherlands Railways (NS, Nederlandse Spoorwegen) also started investigations in this direction. The authors in [78] investigated the optimal driving strategy and found the four optimal driving regimes by measurements and experience. Results with the optimal driving strategy indicated energy savings of 10% compared to the normal practice of train operation. The most important results deduced from this research were that optimizing the cruising speed and coasting distance were the most important factors in energy savings. Another considerable work was published in [75], where the authors considered the EETC problem on level track with the simplifying assumption that the maximum traction, braking and resistance forces are all constant, which made it easier for them to derive the analytical expressions for all driving schemes based on the PMP. This work was futher extended in [76],

where maximum traction, braking and resistance forces were now considered as functions of speed although the exact functions were not given. The developed algorithms were used on the Beijing Yizhuang metro line in China in a timetabling algorithm.

Till now, all the strategies developed were with a time domain model. Since, both the gradient, curvature and velocity limits are a function of distance, [43, 64] suggested a change of independent variable from time to distance. This model was further used in [52], where the authors considered varying gradients and speed limits. The model, the resulting OCP and Pontryagins principle has already been discussed in detail in Subsection 2.1.3. The same results as in (2.17) were derived in [52], where cruising speed is split into partial power and partial braking. The use of the space domain model was continued in [79], where the concept of steep track was also introduced. A steep uphill section is a section in which the train has insufficient power to maintain a cruising speed when climbing, while a steep downhill section is a section where the train is increasing speed while coasting. In [79], the author showed that the optimal control for a specific journey on a non-steep track is unique. This concept was further extended to steep tracks in [45], where a new local minimization principle to calculate the critical switching points on tracks with steep gradients was developed. Furthermore, the authors in [7] proved that these critical switching points are uniquely defined for each steep section of track and deduced that the global optimal strategy is unique, while in [4], it was shown by means of numerical examples that the optimal train control strategy indeed consists of maximum power instead of partial power for acceleration. For more of their work, see [6] [5]. In [69, 70], the authors also considered varying gradients and speed limits and derived the PMP optimality conditions by developing a two-stage iterative algorithm based on Fibonacci search and bisection method. Moreover, in [80], along with time and speed restrictions, also signaling constraints associated with safety requirements are considered, when solving the EETC problem. The EETC problem in this case was modeled as a multiple phase optimal control model.

Finally, MPC has also been applied in this context. In [9], they used the space model and considered varying gradients and speed limits. The optimization problem was solved as a tracking problem, where a reference velocity was tracked and was similar to the previous MPC approaches applied to high speed train in [30, 88]. While in [30], the additional contribution was in the form of parameter adaptation using an update strategy in case of uncertainties in the parameter values caused by friction and track features, in [88] a MPC based hierarchical integration architecture for

real time scheduling and control was introduced. Similarly speed tracking MPC based controller to solve EETC problem has also been developed in [51,53,73,83]. For example, in [53], Particle Swarm Optimization (PSO) based MPC was used to track the reference velocity curve. In [11,46], fuzzy predictive control has been used to solve the EETC problem. In [82], an online cooperative energy efficient trajectory planning for multiple high speed trains is designed, where MPC has been used at a local level. In [87], MPC has also been applied to operational planning involving high speed trains. The main aim was to manage real-time conflict, when disturbances occur during high speed train operations to guarantee the safety and efficiency of networked railway traffic. There were both EETC and EETT problems involved but the focus was on solving EETT/ scheduling problem with EETC solution activated only under certain circumstances. In [21, 21, 81], MPC has been applied for solving conflicting, delays and scheduling problems associated with EETT problems.

Although application of MPC to EETC problem has been investigated in the literature, it has been mostly based on speed tracking. In the next chapters, we will present MPC based strategies but usually different and novel approaches. At last, we would like to mention that this thesis is an extension of a master thesis [34], where an EETC control strategy was proposed using Genetic Algorithm and is being presently in use by Alstom.

CHAPTER 3

Preliminaries: Energy Efficient Train Control (EETC) Strategies

The basic system dynamics of a single train along with the constraints that it is subjected to have already been defined in Chapter 2 (see Subsection 2.1.1 for details). Also, due to the nature of traction, braking and resistance forces (see (2.2) and Fig.2.1), the considered train model is nonlinear in nature. Now, referring to Remark 2.1.2, this work focuses on electrical trains for which the input handle $u \in [1, -1]$, which represents the allowed traction (positive) and braking (negative) force that the train can use at a particular time instant, is continuous in nature. Having said that, in the beginning of Chapter 2, it was mentioned that the EETC algorithms can be classified into two categories, the DAS strategies and the ATO strategies. These strategies and how they impact our optimization problem are better explained in Section 3.1.

3.1 ATO and DAS Strategies

EETC algorithms can be either fully automated (ATO) or serve as an advisory system to the driver (DAS). Mathematically, the choice of the strategy

impacts the optimization problem involved , which is explained in the following subsections.

3.1.1 ATO Strategy

When the controller operates fully autonomously as an ATO strategy, i.e. without a human driver in the loop, the whole interval can be used, i.e. $u \in [1, -1]$. Since u is our input to the system and also our optimization variable, hence in this case our optimization problem becomes a nonlinear continuous problem.

3.1.2 DAS Strategy

On the other hand, in a DAS, i.e. when the control algorithm is developed to assist a human driver with a suggested value of the input handle, only a smaller set of possible values can be delivered by the controller, in order to facilitate the human-machine interaction. In particular, in this scenario the input constraints are further tightened according to four possible operating modes prescribed by our industrial partner:

- *Acceleration:* in this mode, the input can take one of three allowed values, i.e. $u \in \{0.5, 0.75, 1\}$.
- *Coasting:* this mode implies that the traction is zero, i.e $u = 0$.
- *Cruising:* in this mode, the train engages a cruise control system that keeps a constant speed, i.e. u is computed by an inner control loop in such a way that $F_T = F_R$ for positive slopes and $F_B = F_R$ for negative slopes.
- *Braking:* in this mode the maximum braking force is used, i.e. $u = -1$.

As a matter of fact, the modes above can be merged in just two: one with a finite integer number of possible input values $u \in \{-1, 0, 0.5, 0.75, 1\}$ (which unites the Acceleration, Coasting and Braking modes), and one with the cruise control engaged. From the above formulation, it is clear that in the case of DAS, our optimization becomes a nonlinear mixed integer programming problem.

The next three chapters will present the developed EETC strategies as a part of this thesis. While Chapter 4 will present a strategy which can act both as a ATO as well as a DAS system, Chapters 5 and 6 will present strategies specifically developed as DAS strategies. All the strategies have

been developed using MPC. In the scope of this work, both time domain and space domain models have been used. In order to use both the time domain model (2.1) and the space domain model (2.7) with MPC, it is important to express them in state space. In all the three control strategies which will be presented in the following chapters, the single train dynamics will be essentially defined as a two state system with $x(k) = [x_1(k), x_2(k)]^T$ being the states of the train. The state x_2 will always represent the main state of the train which is the train velocity, while the heuristic state x_1 will either represent the train's travel time if we are using space domain model (2.7) or train's distance if we are using time domain model (2.1). In accordance with the strategy used, the models (2.1) and (2.7) will be accordingly reformulated.

CHAPTER 4

Shrinking Horizon Move Blocking Predictive Control Strategy

This chapter presents a nonlinear model predictive control approach as a solution to the EETC problem and has been presented in [25]. Model Predictive Control (MPC) is an optimization-based technique with broad success in industry [65] thanks to its capability to deal with multivariable systems, state and input constraints, and both tracking and economic objectives. Research efforts of more than three decades result today in a mature theory for linear systems [39], [14], and several directions are open for further investigation [55]. In this chapter along with its application to EETC problem, new general results pertaining to MPC for nonlinear systems and problems where a finite terminal time is imposed, at which the state has to reach a given terminal set, are provided. The resulting MPC formulation features a shrinking horizon rather than the most common receding one. Moreover, a move blocking strategy to reduce the computational burden of the underlying optimization program is considered. The resulting control approach has been named Shrinking Horizon Move Blocking Predictive Control (SBPC), which consists of a nominal approach and two relaxed ones, where state constraints are softened to retain recursive feasibility. The ex-

isting works on move blocking strategies consider in fact either linear systems, see e.g. [35–38, 72, 77] or nonlinear systems with receding horizon formulations [15, 50, 85].
The approach proposed has the flexibility of considering either a fully autonomous scenario (ATO), where the input variable u (the total traction/braking force applied to the train) can take any value in a connected compact set (see Subsection 3.1.1), or a driver assistance scenario (DAS), where the predictive controller can suggest to the driver one out of a discrete set of possible driving modes (see Subsection 3.1.2). In both scenarios, the uncertainty derived from either system-model mismatch or control input discretization/misapplication by the human driver is considered. The uncertainty is modeled as a bounded additive input disturbance, and theoretical results regarding the guaranteed bound on constraint violation as a function of the disturbance bound are presented.

4.1 Train Optimal Control Problem

Consider an electric train controlled by a digital control unit in discrete time, with sampling period T_s (see for example Fig.4.1, depicting the one considered in the simulations of Section 4.4). Let us denote with $k \in \mathbb{Z}$ the discrete time variable with $x(k) = [x_1(k),\, x_2(k)]^T$ the state of the train, where x_1 is its position and x_2 its speed, and with $u(k) \in [-1, 1]$ a normalized traction force, where $u(k) = 1$ corresponds to the maximum applicable traction and $u(k) = -1$ to the maximum braking. The input u is the available control variable. The train has to move from one station with position $x_1 = 0$ to the next one, with position $x_1 = x_f$, in a prescribed time t_f. In state space modeling, the prescribed arrival position s_f (see Subsection 2.1.1) and the maximum allowed velocity limit $v_{\max}(k)$ (see Eq. 2.5) have been renamed as $s_f = x_f$ and $v_{\max}(k) = \overline{x}_2(k)$ to link them to the states they are representing. For a given pair of initial and final stations, the track features (slopes, curvature) are known in advance. Thus, in nominal conditions (i.e.with rated values of the train parameters, like its mass and the specifications of the powertrain and braking systems), according to Newton's laws and using the forward Euler discretization method, the equations of motion of a reasonably accurate model of this system read:

$$\begin{aligned} x_1(k+1) &= x_1(k) + T_s x_2(k) \\ x_2(k+1) &= x_2(k) + T_s \left(\frac{F_T(x(k),u(k)) - F_B(x(k),u(k)) - F_R(x(k))}{M} \right) \end{aligned} \tag{4.1}$$

The resistive force $F_R(x)$ is also nonlinear, and it is the sum of a first term $R_v(x_2)$, accounting for resistance due to the velocity, and a second

term $R_g(x_1)$, accounting for the effects of slopes and track curvature:

$$\begin{aligned} F_R(x) &= R_v(x_2) + R_g(x_1) \\ R_v(x_2) &= A + Bx_2 + Cx_2^2 \\ R_g(x_1) &= M_s \left(g \tan(\alpha(x_1)) + \frac{\lambda_t}{r_c(x_1)} \right) \end{aligned} \tag{4.2}$$

While M_s is the static mass of the train, i.e. the mass calculated without taking into account the effective inertia of the rotating components, the other parametric symbols have already been defined in Subsection 2.1.1 (see Tables 2.1 and 2.2 for more details). As already discussed in Subsection 2.1.1, besides the prescribed arrival time t_f and position x_f, there are additional state constraints that must be satisfied. These pertain to the limit on the maximum allowed velocity, $\overline{x}_2(x_1)$, which depends on the position x_1, since a different velocity limit is imposed for safety by the regulating authority according to the track features at each position. Overall, by defining the terminal time step $k_f \doteq \lfloor t_f/T_s \rfloor$ (where $\lfloor \cdot \rfloor$ denotes the flooring operation to the closest integer), the state constraints read:

$$\begin{aligned} x(0) &= [0,\ 0]^T \\ x(k_f) &= [x_f,\ 0]^T \\ x_2(k) &\geq 0,\ \ k = 0, \ldots, k_f \\ x_2(k) &\leq \overline{x}_2(x_1(k)),\ \ k = 0, \ldots, k_f \end{aligned} \tag{4.3}$$

Figure 4.1: *One of the Amsterdam metro trains considered in the simulation example of this chapter.*

The control objective is to maximize the energy efficiency of the train while satisfying the constraints above. To translate this goal in mathematical terms, different possible cost functions can be considered. In our case,

we consider the discretized integral of the absolute value of the traction power over time (with a constant scaling factor T_s^{-1}):

$$J = \sum_{k=0}^{k_f} \left| F_T(x(k), u(k)) x_2(k) \right| . \tag{4.4}$$

This choice tends to produce controllers that minimize the traction energy injected into the system. The braking energy is not penalized, since in our case there is no restriction to the use of the braking system, since we are not considering regeneration for a single train EETC problem (see Chapter 7 for details). Finally, a further feature of this application is a relatively small sampling time T_s with respect to the imposed overall time horizon t_f, resulting in a rather large number of sampling periods in the interval $[0,\ t_f]$, typically from several hundreds to a few thousands.

4.1.1 Problem Abstraction

The control problem described above can be cast in a rather standard form:

$$\min_{\boldsymbol{u}} \ \sum_{k=0}^{k_f} \ell(x(k), u(k)) \tag{4.5a}$$

subject to

$$x(k+1) = f(x(k), u(k)) \tag{4.5b}$$

$$u(k) \in U,\ k = 0, \ldots, k_f - 1 \tag{4.5c}$$

$$x(k) \in X,\ k = 1, \ldots, k_f \tag{4.5d}$$

$$x(0) = x_0 \tag{4.5e}$$

$$x(k_f) \in X_f \tag{4.5f}$$

where $x \in \mathbb{X} \subset \mathbb{R}^n$ is the system state, x_0 is the initial condition, $u \in \mathbb{U} \subset \mathbb{R}^m$ is the input, $f(x, u) : \mathbb{X} \times \mathbb{U} \to \mathbb{X}$ is a known nonlinear mapping representing the discrete-time system dynamics, and $\ell(x, u) : \mathbb{X} \times \mathbb{U} \to \mathbb{R}$ is a stage cost function defined by the designer according to the control objective. The symbol $\boldsymbol{u} = \{u(0), \ldots, u(k_f - 1)\} \in \mathbb{R}^{m\,k_f}$ represents the sequence of current and future control moves to be applied to the plant. The sets $X \subset \mathbb{X}$ and $U \subset \mathbb{U}$ represent the state and input constraints, and the set $X_f \subset \mathbb{X}$ the terminal state constraints, which include a terminal equality constraint as a special case. Furthermore, X and U is assumed to be compact, as well as the terminal constraint set X_f.
We recall that a continuous function $a : \mathbb{R}^+ \to \mathbb{R}^+$ is a $\mathcal{K}$-function ($a \in$

$\mathcal{K}$) if it is strictly increasing and $a(0) = 0$. Throughout this chapter, we consider the following lipchitz continuity assumption on the system model f.

Assumption 1. *The function f enjoys the following lipchitz continuity properties:*

$$\begin{aligned} \|f(x^1, u) - f(x^2, u)\| &\leq a_x\left(\|x^1 - x^2\|\right), \forall x^1, x^2 \in \mathbb{X}, u \in \mathbb{U} \\ \|f(x, u^1) - f(x, u^2)\| &\leq a_u\left(\|u^1 - u^2\|\right), \forall u^1, u^2 \in \mathbb{U}, x \in \mathbb{X} \end{aligned} \tag{4.6}$$

where $a_x,\ a_u \in \mathcal{K}$.

In (4.6) and in the remainder of this thesis, any vector norm $\|\cdot\|$ can be considered. Assumption (1) is reasonable in most real-world applications, and it holds in the railway application considered here.
The nonlinear program (4.5) is a Finite Horizon Optimal Control Problem (FHOCP). In the literature, many different solutions to solve this kind of a problem can be found, depending on the actual form of the system dynamics and constraints. One approach is to compute a (typically local) optimal sequence of inputs $\boldsymbol{u}^*$ and to apply it in open loop. This might be convenient when little uncertainty is present and the system is open-loop stable, which is seldom the case. A much more robust approach is to resort to a feedback control policy $u(k) = \kappa(x(k))$. However, to derive explicitly such a feedback policy in closed form is generally not computationally tractable, due to the presence of system nonlinearities and constraints. A common way to derive implicitly a feedback controller is to adopt a receding horizon strategy, where the input sequence is re-optimized at each sampling time k and only the first element of such a sequence, $u^*(k)$, is applied to the plant. Then, the feedback controller is implicitly defined by the solution of a FHOCP at each k, where the current measured (or estimated) state $x(k)$ is used as initial condition. This approach is well-known as Nonlinear Model Predictive Control (NMPC), and is adopted here as well, however with two particular differences with respect to the standard formulation:

- First, since in our problem the terminal time k_f is fixed, the resulting strategy features a shrinking horizon rather than a receding one. Indeed, here the goal is to make the state converge to the terminal set in the required finite time, and not asymptotically as usually guaranteed by a receding horizon strategy;
- Second, we adopt a move-blocking strategy (see e.g. [15]) to reduce the computational burden required by the feedback controller. This is motivated by the train application, featuring values of k_f of the order

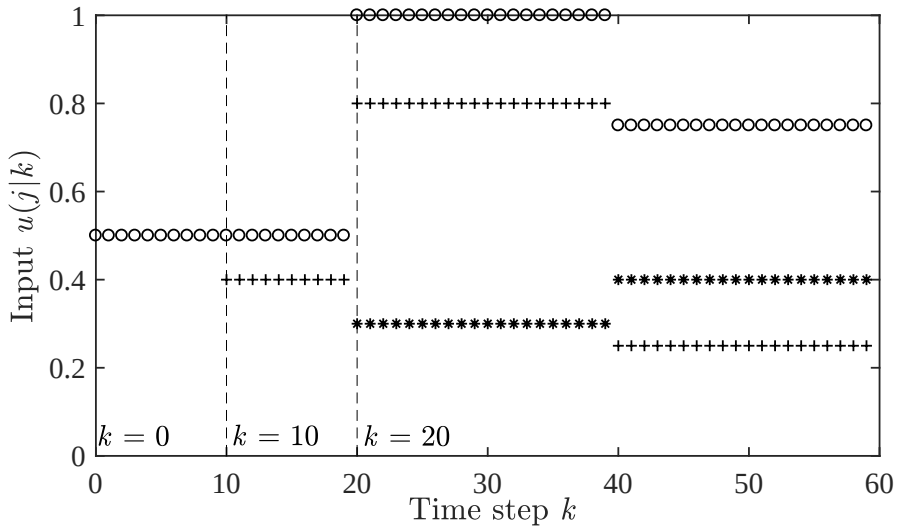

Figure 4.2: *SBPC scheme with $L = 20$ and $k_f = 60$. As an example, possible courses of predicted inputs at time $k = 0$ ('$\circ$'), $k = 10$ ('$+$'), and $k = 20$ ('$*$') are depicted. It can be noted that for $k = 20$ the number of decision variables reduces from 3 to $N(20) = 2$, and that as k increases, the number of blocked moves in the first block decreases.*

of several hundreds to thousands. The corresponding number of decision variables, combined with the system nonlinearity, often results in a prohibitive computational complexity when all the predicted control moves are free optimization variables.

The next section presents the optimal control problem to be solved at each time step in SBPC, followed by a pseudo-algorithm that realizes this control approach and by a proof of convergence in nominal conditions.

4.2 Shrinking Horizon Blocking Predictive Control (SBPC)

We consider a move blocking strategy, where the control input is held constant for a certain time interval. Let us denote with L the maximum number of blocked control moves in each interval within the prediction horizon. Moreover, we consider that each interval contains exactly L blocked moves, except possibly the first one, which can contain a number between 1 and L of blocked input vectors. In this way, for a given value of $k \in [0,\, k_f - 1]$, the number $N(k)$ of intervals (i.e. of different blocked input vector values

to be optimized) is equal to (see Fig. 4.2 for a graphical representation):

$$N(k) = \left\lceil \frac{k_f - k}{L} \right\rceil, \tag{4.7}$$

where $\lceil . \rceil$ denotes the ceiling operation to the closest integer. Let us denote with $\boldsymbol{v}_{N(k)} = \{v(1), \ldots, v(N(k))\} \in \mathbb{R}^{m\,N(k)}$, where $v(\cdot) \in \mathbb{U}$, the sequence of free input values to be optimized, i.e. the values that are held constant within each interval of the blocked input sequence (see Fig. 4.2) and with $u(j|k)$ the input vector at time $k+j$ predicted at time k. Then, with the described blocking strategy, at each k the values of $u(j|k)$ are computed as:

$$u(j|k) = g(\boldsymbol{v}_{N(k)}, j, k) \doteq v\left(\left\lfloor \frac{j + k - \left\lfloor \frac{k}{L} \right\rfloor L}{L} \right\rfloor + 1\right) \tag{4.8}$$

Finally, let us denote with $x(j|k)$, $j = 0, ..., k_f - k$ the state vectors predicted at time $k + j$ starting from the one at time k. At each time $k \in [0,\ k_f - 1]$, we formulate the following FHOCP:

$$\min_{\boldsymbol{v}_{N(k)}} \sum_{j=0}^{k_f-k} \ell(x(j|k), u(j|k)) \tag{4.9a}$$

subject to

$$u(j|k) = g(\boldsymbol{v}_{N(k)}, j, k),\ j = 0, \ldots, k_f - k - 1 \tag{4.9b}$$
$$x(j+1|k) = f(x(j|k), u(j|k)),\ j = 0, \ldots, k_f - k - 1 \tag{4.9c}$$
$$u(j|k) \in U,\ j = 0, \ldots, k_f - k - 1 \tag{4.9d}$$
$$x(j|k) \in X,\ j = 1, \ldots, k_f - k \tag{4.9e}$$
$$x(0|k) = x(k) \tag{4.9f}$$
$$x(k_f - k|k) \in X_f \tag{4.9g}$$

We denote with $\boldsymbol{v}^*_{N(k)} = \{v^*(1), \ldots, v^*(N(k))\}$ a solution (in general only locally optimal) of (4.9). Moreover, we denote with $\boldsymbol{x}^*(k)$ and $\boldsymbol{u}^*(k)$ the corresponding predicted sequences of state and input vectors:

$$\boldsymbol{x}^*(k) = \{x^*(0|k), \ldots, x^*(k_f - k|k)\} \tag{4.10a}$$
$$\boldsymbol{u}^*(k) = \{u^*(0|k), \ldots, u^*(k_f - 1 - k|k)\} \tag{4.10b}$$

where

$$x^*(0|k) = x(k) \tag{4.10c}$$
$$x^*(j+1|k) = f(x^*(j|k), u^*(j|k)) \tag{4.10d}$$
$$u^*(j|k) = g(\boldsymbol{v}^*_{N(k)}, j, k) \tag{4.10e}$$

The SBPC strategy is obtained by recursively solving (4.9), as described by the following pseudo-algorithm.

Algorithm 1 Nominal SBPC Strategy

1. At sampling instant k, measure the state $x(k)$ and solve the FHOCP (4.9). Let $\boldsymbol{v}^*_{N(k)}$ be the computed solution;
2. Apply to the plant the first element of the sequence $\boldsymbol{v}^*_{N(k)}$, i.e. the control vector $u(k) = u^*(0|k) = v^*(1)$;
3. Repeat the procedure from 1) at the next sampling period.

Algorithm 1 defines the following feedback control law:

$$u(k) = \mu(x(k)) := u^*(0|k), \tag{4.11}$$

and the resulting model of the closed-loop system is:

$$x(k+1) = f(x(k), \mu(x(k)) \tag{4.12}$$

Remark 4.2.1. *In the approach described so far, the number $N(k)$ of predicted inputs to be optimized decreases from $N(1) = \left\lceil \frac{k_f}{L} \right\rceil$ to $N(k_f - 1) = 1$, see Fig. 4.2. Another approach that can be used with little modifications is to keep a constant value of $N = N(1)$, and to reduce the number of blocked input values in each interval as k increases, up until the value $k = k_f - N(1)$ is reached, after which each predicted input vector is a free variable and their number shrinks at each k. This second strategy has the advantage to retain more degrees of freedom in the optimization as time approaches its final value.*

We conclude this section with a proposition on the recursive feasibility of (4.9) and convergence of the state of (4.12) to the terminal set.

Proposition 4.2.1. *Assume that the FHOCP* (4.9) *is feasible at time $k = 0$. Then, the FHOCP* (4.9) *is recursively feasible at all $k = 1, \ldots, k_f - 1$ and the state of the closed loop system* (4.12) *converges to the terminal set X_f at time k_f.*

Proof. Recursive feasibility is established by construction, since at any time $k + 1$ one can build a feasible sequence $\boldsymbol{v}_{N(k+1)}$ either by taking $\boldsymbol{v}_{N(k+1)} = \boldsymbol{v}^*_{N(k)}$, if $N(k+1) = N(k)$, or by taking $\boldsymbol{v}_{N(k+1)} = \{v^*(2), \ldots, v^*(N(k))\}$ (i.e. the tail of $\boldsymbol{v}^*_{N(k)}$), if $N(k+1) = N(k) - 1$.

Convergence to the terminal set is then achieved by considering that constraint (4.9g) is feasible at time $k = k_f - 1$. ■

Remark 4.2.2. *So far, we have disregarded any mismatch between the model $f(x, u)$ and the real plant, like the presence of model uncertainty and external disturbances. For this reason, we termed the SBPC approach of Algorithm 1 the "nominal" one. In the next section, we introduce a model of uncertainty, whose form is motivated again by the railway application and two possible variations of Algorithm 1 to deal with it, along with their guaranteed convergence properties. We term these variations the "relaxed" approaches, since they involve the use of suitable soft (i.e. relaxed) constraints to guarantee recursive feasibility.*

Remark 4.2.3. *Convergence to X_f does not necessarily imply forward invariance of such a set under the described control scheme (which is by the way not well defined for $k > k_f$). The capability to keep the state within the terminal set depends on how such a set is defined (e.g. it holds when X_f contains equilibrium points for the model $f(x, u)$) and in general it is not required by the considered problem setup. This automatically implies that we do not have to assume the existence of any terminal control law as usually done in standard NMPC formulations. On the other hand, in our motivating application the terminal set X_f actually corresponds to an equilibrium point (namely with zero speed, and position equal to the arrival station, see* (4.3)*), thus in this case nominal forward invariance is guaranteed for $k > k_f$.*

4.3 Relaxed SBPC Approaches: Algorithms and Properties

Following Remark 4.2.2, to model the system uncertainty and disturbances we consider an additive term $d(k)$ acting on the input vector, i.e.:

$$\tilde{u}(k) = u(k) + d(k) \tag{4.13}$$

where $\tilde{u}(k)$ is the disturbance-corrupted input provided to the plant. This model represents well all cases where plant uncertainty and exogenous disturbances can be translated into an effect similar to the control input (the so-called matched uncertainty). For example, in our train model (4.1) with straightforward manipulations, Eq.(4.13) can describe uncertainty in the train mass, drivetrain specs, track slope and curvature, as well as the discretization of $u^*(0|k)$ and/or misapplication by the human operator in a

driver assistance scenario (see Subsection 3.1.2).
We consider the following assumption on d:

Assumption 2. *The disturbance term d belongs to a compact set $\mathbb{D} \subset \mathbb{R}^m$ such that:*

$$\|d\| \leq \overline{d},\ \forall d \in \mathbb{D} \tag{4.14}$$

where $\overline{d} \in (0, +\infty)$.

This assumption holds in many practical cases and in the considered train application as well. We indicate the perturbed state trajectory due to the presence of d as:

$$\tilde{x}(k+1) = f(\tilde{x}(k), \tilde{u}(k)),\ k = 0, \ldots, k_f \tag{4.15}$$

where $\tilde{x}(0) = x(0)$. Now, referring to Proposition 4.2.1, the convergence guarantees achieved in the nominal case are a direct consequence of the recursive feasibility property, which can be easily lost in presence of the disturbance d, due to the deviation of perturbed trajectory from the nominal one. As commonly done in standard NMPC, to retain recursive feasibility, we therefore soften the constraints in the FHOCP. However, in general the use of soft constraints does not guarantee that, in closed-loop operation, the operational constraints are satisfied, or even that the constraint violation is uniformly decreasing as the worst-case disturbance bound $\overline{d}$ gets smaller. For simplicity and to be more specific, from now on let us restrict our analysis to the terminal state constraint in (4.5f), i.e. $x(k_f) \in X_f$. We do so without loss of generality, since the results and approaches below can be extended to any state constraint in the control problem. On the other hand, in our railway application the terminal state constraint is the most important one from the viewpoint of system performance. The other constraints (velocity limits) are always enforced for safety by modulating traction or by braking. Let us denote the distance between a point x and a set X as:

$$\Delta(x, X) = \min_{y \in X} \|x - y\|. \tag{4.16}$$

Then, we want to derive a modified SBPC strategy with softened terminal state constraint (to ensure recursive feasibility) that guarantees a property of the following form in closed loop:

$$\Delta(\tilde{x}(k_f), X_f) \leq \beta(\overline{d}),\ \beta \in \mathcal{K}. \tag{4.17}$$

That is, the distance between the terminal state and the terminal constraint is bounded by a value that decreases strictly to zero as $\overline{d} \to 0$. In order to obtain this property, we propose a relaxed SBPC approach using a two-step constraint softening procedure, described next.

4.3.1 Two-step Relaxed SBPC Strategy

At each time k we consider a strategy consisting of two optimization problems to be solved in sequence:

a) we compute the best (i.e. smallest) achievable distance between the terminal state and the terminal set, starting from the current perturbed state $\tilde{x}(k)$:

$$\underline{\gamma}(k) = \min_{\boldsymbol{v}_{N(k)},\gamma} \ \gamma \tag{4.18a}$$

subject to

$$u(j|k) = g(\boldsymbol{v}_{N(k)}, j, k),\ j = 0, \dots, k_f - k - 1 \tag{4.18b}$$
$$x(j+1|k) = f(x(j|k), u(j|k)),\ j = 0, \dots, k_f - k - 1 \tag{4.18c}$$
$$u(j|k) \in U,\ j = 0, \dots, k_f - k - 1 \tag{4.18d}$$
$$x(j|k) \in X,\ j = 1, \dots, k_f - k \tag{4.18e}$$
$$x(0|k) = \tilde{x}(k) \tag{4.18f}$$
$$\Delta(x(k_f - k|k), X_f) \leq \gamma \tag{4.18g}$$

b) we optimize the input sequence using the original cost function, and softening the terminal constraint by $\underline{\gamma}(k)$:

$$\min_{\boldsymbol{v}_{N(k)}} \ \sum_{j=0}^{k_f-k} \ell(x(j|k), u(j|k)) \tag{4.19a}$$

subject to

$$u(j|k) = g(\boldsymbol{v}_{N(k)}, j, k),\ j = 0, \dots, k_f - k - 1 \tag{4.19b}$$
$$x(j+1|k) = f(x(j|k), u(j|k)),\ j = 0, \dots, k_f - k - 1 \tag{4.19c}$$
$$u(j|k) \in U,\ j = 0, \dots, k_f - k - 1 \tag{4.19d}$$
$$x(j|k) \in X,\ j = 1, \dots, k_f - k \tag{4.19e}$$
$$x(0|k) = \tilde{x}(k) \tag{4.19f}$$
$$\Delta(x(k_f - k|k), X_f) \leq \underline{\gamma}(k) \tag{4.19g}$$

By construction, both problems are always feasible (with the caveat that state constraints are considered to be always feasible, as discussed above, otherwise the softening shall be applied to these constraints as well). We denote with $\boldsymbol{v}^r_{N(k)}$, $\boldsymbol{x}^r(k)$ and $\boldsymbol{u}^r(k)$ the optimized sequences of decision variables, state and inputs resulting from the solution of (4.19). The sequences $\boldsymbol{x}^r(k)$ and $\boldsymbol{u}^r(k)$ are computed as:

$$\begin{aligned}
\boldsymbol{x}^r(k) &= \{x^r(0|k), \ldots, x^r(k_f - k|k)\} && \text{(4.20a)}\\
\boldsymbol{u}^r(k) &= \{u^r(0|k), \ldots, u^r(k_f - 1 - k|k)\} && \text{(4.20b)}\\
&\text{where} \\
x^r(0|k) &= \tilde{x}(k) && \text{(4.20c)}\\
x^r(j+1|k) &= f(x^r(j|k), u^r(j|k)) && \text{(4.20d)}\\
u^r(j|k) &= g(\boldsymbol{v}^r_{N(k)}, j, k) && \text{(4.20e)}
\end{aligned}$$

Finally, we note that the disturbance is not explicitly considered in problems (4.18)-(4.19), which still employ the nominal model for the predictions.
The resulting relaxed SBPC strategy is implemented by the following pseudo-algorithm.

Algorithm 2 Two-stage Relaxed SBPC Strategy

1. At sampling instant k, measure the state $\tilde{x}(k)$ and solve in sequence the optimization problems (4.18)-(4.19). Let $\boldsymbol{v}^r_{N(k)}$ be the computed solution;
2. Apply to the plant the first element of the sequence $\boldsymbol{v}^r_{N(k)}$, i.e. the control vector $u(k) = u^r(0|k) = v^r(1)$;
3. Repeat the procedure from (1) at the next sampling period.

Algorithm 2 defines the following feedback control law:

$$u(k) = \mu^r(\tilde{x}(k)) := u^r(0|k), \tag{4.21}$$

and the resulting closed-loop dynamics are given by:

$$\tilde{x}(k+1) = f(\tilde{x}(k), \mu^r(\tilde{x}(k)) + d(k)). \tag{4.22}$$

The next result shows that the closed-loop system (4.22) enjoys a uniformly bounded accuracy property of the form (4.17), provided that the relaxed SBPC problem (4.19) is feasible at $k = 0$.

Theorem 4.3.1. *Let Assumptions 1 and 2 hold and let the FHOCP* (4.19) *be feasible at time* $k = 0$*. Then, the terminal state* $\tilde{x}(k_f)$ *of system* (4.22) *enjoys property* (4.17) *with*

$$\Delta(\tilde{x}(k_f), X_f) \leq \beta(\overline{d}) = \sum_{k=0}^{k_f-1} \beta_{k_f-k-1}(\overline{d}) \tag{4.23}$$

where

$$\begin{array}{rcl} \beta_0(\overline{d}) & = & a_u(\overline{d}) \\ \beta_k(\overline{d}) & = & a_u(\overline{d}) + a_x(\beta_{k-1}(\overline{d})),\ k = 1, \ldots, k_f - 1 \end{array} \tag{4.24}$$

Proof. The proof is by induction. Start at $k = 0$ and consider the relaxed optimized sequences $\boldsymbol{x}^r(k),\ \boldsymbol{u}^r(k)$ obtained by solving problem (4.19). We first evaluate the worst-case perturbation induced by the disturbance with respect to the open-loop state trajectory $\boldsymbol{x}^r(k)$. For a sequence of disturbances $d(k),\ k = 0, \ldots, k_f$, the corresponding open-loop input and state trajectories are:

$$\begin{array}{l} \tilde{u}(k) = u^r(k) + d(k),\ j = 0, \ldots, k_f - k - 1 \\ \tilde{x}(0|k) = x^r(0|k) \\ \tilde{x}(k+1) = f(\tilde{x}(k), \tilde{u}(k)),\ k = 1, \ldots, k_f \end{array} \tag{4.25}$$

From (4.6) we have:

$$\begin{array}{l} \|\tilde{x}(1) - x^r(1|0)\| = \|f(\tilde{x}(0), \tilde{u}(0)) - f(x(0), u^r(0|0))\| \leq \\ a_u\left(\|\tilde{u}(0) - u^r(0|0)\|\right) \leq a_u\left(\overline{d}\right) = \beta_0\left(\overline{d}\right) \end{array}$$

Consider now the perturbation 2-steps ahead:

$$\begin{array}{l} \|\tilde{x}(2) - x^r(2|0)\| = \\ \|f(\tilde{x}(1), \tilde{u}(1)) - f(x^r(1|0), u^r(1|0))\| = \\ \|f(\tilde{x}(1), \tilde{u}(1)) - f(\tilde{x}(1), u^r(1|0)) + \\ f(\tilde{x}(1), u^r(1|0)) - f(x^r(1|0), u^r(1|0))\| \leq \\ a_u\left(\overline{d}\right) + a_x\left(\|\tilde{x}(1) - x^r(1|0)\|\right) \leq \\ a_u\left(\overline{d}\right) + a_x\left(\beta_0\left(\overline{d}\right)\right) = \beta_1\left(\overline{d}\right). \end{array}$$

By iterating up until the second last time step we obtain:

$$\|\tilde{x}(k_f) - x^r(k_f|0)\| \leq \beta_{k_f-1}\left(\overline{d}\right), \tag{4.26}$$

where $\beta_{k_f-1} \in \mathcal{K}$ since it is given by compositions and summations of class-$\mathcal{K}$ functions. Since the FHOCP (4.19) is feasible, we have $x^r(k_f|0) \in X_f$ and thus:

$$\begin{array}{rcl} \Delta(\tilde{x}(k_f), X_f) & \leq & \|\tilde{x}(k_f) - x^r(k_f|0)\| + \Delta(x^r(k_f|0), X_f) \\ & \leq & \beta_{k_f-1}(\overline{d}). \end{array} \tag{4.27}$$

Now consider $k = 1$ and the FHOCP (4.18). If the optimizer is initialized with blocked control moves $\boldsymbol{v}_{N(1)}$ such that the tail of the previous optimal sequence $\boldsymbol{u}^r(0)$ is applied to the system, the corresponding minimum γ in

(4.18) results to be upper bounded by $\beta_{k_f-1}(\overline{d})$, in virtue of (4.27). The optimal value $\underline{\gamma}(k)$ is therefore not larger than this bound as well:

$$\underline{\gamma}(1) \leq \beta_{k_f-1}(\overline{d}). \tag{4.28}$$

Now take the optimal sequences $\boldsymbol{x}^r(1)$ and $\boldsymbol{u}^r(1)$ computed by solving the FHOCP (4.19). By applying the same reasoning as we did for $k = 0$, we have (compare with (4.26)):

$$\|\tilde{x}(k_f) - x^r(k_f|1)\| \leq \beta_{k_f-2}(\overline{d}). \tag{4.29}$$

Moreover, equation (4.28) implies that the solution of (4.19) satisfies the following inequality:

$$\Delta(x^r(k_f|1), X_f) \leq \underline{\gamma}(k). \tag{4.30}$$

From (4.28)-(4.30) we have:

$$\Delta(\tilde{x}(k_f), X_f) \leq \|\tilde{x}(k_f) - x^r(k_f|1)\| + \Delta(x^r(k_f|1), X_f) \leq$$
$$\beta_{k_f-2}(\overline{d}) + \beta_{k_f-1}(\overline{d}) = \sum_{k=0}^{1} \beta_{k_f-k-1}(\overline{d}).$$

By applying recursively the same arguments, the bound (4.23) is obtained. ■

Theorem 4.3.1 indicates that the worst-case distance between the terminal state and the terminal set is bounded by a value which is zero for $\overline{d} = 0$ and increases strictly with the disturbance bound. In the train application, this means that, for example, the worst-case accuracy degradation in reaching the terminal station due to a discretization of the input, as done in the driver assistance mode, is proportional to the largest employed quantization interval of the input handle. This result provides a theoretical justification to the proposed two-step relaxed SBPC approach. The bound (4.23) is conservative, since it essentially results from the accumulation of worst-case perturbations induced by the disturbance on the open-loop trajectories computed at each k. As we show in our simulation results, in practice the resulting closed-loop performance are usually very close to those of the nominal case, thanks to recursive optimization in the feedback control loop.

4.3.2 Multi-objective Relaxed SBPC Strategy

As an alternative to the two-step approach described above, one can also consider a multi-objective minimization:

$$\min_{\boldsymbol{v}_{N(k)},\gamma} \sum_{j=0}^{k_f-k} \ell(x(j|k), u(j|k)) + \omega\gamma \tag{4.31a}$$

subject to

$$u(j|k) = g(\boldsymbol{v}_{N(k)}, j, k),\ j = 0, \ldots, k_f - k - 1 \tag{4.31b}$$
$$x(j+1|k) = f(x(j|k), u(j|k)),\ j = 0, \ldots, k_f - k - 1 \tag{4.31c}$$
$$u(j|k) \in U,\ j = 0, \ldots, k_f - k - 1 \tag{4.31d}$$
$$x(j|k) \in X,\ j = 1, \ldots, k_f - k \tag{4.31e}$$
$$x(0|k) = \tilde{x}(k) \tag{4.31f}$$
$$\Delta(x(k_f - k|k), X_f) \leq \gamma \tag{4.31g}$$

where ω is a positive weight on the scalar γ. Problem (4.31) can be solved in Algorithm (2) in place of problems (4.18)-(4.19). In this case, the advantage is that a trade-off between constraint relaxation and performance can be set by tuning ω. Regarding the guaranteed bounds on constraint violation, with arguments similar to those employed in [23] one can under a continuity assumption on ℓ show that, at each $k \in [0, k_f - 1]$, for any $\varepsilon > 0$ there exists a finite value of ω such that the distance between the terminal state and the terminal set is smaller than $\gamma(k_f - k - 1)(\overline{d}) + \varepsilon$. Thus, with large-enough ω, one can recover the behavior obtained with the two-step relaxed SBPC approach. The theoretical derivation is omitted for the sake of brevity, as it is a rather minor extension of the results of [23].

4.4 Simulation Results

We tested the proposed strategies in realistic simulations with real train data provided by Alstom for a section of the Amsterdam metro rail, in particular the track between Rokin and Central Station. The results were also verified on Alstom based train tool CITHEL, which is useful to get a realistic idea of the energy expenditure by the developed SBPC strategies. CITHEL is able to perform a combination of kinematic, electric and thermal calculations all linked together, while considering realistic losses incurred due to the electrical components of the train. The parametric values of the train used in the controller are (see (4.1)-(4.2)) $M = 142403\,\text{kg}$, $M_s = 131403\,\text{kg}$, $A = 3975.9\,\text{N}$, $B = 24.36\,\text{Nsm}^{-1}$ and $C = 4.38\,\text{Nsm}^{-2}$,

while the maximum traction and braking forces allowed for this particular train are in the form of look up tables (see Fig. 4.3). These forces are of the form $F_T(x(k), u(k)) = F_{T_{\max}}(x_2(k))u(k)$, and $F_B(x(k), u(k)) = F_{B_{\max}}(x_2(k))u(k)$. The input variable is constrained in the set $[-1,\ 1]$. The considered track has zero curvature, slopes as plotted in Fig.4.4, and velocity limits reported in Fig. 4.7. The train has to reach the next station at $x_f = 1106\,\text{m}$ in $t_f = 76\,\text{s}$. The sampling time is $T_s = 0.38\,\text{s}$, resulting in $k_f = 200$. The results have been obtained using Matlab® `fmincon` and a laptop equipped with Intel® Core i7-6700Hq processor at 2.6 GHz and 8 GB of memory. All the functions were implemented in Matlab®.

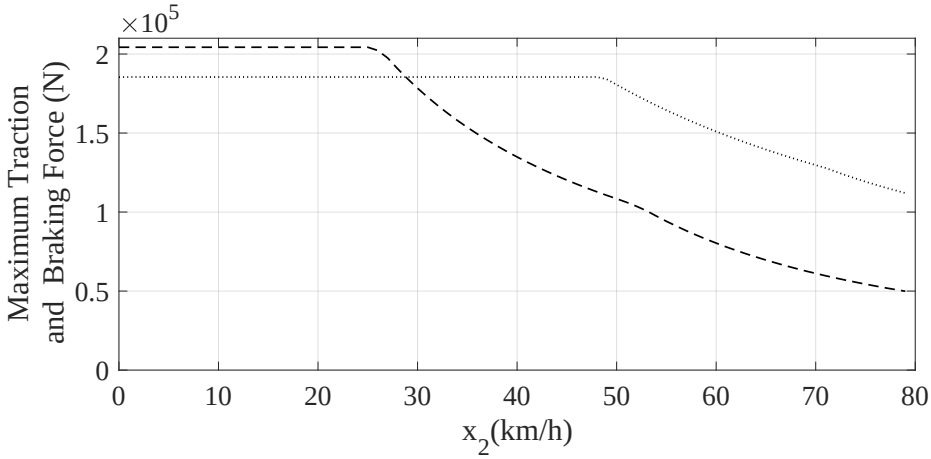

Figure 4.3: *Maximum traction force $F_{T_{\max}}$(dashed) and braking force $F_{B_{\max}}$ (dotted) allowed for the train considered in the simulation.*

Table 4.1: *Comparison results with different values of L for nominal SBPC strategy*

	L	Comp.Time per step (s)	Max. Comp.Time per step (s)	Comp. Time (s)	E_{T} (KWH)	t_f (s)
	1	24.02	70.2	5285	5.8	76
Nominal	20	3.32	38.4727	731	5.9497	76
SBPC strategy	45	0.78	23.0440	172	10.3	76

Firstly, we present a comparison of the results obtained with and without the use of move-blocking. The obtained input and velocity profiles for different values of L in the nominal case have been presented in Fig. 4.5-4.6 respectively. By fair comparisons, we show the computational advantage obtained due to the use of move-blocking as compared to no blocking. While without the use of move-blocking (see Table 4.1), the simulation finishes in $5285\,\text{s}$, taking an average of $24.02\,\text{s}$ and a maximum of $70.2\,\text{s}$

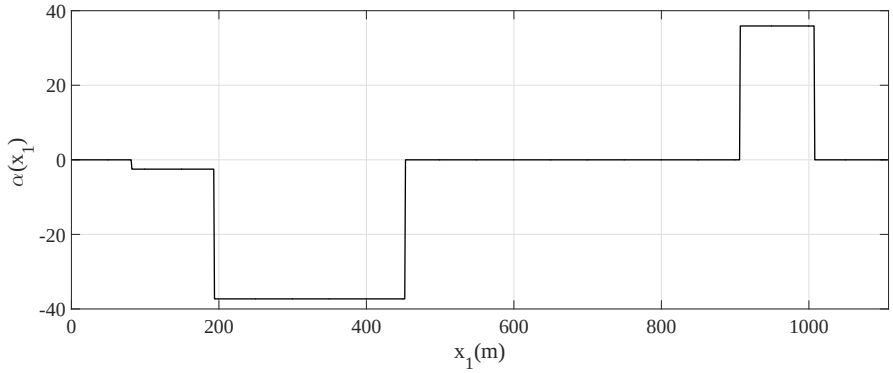

Figure 4.4: *Slopes of the Amsterdam metro track segment considered in the simulation. The units of the slopes are in per mille.*

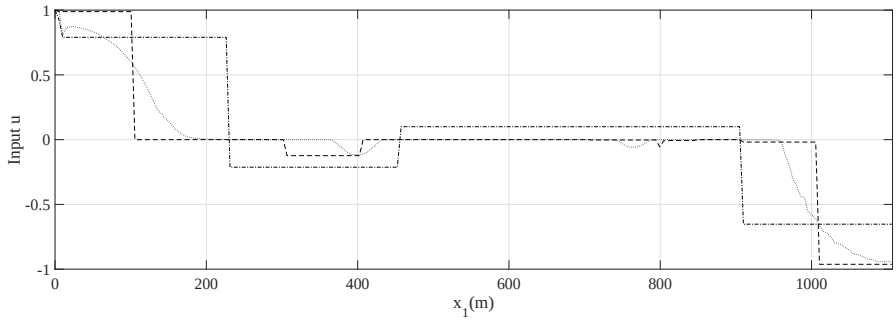

Figure 4.5: *Simulation results. Input handle as a function of the train position obtained with different values of L for nominal SBPC strategy:* $L = 1$ *(dotted line),* $L = 20$ *(dashed),* $L = 45$ *(dash-dot).*

per optimization step, with the use of move-blocking techniques, it reduces considerably (see Table 4.1). For example, when using move-blocking with $L = 20$, in the nominal case the average computational time per optimization step reduces to $3.32\,\mathrm{s}$. Another observation is the effect of blocking on the control performance. From Table 4.1, it is clear that with an increased number of blocked control values, with for example $L = 45$, there is a degradation in the performance and the traction energy consumption E_{T} increases considerably. Hence a trade-off between the two needs to be maintained. In our case, this was achieved for $L = 20$.

Secondly, we compare a nominal situation, where Algorithm 1 is applied and no model uncertainty is present, with a case where we employ Algorithm 2 (both the two-stage approach and the multi-objective optimiza-

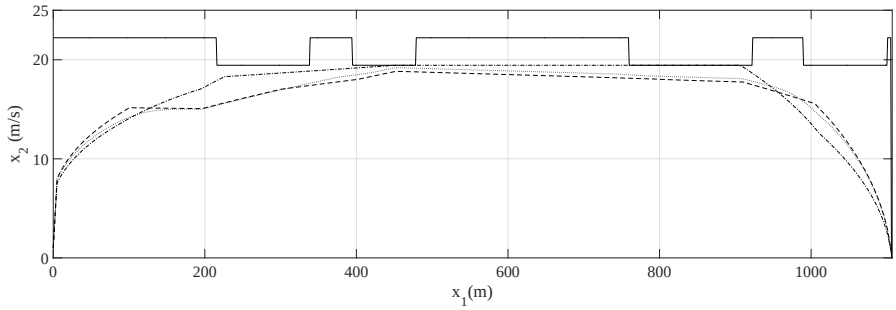

Figure 4.6: *Simulation results. Velocity profiles as a function of the train position obtained with different values of L in case of nominal SBPC strategies: $L = 1$ (dotted line), $L = 20$ (dashed), $L = 45$ (dash-dot). Velocity limits are denoted with a solid line.*

Table 4.2: *Comparison results with different strategies tested in Alstom based tool CITHEL*

	L	E_{T} (KWH)	t_f (s)
All-out solution	-	13.19	73
Genetic algorithm based Eco-drive	-	9.05	77
SBPC strategy	20	5.9497	78

tion variant) in presence of random parameter uncertainty ($\pm 10\%$ of each model parameter) and input variable discretization, considering a discrete set of operating modes as described in SubSection 3.1.2(driver assistance scenario). In particular, we compute the actual input as the nearest neighbor, in the set $\{-1, 0, 0.5.0.75, 1\}$, to the one given by the SBPC strategy in case when the train is not cruising. For the multi-objective approach, we set $\omega = 3505$ (see (4.31)).
The obtained velocity profiles are presented in Fig. 4.7. From the plots, it is evident that in order to save energy, after accelerating to a certain velocity, the train mostly coasts also taking advantage of the negative slopes. All the velocity constraints are always satisfied. Regarding the obtained final distance between the terminal state and the target one at $t = t_f$, in the presence of uncertainty this is smaller than 1 m for both the 2-stage approach and the multi-objective one. This result is perfectly compatible with the desired performance in this application. Fig. 4.7 presents also the "all-out" solution, which achieves the shortest arrival time compatible with all the constraints. This corresponds to $t_f = 72$ s.

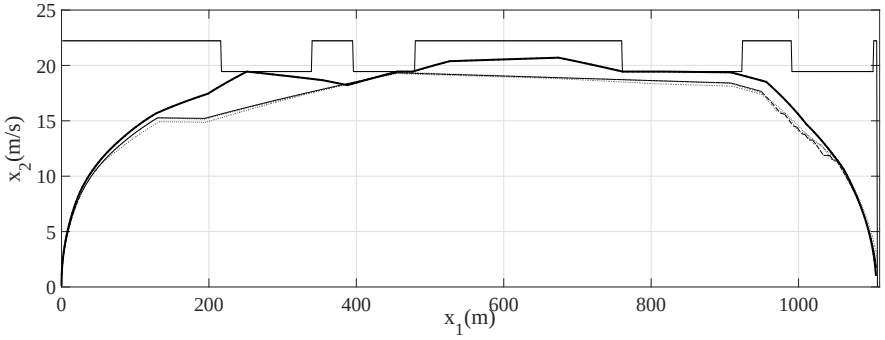

Figure 4.7: *Simulation results. Velocity profiles as a function of the train position obtained with different SBPC strategies: nominal (dotted line), two-step relaxed (dashed), multi-objective (dash-dot). All these approaches share the same final time of $t_f = 76\,s$. The "all-out" solution ($t_f = 72\,s$) is shown with a thick solid line, and velocity limits with a thin solid line.*

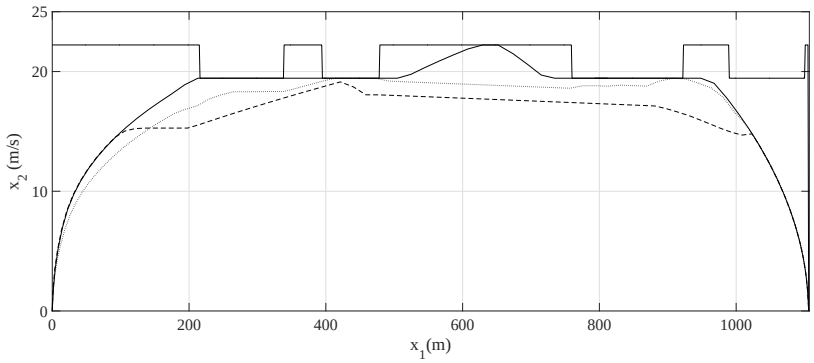

Figure 4.8: *Simulation results. Velocity profiles as a function of the train position obtained with Alstom based CITHEL tool: genetic algorithm based eco-drive (dotted line), SBPC strategy (dashed). All these approaches share the same final time of $t_f = 76\,s$ with $L = 20$ used in SBPC strategy. The "all-out" solution ($t_f = 73\,s$) is shown with a thick solid line, and velocity limits with a thin solid line.*

Finally, the results were tested on Alstom based tool CITHEL and also compared with their existing eco-drive strategy based on Genetic algorithm. The results are presented in Table.4.2 and the obtained velocity profiles in Fig.4.8. Though, the SBPC strategies arrive with a delay of 2 s at the prescribed station, the energy consumption is considerably lower as compared

to the existing Genetic-algorithm based eco-drive approach. One reason for this energy saving is due to the maximum use of coasting mode both in the case of negative as well as zero slopes, resulting in increased energy efficiency.

4.5 Conclusion

We proposed a predictive control approach to solve problems where a finite terminal time and corresponding state constraint set are imposed. The approach features a shrinking horizon and exploits move blocking to reduce the computational burden. We derived convergence guarantees in both nominal conditions and under uncertainty, and showcased the technique in realistic simulations pertaining to a motivating industrial application in train control. All the strategies were tested on official Alstom based tool CITHEL and proved to provide better results in terms of energy efficiency as compared to the existing benchmarks. Extensions of the approach to more general input parameterizations are presented in Chapter 5.

CHAPTER 5

Shrinking Horizon Parametrized Predictive Control Strategy

In this chapter, a new MPC approach for the efficient operation of trains is presented (see [24]). This strategy has been developed specifically for the case of DAS (see Subsection 3.1.2 for details), where the control input (usually the traction/braking force applied to the train) is constrained to belong to a set of discrete values or operating modes, which would naturally result in a mixed-integer nonlinear program to be solved at each sampling instant. To cope with this problem, the formulation proposed features an input parametrization strategy that yields a continuous optimization program. Moreover, a shrinking horizon is adopted. The resulting approach has been named Shrinking Horizon Parametrized Predictive Control (SPPC). As in Chapter 4, both a nominal approach and two relaxed ones, where state constraints are softened to retain recursive feasibility in case of model uncertainty are presented.

5.1 Train Optimal Control Problem

Consider an electric train controlled by a digital control unit. In this strategy, we consider space as the independent variable, while time will be one of the system's states. Thus, we denote with $k \in \mathbb{Z}$ the discrete space variable, and with D_s the sampling distance, so that the actual distance along the track at each sampling instant is equal to kD_s. From the point of view of practical implementation, we assume that the controller has a high enough sampling rate, such that the discrete space instants can be met with high accuracy. For example, with a train speed of about $100\,\mathrm{ms}^{-1}$, a space discretization of 5 m, and a controller sampling rate of 1 kHz the maximum space delay in actuating the input would be equal to 0.1 m. i.e. 2% of the sampling distance. We denote with $x(k) = [x_1(k),\, x_2(k)]^T$ the state of the train, where x_1 is its travel time and x_2 the train speed, and with $u(k) \in [-1, 1]$ a normalized traction force, where $u(k) = 1$ corresponds to the maximum applicable traction and $u(k) = -1$ to the maximum braking. The input u is the available control variable. The input u is the available control variable. The train has to move from one station at time $x_1 = 0$ and reach the next one at time $x_1 = x_f$, covering the corresponding distance s_f. In state space modeling , the prescribed arrival time t_f (see Eq. 2.6) and the maximum allowed velocity limit $v_{\max}(k)$ (see Eq. 2.5) have been renamed as $t_f = x_f$ and $v_{\max}(k) = \overline{x}_2(k)$ to link them to the states they are representing. For a given pair of initial and final stations, the track features (slopes, curvature) are known in advance. Thus, in nominal conditions (i.e. with rated values of the train parameters, like its mass and the specifications of the powertrain and braking systems), according to Newton's laws and using the forward Euler discretization method, the equations of motion of a reasonably accurate model of this system read:

$$\begin{aligned} x_1(k+1) &= x_1(k) + \tfrac{D_s}{x_2(k)} \\ x_2(k+1) &= x_2(k) + D_s \left(\tfrac{F_T(x(k),u(k)) - F_B(x(k),u(k)) - F_R(k,x(k))}{M x_2(k)} \right) \end{aligned} \tag{5.1}$$

The resistive force $F_R(k, x)$ is also nonlinear, and it is the sum of a first term $R_v(x_2)$, accounting for resistance due to the velocity, and a second term $R_g(k)$, accounting for the effects of slopes and track curvature:

$$\begin{aligned} F_R(k, x) &= R_v(x_2) + R_g(k) \\ R_v(x_2) &= A + Bx_2 + Cx_2^2 \\ R_g(k) &= M_s \left(g \tan(\alpha(k)) + \frac{\lambda_t}{r_c(k)} \right) \end{aligned} \tag{5.2}$$

The parametric symbols have already been defined in Subsection 2.1.1 (see Tables 2.1 and 2.2 for more details). As already discussed in Subsection 2.1.1, besides the prescribed arrival time x_f and position s_f, there are additional state constraints that must be satisfied. These pertain to the limit on the maximum allowed velocity, $\overline{x}_2(k)$, which depends on the position k, since a different velocity limit is imposed for safety by the regulating authority according to the track features at each position. Overall, by defining the terminal space step as $k_f \doteq \lfloor s_f/D_s \rfloor$ (where $\lfloor \cdot \rfloor$ denotes the flooring operation to the closest integer), the state constraints read:

$$\begin{array}{ll} x(0) & = [0,\ 0]^T \\ x(k_f) & = [x_f,\ 0]^T \\ x_2(k) & \geq 0,\ \ k = 0, \ldots, k_f \\ x_2(k) & \leq \overline{x}_2(k),\ \ k = 0, \ldots, k_f \end{array} \tag{5.3}$$

The control objective is to maximize the energy efficiency of the train while satisfying the constraints above. To translate this goal in mathematical terms, different possible cost functions can be considered. In our case, we consider the discretized integral of the absolute value of the traction power over space (with a constant scaling factor D_s^{-1}):

$$J = \sum_{k=0}^{k_f} \left| F_T(x(k), u(k)) \right|. \tag{5.4}$$

This choice tends to produce controllers that minimize the traction energy injected into the system.

As already pointed out, the input variable is also constrained in the interval $u \in [-1, 1]$. However, since this strategy has been specially designed keeping in mind the DAS scenario, our input is further constrained to belong to only a smaller set of possible values which can be delivered by the controller, in order to facilitate the human-machine interaction. In particular, in this scenario the input constraints are further tightened according to four possible operating modes prescribed by our industrial partner i.e. $u \in \{1, 0, u_{CR}, -1\}$, where u_{CR} identifies the cruising mode (see Subsection 3.1.2 for details). Finally, a further feature of this application is a relatively small sampling space D_s with respect to the imposed overall space horizon s_f, resulting in a rather large number of sampling periods in the interval $[0,\ s_f]$, typically from several hundreds to a few thousands.

5.1.1 Problem Abstraction

The control problem described above can be cast in a rather standard form:

$$\min_{\boldsymbol{u}} \sum_{k=0}^{k_f} \ell(x(k), u(k)) \tag{5.5a}$$

subject to

$$x(k+1) = f(x(k), u(k)) \tag{5.5b}$$
$$u(k) \in U,\ k = 0, \ldots, k_f - 1 \tag{5.5c}$$
$$x(k) \in X,\ k = 1, \ldots, k_f \tag{5.5d}$$
$$x(0) = x_0 \tag{5.5e}$$
$$x(k_f) \in X_f \tag{5.5f}$$

where $x \in \mathbb{X} \subset \mathbb{R}^n$ is the system state, x_0 is the initial condition, $u \in \mathbb{U} \subset \mathbb{R}^m$ is the input, $f(x,u) : \mathbb{X} \times \mathbb{U} \to \mathbb{X}$ is a known nonlinear mapping representing the system dynamics, and $\ell(x,u) : \mathbb{X} \times \mathbb{U} \to \mathbb{R}$ is a stage cost function defined by the designer according to the control objective. The symbol $\boldsymbol{u} = \{u(0), \ldots, u(k_f - 1)\} \in \mathbb{R}^{m\,k_f}$ represents the sequence of current and future control moves to be applied to the plant. The sets $X \subset \mathbb{X}$ and $U \subset \mathbb{U}$ represent the state and input constraints (including the discrete set of allowed inputs or input modes as described above), and the set $X_f \subset \mathbb{X}$ the terminal state constraints, which include a terminal equality constraint as a special case. Furthermore, X and U is assumed to be compact, as well as the terminal constraint set X_f.
We recall that a continuous function $a : \mathbb{R}^+ \to \mathbb{R}^+$ is a $\mathcal{K}$-function ($a \in \mathcal{K}$) if it is strictly increasing and $a(0) = 0$. Throughout this chapter, we consider the following continuity assumption on the system model f.

Assumption 3. *The function f enjoys the following lipchitz continuity properties:*

$$\begin{aligned} \|f(x^1, u) - f(x^2, u)\| &\leq a_x\left(\|x^1 - x^2\|\right),\ \forall x^1, x^2 \in \mathbb{X}, u \in \mathbb{U} \\ \|f(x, u^1) - f(x, u^2)\| &\leq a_u\left(\|u^1 - u^2\|\right),\ \forall u^1, u^2 \in \mathbb{U}, x \in \mathbb{X} \end{aligned} \tag{5.6}$$

where $a_x,\ a_u \in \mathcal{K}$.

5.2 Nominal Shrinking Horizon Parametrized Predictive Control

To solve problem (5.5), we again resort to Nonlinear Model Predictive Control (NMPC), however with two particular differences with respect to the standard formulation:

- First, since in our problem the terminal space s_f is fixed, the resulting strategy features a shrinking horizon rather than a receding one. Indeed, here the goal is to make the state converge to the terminal set in the required finite time, and not asymptotically as usually guaranteed by a receding horizon strategy;
- Second, we adopt an input-parametrization strategy (see e.g. [22]) to reduce the computational burden required by the feedback controller as well as to enforce the discrete constraints on the input while retaining a continuous optimization program, instead of the mixed-integer one that would result from direct optimization of the input.

5.2.1 Parametrization Setup

We adopt a parametrization of the control input that allows us to naturally incorporate the presence of the discrete (switched) driving modes described. The main idea is to first split the track (i.e. the whole prediction horizon from 0 to k_f) into sectors. Then, in each sector, we pre-define a switching sequence of the four driving modes, and we optimize over the switching (space) instants of the sequence. In this way, we retain a continuous vector of optimization variables, thus improving the computational efficiency, while still providing the controller with enough degrees-of-freedom to optimize the predicted system behavior. Specifically, we consider a number $s_n \in \mathbb{N}$ of sectors, each one with length Γ_i, such that

$$\sum_{i=1}^{s_n} \Gamma_i = s_f. \tag{5.7}$$

The choice of sectors is carried out by considering characteristics such as the presence of constant velocity limits and the resistance force due to the slopes and track curvature $R_g(k)$, which are known in advance, see Fig. 5.1 for an example. Regarding the switching sequence ("driving style") adopted in each sector, denoted with $\boldsymbol{u_{d_i}}$, we choose the following:

$$\begin{array}{rcl} \boldsymbol{u_{d_i}} & = & \{ \quad u_{(i,1)}, \quad u_{(i,2)}, \quad u_{(i,3)}, \quad u_{(i,4)} \quad \} \\ & = & \{ \quad 1, \quad u_{CR}, \quad 0, \quad -1 \quad \}, \quad \forall i \in [1, \ldots, s_n] \end{array} \tag{5.8}$$

where $u_{(i,\ell)}$ is the input issued in the $\ell-$th phase of the $i-$th sector (with $\ell \in \{1, 2, 3, 4\}$) and u_{CR} identifies the cruising mode (see Subsection 3.1.2 for details), i.e. where the actual input $u(k)$ is computed by a cruise control system in order to maintain a constant speed. The chosen switching

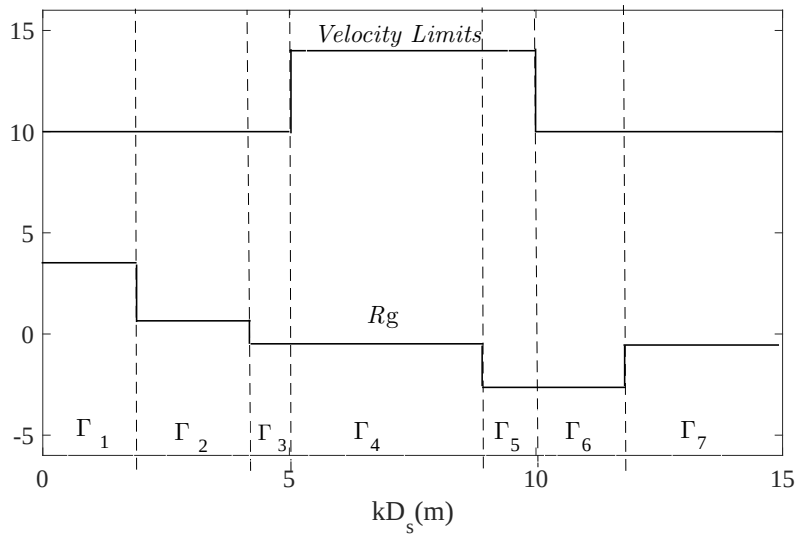

Figure 5.1: *Example of sector choice for a track with $s_f = 15$ and s_n= 7. Possible sectors based on similar characteristics such as velocity limits and R_g values are depicted.*

sequence is such that in each sector, theoretically, the controller can choose to have a traction phase, a cruising one, a coasting one, and finally a braking phase. Thus, the maximum number of operating modes that can be set in the whole optimization horizon is equal to $4\,s_n$. As anticipated, our optimization variables will be the switching instants, or more precisely the duration of each phase within each switching sequence. We denote these quantities with $\delta s_{(i,\ell)}$, such that:

$$\begin{aligned} &0 \leq \delta s_{(i,\ell)} \leq \Gamma_i \\ &\sum_{\ell=1}^{4} \delta s_{(i,\ell)} = \Gamma_i. \end{aligned} \tag{5.9}$$

As an example, values of $(s_{(i,1)}, s_{(i,2)}, s_{(i,3)}, s_{(i,4)})$ equal to $(0, 0, \Gamma_i, 0)$ correspond to the train coasting throughout sector i, and so on.

Remark 5.2.1. *The presented parametrization provides the controller with enough degrees of freedom to choose a single mode or multiple modes of operation in each sector, in order to compensate the presence of uncertainty and to adapt to the track features and constraints. Additionally, the constraint on prescribed arrival position needs to be satisfied: this is done implicitly by imposing* (5.9) *for each sector, which implies* (5.7)*.*

We are now in position to introduce the optimal control problem to be solved at each time step in our shrinking horizon approach and the resulting SPPC approach presented next.

5.2.2 Shrinking Horizon Parametrized Predictive Control (SPPC)

We start by defining the optimization variables available at each step k. The set of indexes identifying the current and future sectors, from the current position kD_s until the end of the track s_f, is given by:

$$\{i : \underline{i}(k) + 1 \leq i \leq s_n\}, \tag{5.10}$$

where

$$\underline{i}(k) \doteq \begin{cases} \max\limits_{\bar{i} \geq 1} \bar{i} \;\; \text{s.t.} \sum\limits_{i=1}^{\bar{i}} \Gamma_i < kD_s, & \text{if } \; \Gamma_1 < kD_s \\ 0, & \text{otherwise} \end{cases}$$

Then, the number $N(k)$ of free variables to be computed corresponds to the number of remaining sectors, equal to $(s_n - \underline{i}(k))$, times the number of modes in each sector, i.e. 4 in our case. Therefore, we have $N(k) = 4(s_n - \underline{i}(k))$. We denote the vector of optimization variables with

$$\boldsymbol{v}_{N(k)} \doteq \{\delta s_{(\underline{i}(k)+1,1)}, \ldots, \delta s_{(\underline{i}(k)+1,4)}, \ldots, \delta s_{(s_n,4)}\}^T \in \mathbb{R}^{N(k)}. \tag{5.11}$$

Let us indicate with $u(j|k)$ the input vector at each space sample $k+j$ predicted at step k. Considering the parametrization described in Subsection 5.2.1, we can define the function $g(\boldsymbol{v}_{N(k)}, j, k)$ that links, at each step k and for each $j = 0, \ldots, k_f - k - 1$, the optimization variables $\boldsymbol{v}_{N(k)}$ with the predicted input $u(j|k)$:

$$u(j|k) = g(\boldsymbol{v}_{N(k)}, j, k) \doteq u_{(\hat{i}(j,k), \hat{\ell}(\boldsymbol{v}_{N(k)}, j, k))}, \tag{5.12}$$

where (compare with (5.8)):

$$\begin{aligned} \hat{i}(j,k) \doteq \; & \min_{\bar{i}=1,\ldots,s_n} \bar{i} \\ & \text{s.t.} \\ & \sum_{i=1}^{\bar{i}} \Gamma_i \geq (k+j)D_s \end{aligned}$$

and

$$\begin{aligned} \hat{\ell}(\boldsymbol{v}_{N(k)}, j, k) \doteq \; & \min_{\bar{\ell}=1,\ldots,4} \bar{\ell} \\ & \text{s.t.} \\ & \sum_{i=1}^{\hat{i}(j,k)} \Gamma_i + \sum_{\ell=1}^{\bar{\ell}} \delta s_{(\hat{i}(j,k),\ell)} \geq (k+j)D_s. \end{aligned}$$

Note that the evaluation of (5.12) is very efficient, since it just amounts to finding, for each space sample $k+j$, the indexes of the corresponding sector and phase and then to apply the corresponding pre-defined driving mode from (5.8). Finally, let us denote with $x(j|k)$, $j = 0, ..., k_f - k$ the state vectors predicted at space sample $k+j$ starting from the one at step k. At each step $k \in [0,\ k_f - 1]$, we formulate the following FHOCP:

$$\min_{\boldsymbol{v}_{N(k)}} \sum_{j=0}^{k_f-k} \ell(x(j|k), u(j|k)) \tag{5.13a}$$

subject to

$$u(j|k) = g(\boldsymbol{v}, \boldsymbol{v}_{N(k)}, j, k),\ j = 0, \ldots, k_f - k - 1 \tag{5.13b}$$
$$x(j+1|k) = f(x(j|k), u(j|k)),\ j = 0, \ldots, k_f - k - 1 \tag{5.13c}$$
$$u(j|k) \in U,\ j = 0, \ldots, k_f - k - 1 \tag{5.13d}$$
$$x(j|k) \in X,\ j = 1, \ldots, k_f - k \tag{5.13e}$$
$$x(0|k) = x(k) \tag{5.13f}$$
$$\boldsymbol{A}(k)\boldsymbol{v}_{N(k)} \leq b(k) \tag{5.13g}$$
$$x(k_f - k|k) \in X_f \tag{5.13h}$$

Where the matrices $\boldsymbol{A}(k)$, $b(k)$ in (5.13g) are built to enforce the constraints (5.9). We denote with $\boldsymbol{v}^*_{N(k)} = \{\delta s^*_{(i(k)+1,1)}, \ldots, \delta s^*_{(s_n,4)}\}^T$ a solution (in general only locally optimal) of (5.13). Moreover, we denote with $\boldsymbol{x}^*(k)$ and $\boldsymbol{u}^*(k)$ the corresponding predicted sequences of state and input vectors:

$$\boldsymbol{x}^*(k) = \{x^*(0|k), \ldots, x^*(k_f - k|k)\} \tag{5.14a}$$
$$\boldsymbol{u}^*(k) = \{u^*(0|k), \ldots, u^*(k_f - 1 - k|k)\} \tag{5.14b}$$

where

$$x^*(0|k) = x(k) \tag{5.14c}$$
$$x^*(j+1|k) = f(x^*(j|k), u^*(j|k)) \tag{5.14d}$$
$$u^*(j|k) = g(\boldsymbol{v}^*_{N(k)}, j, k) \tag{5.14e}$$

The SPPC strategy is obtained by recursively solving (5.13), as described by the following pseudo-algorithm.
Algorithm 3 defines the following feedback control law:

$$u(k) = \mu(x(k)) = u^*(0|k), \tag{5.15}$$

and the resulting model of the closed-loop system is:

$$x(k+1) = f(x(k), \mu(x(k)) \tag{5.16}$$

Algorithm 3 Nominal SPPC Strategy

1. At sampling instant k, measure the state $x(k)$ and solve the FHOCP (5.13). Let $\boldsymbol{v}^*_{N(k)}$ be the computed solution;
2. Apply to the plant the first element of the control sequence $\boldsymbol{u}^*(k)$, i.e. $u(k) = u^*(0|k) = g(\boldsymbol{v}^*_{N(k)}, 0, k)$;
3. Repeat the procedure from 1) at the next sampling period.

We conclude this section with a Proposition on the recursive feasibility of (5.13) and convergence of the state of (5.16) to the terminal set.

Proposition 5.2.1. *Assume that the FHOCP* (5.13) *is feasible at space* $k = 0$*. Then, the FHOCP* (5.13) *is recursively feasible at all* $k = 1, \dots, k_f - 1$ *and the state of the closed loop system* (5.16) *converges to the terminal set* X_f *at space* k_f*.*

Proof. Recursive feasibility is established by construction, since at any step $k+1$, one can build a feasible sequence $\boldsymbol{v}_{N(k+1)}$ by taking either $\boldsymbol{v}_{N(k+1)} = \boldsymbol{v}^*_{N(k)}$ (if $N(k+1) = N(k)$) or $\boldsymbol{v}_{N(k+1)} = \{\delta s^*_{(\underline{i}(k+1)+1,1)}, \dots, \delta s^*_{(s_n,4)}\}^T$ (if $N(k+1) < N(k)$, i.e. the values in $\boldsymbol{v}^*_{N(k)}$ excluding its first four elements). Convergence to the terminal set is then achieved by considering that constraint (5.13h) is feasible at space $k = k_f - 1$. □

Remark 5.2.2. *As in Chapter 4, the next section will consider the presence of model uncertainty and external disturbances on the model* $f(x, u)$*.*

5.3 Relaxed SPPC Approach: Algorithm and Properties

To model uncertainty and disturbances, we consider an additive term $d(k)$ acting on the input vector, i.e.:

$$\tilde{u}(k) = u(k) + d(k) \tag{5.17}$$

where $\tilde{u}(k)$ is the disturbance-corrupted input provided to the plant. This model represents well all cases where plant uncertainty and exogenous disturbances can be translated into an effect similar to the control input (the so-called matched uncertainty). For example, in our train model, Eq. (5.17) can describe uncertainty in the train mass, drivetrain specs, track slope and misapplication of the computed input by the human operator in a driver assistance scenario .
We consider the following assumption on d:

Assumption 4. *The disturbance term d belongs to a compact set $\mathbb{D} \subset \mathbb{R}^m$ such that:*

$$\|d\| \leq \overline{d},\ \forall d \in \mathbb{D} \tag{5.18}$$

where $\overline{d} \in (0, +\infty)$. □

This assumption holds in many practical cases and in the considered train application as well. We indicate the perturbed state trajectory due to the presence of d as:

$$\tilde{x}(k+1) = f(\tilde{x}(k), \tilde{u}(k)),\ k = 0, \ldots, k_f \tag{5.19}$$

where $\tilde{x}(0) = x(0)$. To retain recursive feasibility in presence of the disturbance, we soften the constraints in the FHOCP. However, in general the use of soft constraints does not guarantee that, in closed-loop operation, the operational constraints are satisfied, or even that the constraint violation is uniformly decreasing as the worst-case disturbance bound $\overline{d}$ gets smaller. For simplicity and to be more specific, from now on let us restrict our analysis to the terminal state constraint in (5.5f), i.e. $x(k_f) \in X_f$. We do so without loss of generality, since the results and approaches below can be extended to any state constraint in the control problem. Moreover, in our railway application the terminal state constraint is the most important one from the viewpoint of system performance. The other constraints (velocity limits) are always enforced for safety by modulating traction or by braking. Let us denote the distance between a point x and a set X as:

$$\Delta(x, X) = \min_{y \in X} \|x - y\|. \tag{5.20}$$

Then, we want to derive a modified SPPC strategy with softened terminal state constraint (to ensure recursive feasibility) that guarantees a property of the following form in closed loop:

$$\Delta(\tilde{x}(k_f), X_f) \leq \beta(\overline{d}),\ \beta \in \mathcal{K}. \tag{5.21}$$

That is, the distance between the terminal state and the terminal constraint is bounded by a value that decreases strictly to zero as $\overline{d} \to 0$. In order to obtain this property, we propose a relaxed SPPC approach using a two-step constraint softening procedure, described next.

5.3.1 Two-step Relaxed SPPC Strategy

At each step k we consider a strategy consisting of two optimization problems to be solved in sequence:

a) we compute the best (i.e. smallest) achievable distance between the terminal state and the terminal set, starting from the current perturbed state $\tilde{x}(k)$:

$$\begin{aligned}
&\underline{\gamma}(k) = \arg \min_{\boldsymbol{v}_{N(k)}, \gamma(k)} \ \gamma(k) \\
&\text{subject to} \\
&u(j|k) = g(\boldsymbol{v}_{N(k)}, j, k),\ j = 0, \dots, k_f - k - 1 \\
&x(j+1|k) = f(x(j|k), u(j|k)),\ j = 0, \dots, k_f - k - 1 \\
&u(j|k) \in U,\ j = 0, \dots, k_f - k - 1 \\
&x(j|k) \in X,\ j = 1, \dots, k_f - k \\
&x(0|k) = \tilde{x}(k) \\
&A(k)\boldsymbol{v}_{N(k)} \leq b(k) \\
&\Delta(x(k_f - k|k), X_f) \leq \gamma(k)
\end{aligned} \tag{5.22}$$

b) we optimize the input sequence using the original cost function, and softening the terminal constraint by $\underline{\gamma}(k)$:

$$\begin{aligned}
&\min_{\boldsymbol{v}_{N(k)}} \sum_{j=0}^{k_f - k} \ell(x(j|k), u(j|k)) \\
&\text{subject to} \\
&u(j|k) = g(\boldsymbol{v}_{N(k)}, j, k),\ j = 0, \dots, k_f - k - 1 \\
&x(j+1|k) = f(x(j|k), u(j|k)),\ j = 0, \dots, k_f - k - 1 \\
&u(j|k) \in U,\ j = 0, \dots, k_f - k - 1 \\
&x(j|k) \in X,\ j = 1, \dots, k_f - k \\
&x(0|k) = \tilde{x}(k) \\
&A(k)\boldsymbol{v}_{N(k)} \leq b(k) \\
&\Delta(x(k_f - k|k), X_f) \leq \underline{\gamma}(k)
\end{aligned} \tag{5.23}$$

By construction, both problems are always feasible (with the caveat that state constraints are considered to be always feasible, as discussed above, otherwise the softening shall be applied to these constraints as well). We denote with $\boldsymbol{v}^r_{N(k)}$, $\boldsymbol{x}^r(k)$ and $\boldsymbol{u}^r(k)$ the optimized sequences of decision variables, state and inputs resulting from the solution of (5.23). The sequences $\boldsymbol{x}^r(k)$ and $\boldsymbol{u}^r(k)$ are computed as:

$$\begin{aligned}
\boldsymbol{x}^r(k) &= \{x^r(0|k), \ldots, x^r(k_f - k|k)\} && \text{(5.24a)}\\
\boldsymbol{u}^r(k) &= \{u^r(0|k), \ldots, u^r(k_f - 1 - k|k)\} && \text{(5.24b)}\\
&\text{where} \\
x^r(0|k) &= \tilde{x}(k) && \text{(5.24c)}\\
x^r(j+1|k) &= f(x^r(j|k), u^r(j|k)) && \text{(5.24d)}\\
u^r(j|k) &= g(\boldsymbol{v}^r_{N(k)}, j, k) && \text{(5.24e)}
\end{aligned}$$

The resulting relaxed SPPC strategy is implemented by the following pseudo-algorithm.

Algorithm 4 Two-stage Relaxed SPPC Strategy

1. At sampling instant k, measure the state $\tilde{x}(k)$ and solve in sequence the optimization problems (5.22)-(5.23). Let $\boldsymbol{v}^r_{N(k)}$ be the computed solution;
2. Apply to the plant the control vector $u(k) = u^r(0|k) = g(\boldsymbol{v}^r_{N(k)}, 0, k)$;
3. Repeat the procedure from (1) at the next sampling period.

Algorithm 4 defines the following feedback control law:

$$u(k) = \mu^r(\tilde{x}(k) = u^r(0|k), \tag{5.25}$$

and the resulting closed-loop dynamics are given by:

$$\tilde{x}(k+1) = f(\tilde{x}(k), \mu^r(\tilde{x}(k)) + d(k)). \tag{5.26}$$

The next result shows that the closed-loop system (5.26) enjoys a uniformly bounded accuracy property of the form (5.21), provided that the nominal SPPC problem (5.13) is feasible at $k = 0$.

Theorem 5.3.1. *Let Assumptions 3 and 4 hold and let the FHOCP* (5.13) *be feasible at step $k = 0$. Then, the terminal state $\tilde{x}(k_f)$ of system* (5.26) *enjoys property* (5.21) *with*

$$\Delta(\tilde{x}(k_f), X_f) \leq \beta(\overline{d}) = \sum_{k=0}^{k_f-1} \beta_{k_f-k-1}(\overline{d}) \tag{5.27}$$

where

$$\begin{aligned}
\beta_0(\overline{d}) &= a_u(\overline{d}) \\
\beta_k(\overline{d}) &= a_u(\overline{d}) + a_x(\beta_{k-1}(\overline{d})),\ k = 1, \ldots, k_f - 1
\end{aligned} \tag{5.28}$$

Proof. The proof is by induction. Start at $k = 0$ and consider the relaxed optimized sequences $\boldsymbol{x}^r(k)$, $\boldsymbol{u}^r(k)$ obtained by solving problem (5.23). We first evaluate the worst-case perturbation induced by the disturbance with respect to the open-loop state trajectory $\boldsymbol{x}^r(k)$. For a sequence of disturbances $d(k)$, $k = 0, \ldots, k_f$, the corresponding open-loop input and state trajectories are:

$$\begin{array}{l} \tilde{u}(k) = u^r(k) + d(k),\ j = 0, \ldots, k_f - k - 1 \\ \tilde{x}(0|k) = x^r(0|k) \\ \tilde{x}(k+1) = f(\tilde{x}(k), \tilde{u}(k)),\ k = 1, \ldots, k_f \end{array} \tag{5.29}$$

From (5.6) we have:

$$\begin{array}{l} \|\tilde{x}(1) - x^r(1|0)\| = \|f(\tilde{x}(0), \tilde{u}(0)) - f(x(0), u^r(0|0))\| \leq \\ a_u\left(\|\tilde{u}(0) - u^r(0|0)\|\right) \leq a_u\left(\overline{d}\right) = \beta_0\left(\overline{d}\right) \end{array}$$

Consider now the perturbation 2-steps ahead:

$$\begin{array}{l} \|\tilde{x}(2) - x^r(2|0)\| = \\ \|f(\tilde{x}(1), \tilde{u}(1)) - f(x^r(1|0), u^r(1|0))\| = \\ \|f(\tilde{x}(1), \tilde{u}(1)) - f(\tilde{x}(1), u^r(1|0)) + \\ f(\tilde{x}(1), u^r(1|0)) - f(x^r(1|0), u^r(1|0))\| \leq \\ a_u\left(\overline{d}\right) + a_x\left(\|\tilde{x}(1) - x^r(1|0)\|\right) \leq \\ a_u\left(\overline{d}\right) + a_x\left(\beta_0\left(\overline{d}\right)\right) = \beta_1\left(\overline{d}\right). \end{array}$$

By iterating up until the second last time step we obtain:

$$\|\tilde{x}(k_f) - x^r(k_f|0)\| \leq \beta_{k_f-1}\left(\overline{d}\right), \tag{5.30}$$

where $\beta_{k_f-1} \in \mathcal{K}$ since it is given by compositions and summations of class-$\mathcal{K}$ functions. Since the FHOCP (5.23) is feasible, we have $x^r(k_f|0) \in X_f$ and thus:

$$\begin{array}{rcl} \Delta(\tilde{x}(k_f), X_f) & \leq & \|\tilde{x}(k_f) - x^r(k_f|0)\| + \Delta(x^r(k_f|0), X_f) \\ & \leq & \beta_{k_f-1}(\overline{d}). \end{array} \tag{5.31}$$

Now consider $k = 1$ and the FHOCP (5.22). If the optimizer is initialized with parametrized control moves $\boldsymbol{v}_{N(1)}$ such that the tail of the previous optimal sequence $\boldsymbol{u}^r(0)$ is applied to the system, the corresponding minimum $\gamma(k)$ in (5.22) results to be upper bounded by $\beta_{k_f-1}(\overline{d})$, in virtue of (5.31). The optimal value $\underline{\gamma}(k)$ is therefore not larger than this bound as well:

$$\underline{\gamma}(1) \leq \beta_{k_f-1}(\overline{d}). \tag{5.32}$$

Now take the optimal sequences $\boldsymbol{x}^r(1)$ and $\boldsymbol{u}^r(1)$ computed by solving the FHOCP (5.23). By applying the same reasoning as we did for $k = 0$, we have (compare with (5.30)):

$$\|\tilde{x}(k_f) - x^r(k_f|1)\| \leq \beta_{k_f-2}(\overline{d}). \tag{5.33}$$

Moreover, equation (5.32) implies that the solution of (5.23) satisfies the following inequality:

$$\Delta(x^r(k_f|1), X_f) \leq \underline{\gamma}(k). \tag{5.34}$$

From (5.32)-(5.34) we have:

$$\Delta(\tilde{x}(k_f), X_f) \leq \|\tilde{x}(k_f) - x^r(k_f|1)\| + \Delta(x^r(k_f|1), X_f) \leq$$
$$\beta_{k_f-2}(\overline{d}) + \beta_{k_f-1}(\overline{d}) = \sum_{k=0}^{1} \beta_{k_f-k-1}(\overline{d}).$$

By applying recursively the same arguments, the bound (5.27) is obtained. ■

Theorem 5.3.1 indicates that the worst-case distance between the terminal state and the terminal set is bounded by a value which is zero for $\overline{d} = 0$ and increases strictly with the disturbance bound. In the considered railway application this means that, for example, the worst-case accuracy degradation in reaching the terminal station on time due to the changing mass of the train which is a function of the passenger load, is proportional to the largest difference between the nominal mass and its change due to the varying passenger load. This result provides a theoretical justification to the proposed two-step relaxed SPPC approach. The bound (5.27) is conservative, since it essentially results from the accumulation of worst-case perturbations induced by the disturbance on the open-loop trajectories computed at each k. As we show in our simulation results, in practice the resulting closed-loop performance are usually very close to those of the nominal case, thanks to recursive optimization in the feedback control loop.

5.3.2 Multi-objective Relaxed SPPC Strategy

As an alternative to the two-step approach described above, one can also consider a multi-objective minimization:

$$\begin{gathered}\min_{\boldsymbol{v}_{N(k)},\gamma} \sum_{j=0}^{k_f-k} \ell(x(j|k),u(j|k)) + \omega\gamma \\ \text{subject to} \\ u(j|k) = g(\boldsymbol{v}_{N(k)},j,k),\ j=0,\dots,k_f-k-1 \\ x(j+1|k) = f(x(j|k),u(j|k)),\ j=0,\dots,k_f-k-1 \\ u(j|k)\in U,\ j=0,\dots,k_f-k-1 \\ x(j|k)\in X,\ j=1,\dots,k_f-k \\ x(0|k)=\tilde{x}(k) \\ A(k)\boldsymbol{v}_{N(k)} \le b(k) \\ \Delta(x(k_f-k|k),X_f)\le\gamma\end{gathered} \tag{5.35}$$

where ω is a positive weight on the scalar γ. Problem (5.35) can be solved in Algorithm (4) in place of problems (5.22)-(5.23). In this case, the advantage is that a trade-off between constraint relaxation and performance can be set by tuning ω. Regarding the guaranteed bounds on constraint violation, with arguments similar to those employed in [23] one can show that, at each $k \in [0, k_f - 1]$, for any $\varepsilon > 0$ there exists a finite value of ω such that the distance between the terminal state and the terminal set is smaller than $\gamma(k_f - k - 1)(\overline{d}) + \varepsilon$. Thus, with large-enough ω, one can recover the behavior obtained with the two-step relaxed SPPC approach. The theoretical derivation is omitted for the sake of brevity, as it is a rather minor extension of the results of [23].

5.4 Simulation Results

We tested the proposed strategies in realistic simulations with real train data provided by Alstom for a section of the Amsterdam metro rail, in particular the track between Rokin and Central Station. As in Chapter 4, the results have also been verified on Alstom based train tool CITHEL, which is useful to get a realistic idea of the energy expenditure by the developed SPPC strategies. The parametric values of the train used in the controller are (see (5.1)-(5.2)) $M = 142403\,\text{kg}$, $M_s = 131403\,\text{kg}$, $A = 3975.9\,\text{N}$, $B = 24.36\,\text{Nsm}^{-1}$ and $C = 4.38\,\text{Nsm}^{-2}$, while the maximum traction and braking forces allowed for this particular train are in the form of look up tables (see Fig. 5.2). These forces are of the form $F_T(x(k),u(k)) = F_{T_{\max}}(x_2(k))u(k)$, and $F_B(x(k),u(k)) = F_{B_{\max}}(x_2(k))u(k)$. The input

variable is constrained in the set $[-1, 1]$. The train has to reach the next station at $s_f = 1106\,\text{m}$ in $x_f = 76\,\text{s}$. The track is divided into $s_n = 15$ sectors. The employed sampling distance is $D_s = 18.4\,\text{m}$. Again as in Chapter 4, the results have been obtained using Matlab® `fmincon` and a laptop equipped with Intel® Core i7-6700Hq processor at 2.6 GHz and 8 GB of memory. All the functions were implemented in Matlab®.The train has to reach the next station at $s_f = 1106\,\text{m}$ in $x_f = 76\,\text{s}$. The track is divided into $s_n = 15$ sectors. The employed sampling distance is $D_s = 18.4\,\text{m}$. The considered track has zero curvature, slopes as plotted in Fig. 5.3, and velocity limits reported in Fig. 5.5.

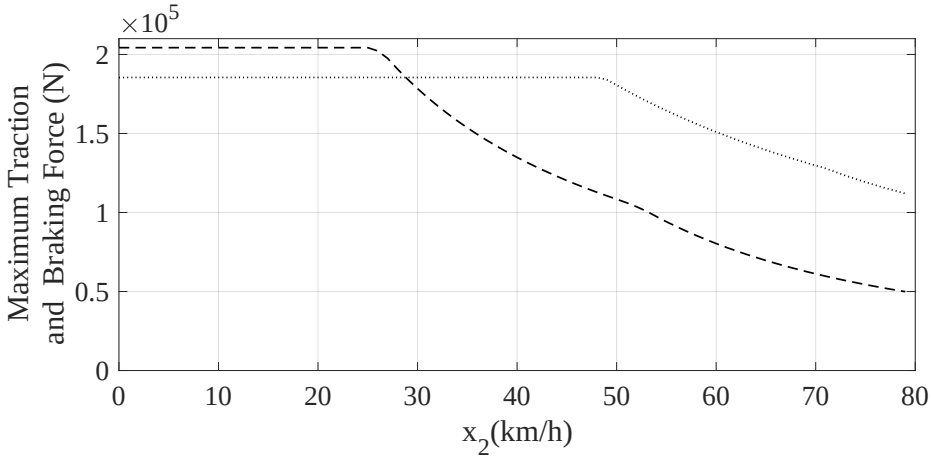

Figure 5.2: *Maximum traction force $F_{T_{\max}}$(dashed) and braking force $F_{B_{\max}}$ (dotted) allowed for the train considered in the simulation.*

We compare a nominal situation, where Algorithm 3 is applied and no model uncertainty is present, with a case where we employ Algorithm 4 (with both the two-stage approach and the multi-objective optimization variants) in presence of random parameter uncertainty ($\pm 10\%$ of each model parameter). For the multi-objective approach, we set $\omega = 160$ (see (5.35)). The obtained input and velocity profiles are presented in Fig.5.4 -5.5. From the plots, it is evident that in order to save energy, after accelerating to a certain velocity, the train mostly coasts or cruises taking advantage of the slopes. All the velocity constraints are always satisfied and the input is allowed to take on only one of the four allowed modes. Regarding the obtained final time between the terminal state and the target one at $k = k_f$, even in the presence of uncertainty the final time was respected for both the

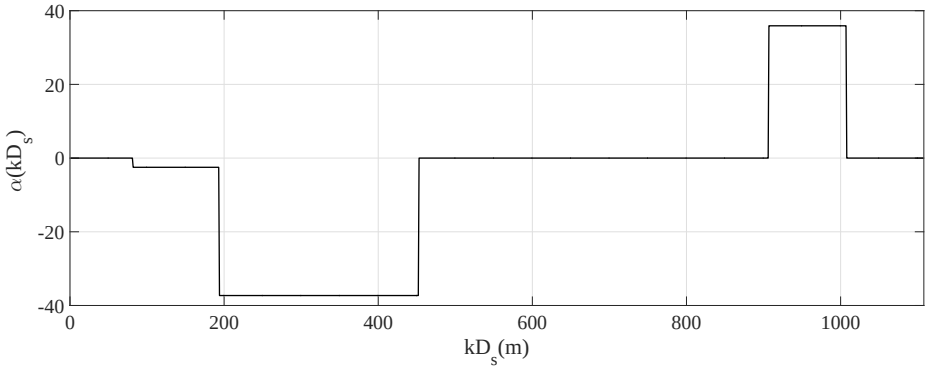

Figure 5.3: *Slopes of the Amsterdam metro track segment considered in the simulation. The unit of slope is in per mille.*

2-stage approach and the multi-objective one. This result is perfectly compatible with the desired performance in this application. Fig. 5.5 presents also the "all-out" solution, which achieves the shortest arrival time compatible with all the constraints. This corresponds to $x_f = 72.2\,\mathrm{s}$. As for the computational time, all the strategies require an average of $2\,\mathrm{s}$ per optimization step.

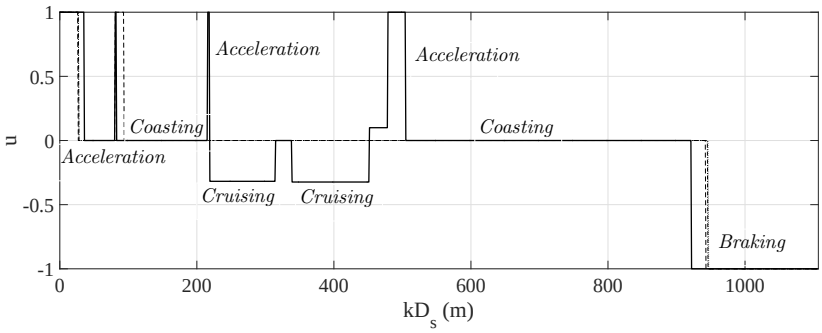

Figure 5.4: *Simulation results. Input handle as a function of the train position obtained with different SPPC strategies: nominal (dotted line), two-step relaxed (dashed), multi-objective (dash-dot). The "all-out" handle is shown with a solid line*

Finally, the results were tested on Alstom based tool CITHEL and also compared with their existing eco-drive strategy based on Genetic algorithm. The results are presented in Table.5.1 and the obtained velocity profiles in Fig.5.6. Though, the SPPC strategies arrive with a delay of $2\,\mathrm{s}$ at the pre-

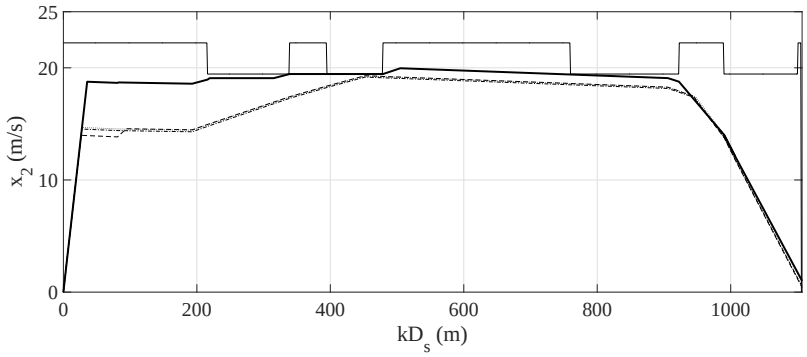

Figure 5.5: *Simulation results. Velocity profiles as a function of the train position obtained with different SPPC strategies: nominal (dotted line), two-step relaxed (dashed), multi-objective (dash-dot). All these approaches share the same final time of $t_f = 76\,s$. The "all-out" solution ($t_f = 72.2\,s$) is shown with a thick solid line, and velocity limits with a thin solid line.*

scribed station, the traction energy consumption E_{T} is considerably lower as compared to the existing Genetic-algorithm based eco-drive approach, which proves the efficiency of the developed SPPC strategies. A final comment is in the observation of different accceleration rates obtained with matlab and CITHEL simulations (see Fig. 5.5 - 5.6) for these strategies and are a consequence of the different space samples used to obtain the velocity profiles. Since, in SPPC strategy the samples are the optimization variables, sometimes it can result in some error in the actual and simulated acceleration rate, which can always be taken care of.

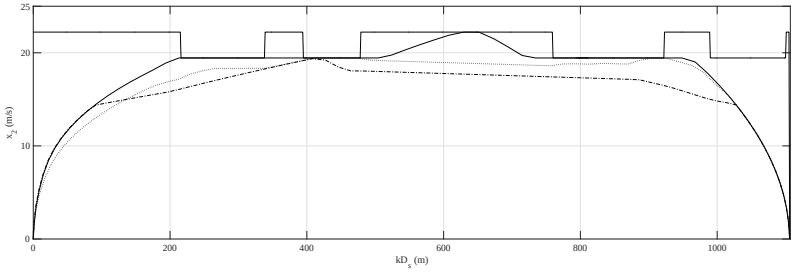

Figure 5.6: *Simulation results. Velocity profiles as a function of the train position obtained with Alstom based CITHEL tool: genetic algorithm based eco-drive (dotted line), SPPC strategy (dash-dot). All these approaches share the same final time of $t_f = 76\,s$. The "all-out" solution ($t_f = 73\,s$) is shown with a thick solid line, and velocity limits with a thin solid line.*

Table 5.1: *Comparison results with different strategies tested in Alstom based tool CITHEL*

	E_{T} (KWH)	t_f (s)
All-out solution	13.19	73
Genetic algorithm based Eco-drive	9.05	77
SPPC strategy	6.2553	78

5.5 Conclusion

We considered the problem of energy-efficient train operation, involving a finite terminal position and corresponding state constraint, and a discrete set of allowed input values or operating modes. To address this problem, we proposed a MPC approach with a shrinking horizon and a particular input parametrization, which allows one retain a continuous optimization problem at each step. We derived convergence guarantees in both nominal conditions and under uncertainty, and showcased the technique in realistic simulations. Comparison of results in terms of energy consumption with the existing benchmark by means of Alstom based tool CITHEL proves the efficiency of the developed SPPC strategies.

CHAPTER 6

Receding Horizon Switched Predictive Control Strategy

In this chapter, a switched NMPC strategy for the EETC problem is presented. This work has been presented in [26]. As explained in the previous chapters, for energy efficient operation of railways, MPC is a suitable approach, thanks to its capability to deal with state and input constraints and economic objectives, see e.g., [49, 54]. Like in Chapter 5, this strategy has also been developed as a DAS strategy. Recalling the DAS strategy described in Subsection 3.1.2, where the input u is actually constrained to belong to a discrete set of modes, the train model can be considered as switching in nature, and hence this was the main idea behind the development of this scheme. On the other hand, while in Chapter 4 and Chapter 5, the MPC strategies presented are based on shrinking horizon, this strategy is based on receding horizon approach. The resulting control approach has been named Receding Horizon Switched Predictive Control (RSPC) strategy.

In general, a switched system is formed of family of subsystems together with a switching signal, which specifies at each sampling instant, the active subsystem dynamics. The aim of a general switched NMPC is to control

this switching signal based on some criteria. Important results for stability and stabilization of switched systems have been presented in [18, 31, 32], while switched NMPC have been investigated in [19, 56]. More recently in [58, 59, 86], important stabilization results for switched MPC have been reported.
Now, consider a generic switched system of the following form

$$x(k+1) = f_{\sigma(k)}(x(k)) \tag{6.1}$$

defined for all $k \in \mathbb{N}$, where $x(k) \in \mathbb{R}^n$ is the state and $\sigma(k)$ is the switching rule. The active model at the time instant k is selected by the integer $\sigma(k) \in \{1, \cdots, P\}$.

6.1 Switched Train Control Problem

Consider an electric train controlled by a digital control unit. In this strategy, we consider space as the independent variable, while time will be one of the system's states. Thus, we denote with $k \in \mathbb{Z}$ the discrete space variable, and with $D_s(k)$ the adaptive sampling distance which is space varying. We denote with $x(k) = [x_1(k),\, x_2(k)]^T$ the state of the train, where x_1 is its travel time and x_2 the train speed, and with $u(k) \in [-1, 1]$ a normalized traction force, where $u(k) = 1$ corresponds to the maximum applicable traction and $u(k) = -1$ to the maximum braking. The input u is the available control variable. The train has to move from one station at time $x_1 = 0$ and reach the next one at time $x_1 = x_f$, covering the corresponding distance s_f. In state space modeling, the prescribed arrival time t_f (see Eq.(2.6)) and the maximum allowed velocity limit $v_{\max}(k)$ (see Eq.(2.5)) have been renamed as $t_f = x_f$ and $v_{\max}(k) = \overline{x}_2(k)$ to link them to the states they are representing. For a given pair of initial and final stations, the track features (slopes, curvature) are known in advance. Thus, in nominal conditions (i.e. with rated values of the train parameters, like its mass and the specifications of the powertrain and braking systems), according to Newton's laws and using the forward Euler discretization method, the equations of motion of a reasonably accurate switched model of this system read:

$$\begin{aligned} x_1(k+1) &= x_1(k) + \tfrac{D_s(k)}{x_2(k)} \\ x_2(k+1) &= x_2(k) + D_s(k) \left(\tfrac{F_T(x(k),u_{\sigma(k)}(k)) - F_B(x(k),u_{\sigma(k)}(k)) - F_R(k,x(k)}{M x_2(k)} \right) \end{aligned} \tag{6.2}$$

The resistive force $F_R(k, x)$ is also nonlinear, and it is the sum of a first term $R_v(x_2)$, accounting for resistance due to the velocity, and a second

term $R_g(k)$, accounting for the effects of slopes and track curvature:

$$\begin{aligned} F_R(k,x) &= R_v(x_2) + R_g(k) \\ R_v(x_2) &= A + Bx_2 + Cx_2^2 \\ R_g(k) &= M_s\left(g\tan(\alpha(k)) + \frac{\lambda_t}{r_c(k)}\right) \end{aligned} \tag{6.3}$$

The parametric symbols have already been defined in Subsection 2.1.1 (see Tables 2.1 and 2.2 for more details). Making reference to the formulation in Eq.(6.1), since the switching signal is externally updated and is a function of space, system (6.2) is a space dependent switching system.

Remark 6.1.1. *The model* (6.2) *has been rewritten in the form of* (6.1)*, where* $\sigma(k) \in \{1, \ldots, 6\}$ *is the switching signal, such that* $u_{\sigma(k)}(k) \in \{-1,\ 0,\ 0.5,\ 0.75,\ 1,\ u_{CR}\}$ *respectively, in terms of switching input handle, where* u_{CR} *identifies the cruising mode (see Subsection 3.1.2). For example,* $\sigma(k) = 1$ *implies that* $u_1(k) = -1$ *is chosen to be applied to the system* (6.2) *at the sampling instant* k*.*

As already discussed in Subsection 2.1.1, besides the prescribed arrival time x_f and position s_f, there are additional state constraints that must be satisfied. These pertain to the limits on the maximum allowed velocity, $\overline{x}_2(k)$, which depends on the position k, since a different velocity limit is imposed for safety by the regulating authority according to the track features at each position. Overall, by defining the terminal space step as k_f, the state constraints read:

$$\begin{aligned} x(0) &= [0,\ 0]^T \\ x(k_f) &= [x_f,\ 0]^T \\ x_2(k) &\geq 0,\ \ k = 0, \ldots, k_f \\ x_2(k) &\leq \overline{x}_2(k),\ \ k = 0, \ldots, k_f \end{aligned} \tag{6.4}$$

The control objective is to maximize the energy efficiency of the train while satisfying the constraints above, which translates mathematically to minimizing the overall traction energy given by:

$$J = \sum_{k=0}^{k_f} F_T(x(k), u_{\sigma(k)}(k)) \tag{6.5}$$

This choice tends to produce controllers that minimize the traction energy injected into the system.

6.1.1 Problem Abstraction

The control problem described above can be cast in a rather standard form:

$$\min_{\boldsymbol{\chi}} \sum_{k=0}^{k_f} \ell_{\sigma(k)}(x(k), u_{\sigma(k)}(k)) \tag{6.6a}$$

subject to

$$x(k+1) = f_{\sigma(k)}(x(k), u_{\sigma(k)}(k)) \tag{6.6b}$$

$$u_{\sigma(k)}(k) \in U,\ k = 0, \ldots, k_f - 1 \tag{6.6c}$$

$$x(k) \in X,\ k = 1, \ldots, k_f \tag{6.6d}$$

$$x(0) = x_0 \tag{6.6e}$$

$$x(k_f) \in X_f \tag{6.6f}$$

where $x \in \mathbb{X} \subset \mathbb{R}^n$ is the system state and x_0 is the initial condition. The symbol $\boldsymbol{\chi} = [\sigma(0), \ldots, \sigma(k_f - 1)]$ represents the vector of switching strategy to be applied to the plant. The sets $X \subset \mathbb{X}$ and $U \subset \mathbb{U}$ represent the state and input constraints (including the discrete set of allowed inputs or input modes as described above), and the set $X_f \subset \mathbb{X}$ the terminal state constraints, which include a terminal equality constraint as a special case. Furthermore, X is assumed to be compact, as well as the terminal constraint set X_f.

6.2 Receding Horizon Switched Predictive Control (RSPC) Approach

To solve (6.6), a switched NMPC strategy with a receding horizon approach (RSPC) is adopted. The main reason for this choice is that solving (6.6) can be computationally very expensive when using a heuristic brute force approach, since there are no solvers available which can directly solve this particular problem due to the non convex nature of the cost function and an optimization problem which becomes a nonlinear mixed integer programming problem due to the discretization of the control variable in the case of a DAS strategy. Hence, the prediction horizon should be as short as possible. Also, due to the receding horizon approach explained in Subsection 6.2.1, the terminal constraint on time (see (6.4)) has been relaxed to be included as a terminal cost. Finally, in order to deal with braking dynamics which is very difficult to capture with receding horizon approach, a separate predictive braking approach in parallel which involves adapting the samples so that the train stops at the arrival station is also included. The

adaptive sampling is adopted not just for capturing braking dynamics but also to capture the track characteristics such as the slopes and the curvature which are a function of the space as well as the changing velocity limits.

6.2.1 Receding Horizon Setup

Consider the receding prediction horizon N. In order to maximize the traction energy efficiency of the train, at any sampling instant k, the cost function was chosen as:

$$J_{\boldsymbol{\chi}}(x) = \sum_{j=0}^{N-1}(1-\gamma_S)\ell_{\sigma(j|k)}(x(j|k), u_{\sigma(j|k)}(j|k)) + \gamma_S F(x(N|k)) \quad (6.7)$$

with $\boldsymbol{\chi} = [\sigma(0|k), \ldots, \sigma(N-1|k)]^\top$ being the predicted switching control sequence. The terms

$$\begin{aligned}\ell_{\sigma(j|k)}(x(j|k), u_{\sigma(j|k)}(j|k)) &= \left(\frac{F_T(x(j|k), u_{\sigma(j|k)}(j|k)) - F_R(x(j|k))}{F_{T_{\max}}}\right)^2 \\ F(x(N|k)) &= \left(\frac{x_1(0|k) + T_{horizon}(k) - x_1(N|k)}{T_{horizon}(k)}\right)^2\end{aligned} \quad (6.8)$$

The cost function is chosen as a combination of the traction energy, the energy losses due to resistance and horizon time error. In the cost function, $T_{horizon}$ is the horizon time. The reason for including losses due to the resistance energy in the cost is to provide a solution which could exploit the track characteristics when the train is descending, thus reducing the energy losses and making use of the negative slopes to reduce energy consumption.

Remark 6.2.1. *At each step k, the horizon time $T_{horizon}(k)$ is the time needed to cover the distance of that particular prediction horizon, given the maximum allowed velocity limits, maximum allowed journey time and the characteristics of the track. In order to compute $T_{horizon}$, a heuristic approach is adopted.*

6.2.2 RSPC Strategy

Let us denote with $x(j|k)$, $j = 0, ..., k_f - k$ the state vectors predicted at space sample $k + j$ starting from the one at step k. At each step $k \in [0,\, k_f - 1]$, we formulate the following FHOCP:

$$\min_{\boldsymbol{\chi}(k)} \sum_{j=0}^{N-1} \ell_{\sigma(j|k)}(x(j|k), u_{\sigma(j|k)}(j|k)) + F(x(N|k)) \tag{6.9a}$$

subject to

$$\boldsymbol{\chi}(k) = [\sigma(0|k), \ldots, \sigma(N-1|k)] \tag{6.9b}$$
$$x(j+1|k) = f_{\sigma(j|k)}(x(j|k), u_{\sigma(j|k)}(j|k)),\ j = 0, \ldots, N-1 \tag{6.9c}$$
$$u_{\sigma(j|k)}(j|k) \in U,\ j = 0, \ldots, N-1 \tag{6.9d}$$
$$x(j|k) \in X,\ j = 1, \ldots, N \tag{6.9e}$$
$$x(0|k) = x(k) \tag{6.9f}$$
$$x(N|k) \in X_f \tag{6.9g}$$

We denote with $\boldsymbol{\chi}^*(k) = [\sigma^*(0|k), \ldots, \sigma^*(N-1|k)]$ the optimal switching strategy obtained by solving (6.9). Moreover, we denote with $\boldsymbol{x}^*(k)$ and $\boldsymbol{u}^*(k)$ the corresponding predicted sequences of state and input vectors:

$$\boldsymbol{x}^*(k) = \{x^*(0|k), \ldots, x^*(N|k)\} \tag{6.10a}$$
$$\boldsymbol{u}^*_{\boldsymbol{\chi}^*(k)}(k) = \{u^*_{\sigma^*(0|k)}(0|k), \ldots, u^*_{\sigma^*(N-1|k)}(N-1|k)\} \tag{6.10b}$$

where

$$x^*(0|k) = x(k) \tag{6.10c}$$
$$x^*(j+1|k) = f(x^*(j|k), u^*_{\sigma^*(j|k)}(j|k)) \tag{6.10d}$$
$$\tag{6.10e}$$

The RSPC strategy is obtained by recursively solving (6.9), as described by the following pseudo-algorithm.

Algorithm 5 RSPC Strategy

1. At sampling instant k, measure the state $x(k)$ and solve the FHOCP (6.9). Let $\boldsymbol{\chi}^*(k)$ be the computed switching strategy solution;
2. Apply to the plant the first element of the control sequence $\boldsymbol{u}^*_{\boldsymbol{\chi}^*(k)}(k)$.
3. Repeat the procedure from 1) at the next sampling period.

Algorithm 5 defines the following switching strategy

$$\chi(k) = \sigma^*(0|k) \tag{6.11}$$

which in turn defines the following feedback control law:

$$u_{\sigma(k)}(k) = \mu(x(k)) = u^*_{\sigma^*(0|k)}(0|k), \tag{6.12}$$

and the resulting model of the closed-loop system is:

$$x(k+1) = f(x(k), \mu(x(k)) \tag{6.13}$$

6.2.3 Adaptive RSPC Strategy

As mentioned in the beginning of this section, with a constant receding prediction horizon, it is not always possible to capture the changing dynamics of the track on which the train is running. Hence, a setup to suitably adapt the sample length and as a consequence the prediction horizon length to the changing dynamics is introduced in this section. The main idea is to first split the track into sectors. Specifically, we consider a number $s_n \in \mathbb{N}$ of sectors as in Chapter 5, Subsection 5.2.1, each one with length Γ_i, such that

$$\sum_{i=1}^{s_n} \Gamma_i = s_f. \tag{6.14}$$

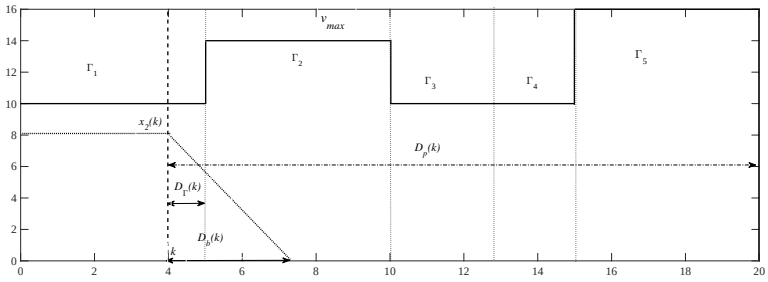

Figure 6.1: *Example of sector choice for a track with $s_f = 20$ and s_n= 5. Possible sectors based on similar characteristics such as velocity limits and R_g values are depicted. Also, as an example, graphical representations of the distances, $D_p(k)$, $D_\Gamma(k)$ and $D_b(k)$ are shown at the current step k.*

The choice of sectors is carried out by considering characteristics such as the presence of constant velocity limits and the resistance force due to the slopes and track curvature $R_g(k)$ throughout that particular sector, which are known in advance, refer to Fig. 5.1 for an example.

At any step k, the braking distance $D_b(k)$ needed for the train to stop based on the current velocity $x_2(k)$ can be calculated by the following equation:

$$0 = x_2(k) + D_b(k) \left(\frac{-F_B(x(k), u_{\sigma(k)}(k)) - F_R(k, x(k)}{M x_2(k)} \right) \tag{6.15}$$

Also, at any step k, let the remaining distance to be covered by the train

to reach the arrival station be denoted by $D_p(k)$. For a graphical representation of $D_b(k)$ and $D_p(k)$, refer to Fig. 8.1 for an example.

Finally, the resultant distance $\delta D(k)$ can be calculated by

$$\delta D(k) = D_p(k) - D_b(k). \tag{6.16}$$

Let $\overline{D}$ be a constant parameter chosen as the sampling distance under normal conditions. At step k, let the remaining distance of the particular sector that the train is in be denoted by $D_\Gamma(k)$. Again, refer to Fig. 8.1 for an example. The adaptive RSPC strategy is obtained by the following algorithm.

Algorithm 6 Adaptive RSPC Algorithm

if $\delta D(k) > 0 \quad \wedge \quad D_\Gamma(k) \geq N\overline{D}$ **then**
  $D_s(k) = \overline{D}, \chi(k) = \sigma^*(0|k)$
else if $\delta D(k) > 0 \quad \wedge \quad D_\Gamma(k) < N\overline{D}$ **then**
  $D_s(k) = D_\Gamma(k), \chi(k) = \sigma^*(0|k)$
else if $\delta D(k) = 0$ **then**
  $D_s(k) = D_\Gamma(k), \chi(k) = \sigma(k) = 1, i.e. \;\; u_1(k) = -1.$
end if

6.3 Results

We tested the proposed strategies in realistic simulations with real train data provided by Alstom for a section of regional trains. The parametric values of the train used in the controller are (see (6.2)-(6.3)) $M = 267464\,\text{kg}$, $M_s = 255200\,\text{kg}$, $A = 3597.6\,\text{N}$, $B = 119.5\,\text{Nsm}^{-1}$ and $C = 6.97\,\text{Nsm}^{-2}$, while the maximum traction and braking forces allowed for this particular train are in the form of look up tables (see Fig. 6.2). These forces are of the form $F_T(x(k), u(k)) = F_{T_{\max}}(x_2(k))u(k)$, and $F_B(x(k), u(k)) = F_{B_{\max}}(x_2(k))u(k)$. The input variable is constrained in the set $[-1,\ 1]$.

The considered track has curvature and slopes as plotted in Fig. 6.3 and Fig.6.4 , and velocity limits reported in Fig. 6.5.The train has to reach the next station at $s_f = 808\,\text{m}$ in $x_f = 80\,\text{s}$. The track is divided into $s_n = 8$ sectors.

The simulation results presented have been obtained using CITHEL, which is the official software developed by Alstom. The resulting velocity profiles using different approaches are shown in Fig. 6.5. We compare strategies where Algorithm 6 is applied with the, "Eco-drive coasting" strategy which is at present being used by Alstom.

The obtained velocity profiles are presented in Fig. 6.5. All the velocity constraints are always satisfied. Regarding the obtained final time between

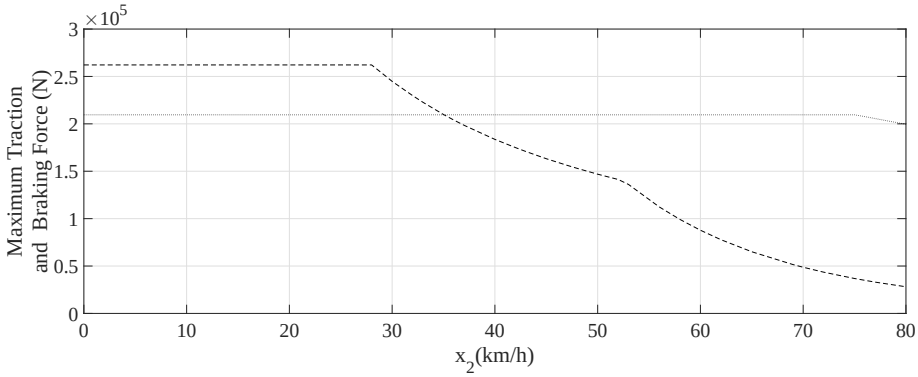

Figure 6.2: *Maximum traction force $F_{T_{\max}}$(dashed) and braking force $F_{B_{\max}}$ (dotted) allowed for the train considered in the simulation.*

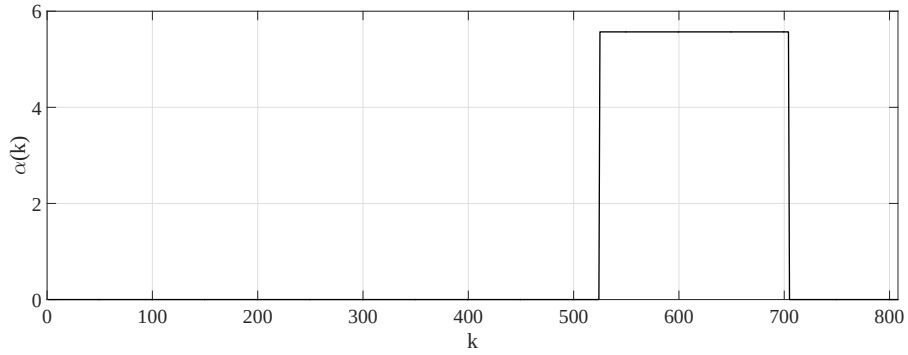

Figure 6.3: *Slopes of the Regional track segment considered in the simulation.*

the terminal state and the target one at $k = k_f$, in our case the train arrived a bit early in $x_f = 77$ s, which essentially depends on tuning of γ_S. This result is perfectly compatible with the desired performance in this application. Fig. 6.5 also presents the "all-out" solution, which achieves the shortest arrival time compatible with all the constraints. This corresponds to $x_f = 61$ s. Table 6.1 provides a summary of obtained results. Analyzing the results, it can be said that with better tuning of γ_S, adaptive RSPC strategy is almost similar to the Eco-drive coasting solution, where the train mostly coasts and arrives the station in a delay of 1 second. The adaptive RSPC algorithm respects the final travel time at the expense of a bit more energy since it arrives earlier but that mostly depends on tuning of γ_S and can be made to arrive on time. In terms of computational time, the adaptive RSPC outperforms the Eco-drive coasting solution by almost 10 times.

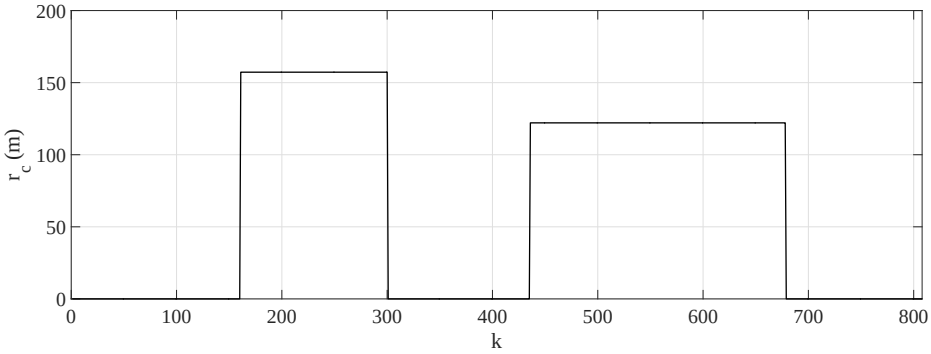

Figure 6.4: *Radius of Curvature of the Regional track segment considered in the simulation.*

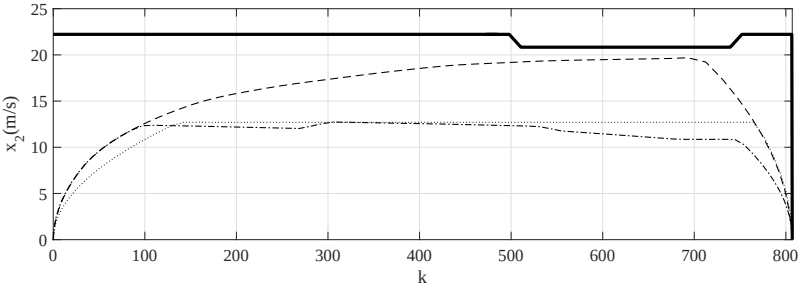

Figure 6.5: *Simulation results. Velocity profiles as a function of the train position obtained with different strategies: Adaptive RSPC (dotted line), Eco-drive Coasting (dash-dot). The "all-out" solution ($x_f = 61\,s$) is shown with a dashed line, and velocity limits with a solid line.*

Table 6.1: *Comparison of results obtained in terms of final arrival times and traction energy E_{T} with tests performed on CITHEL*

	$x_f(s)$	E_{T} (KWH)
all-out	61	24.69
Eco-drive coasting strategy	81	12.58
Adaptive RSPC strategy	77	13.09

6.4 Conclusion

The purpose of this work was to provide a sub-optimal control solution to predict the velocity profile of a railway vehicle by using adaptive RSPC scheme. In the next chapter, this strategy will be further extended to a

network of trains, where the trains will be allowed to exchange regenerated braking energy available in the network.

CHAPTER 7

Collaborative Eco-Drive of Train Networks via Predictive Control Strategies

Historically speaking, one of the earliest examples in railways, where regenerative braking was introduced was the Baku-Tbilisi-Batumi railway (Transcaucasus railway or Georgian railway) in the 1930s. Analyzing railway energy consumption, more than 70 percent of the consumption corresponds to traction requirements while the rest corresponds to non-traction [41]. Hence, most of the new technologies are focused on reducing the traction related energy consumption, for instance, adopting electrical traction systems, which are considered to be the most efficient traction systems in the railway sector, due to their ability to regenerate and recover braking energy which otherwise gets lost as heat into the environment.
Regenerative braking is an energy recovery mechanism that converts the kinetic energy during braking into electricity, also known as regenerative energy. The principle of regenerative energy usually involves a source Pantograph, the traction motor/generator and the trains connected to the Pantograph [84]. During regenerative braking, the traction motor acts as a generator and restores part of the kinetic energy into electrical energy (see Fig. 7.1 for details).

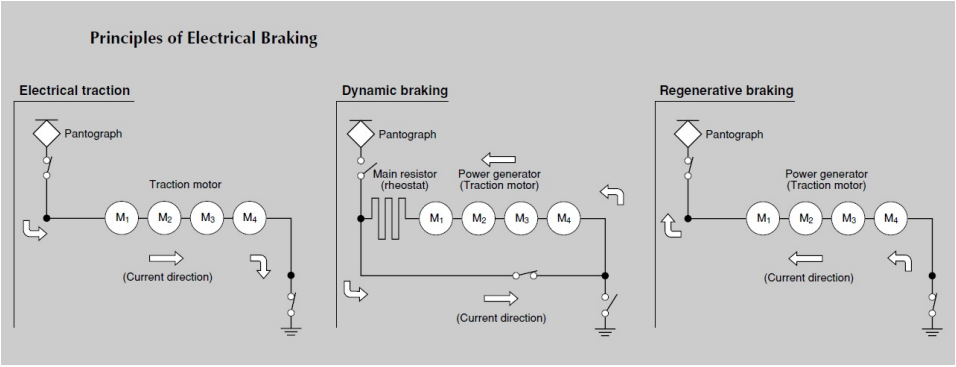

Figure 7.1: *Representational diagram explaining the normal electric traction, dynamic braking and regenerative braking principle for an electrical train. This diagram has been borrowed from [42]*

Today, one of the most important research directions for energy efficient operation of trains is based on developing techniques for efficient utilization of this regeneration energy. Usually, the generated energy can either be fed back to the Pantograph to be used instantaneously by other trains connected to the Pantograph or stored on an energy storage device for later use. The three most common energy storage devices known in the literature are batteries, supercapacitors and flywheels, while other not so common devices include superconductive energy storage and fuel cells. Application-wise, the energy storage technologies used in railway industry can be divided into two categories: on-board (OESS) and stationary (SESS) energy storage systems. OESS are those installed inside the trains and can be used to store the recovered energy of only one train, and hence the power and energy capacity required is lower than SESSs. OSSs serve three main purposes on board railway cars: energy consumption reduction, peak power reduction and catenary-free operation. Catenary-free operation is a type of operation in which a train with electric traction motor runs on a non-electrified line using the energy from an energy storage device. These trains need storage devices capable of not only providing a high peak for instance, but also high energy capacity which is quite challenging and still very much open to further investigation. SESS, on the other hand, when compared to an on-board one, should have a higher energy capacity, while there is more freedom regarding the sizing of the system. It should have both a high power and energy capacity together with a long charge/discharge life cycle. A recent review of the storage devices can be found in [33]. This stored energy could be used in the next acceleration phase by the train. In [61],

MPC was applied to reduce the overall cost of energy demanded from the grid by considering factors influenced by energy storage devices and energy exchange due to acceleration and deceleration of the trains connected to the substation. While storing regenerative energy for later use can be good option, it requires huge changes in the present railway infrastructure and can be economically quite demanding. Another direction to investigate is the instantaneous use of this regenerated energy. Regenerated braking can or cannot be directly incorporated into the EETC problem. With respect to the incorporation in the EETC problem, it was first introduced in 1985 in [10], where OCP (2.8) was reformulated to include regenerative braking. In particular, the reformulated objective problem is described below:

$$J = \min_{h} \int_0^{t_f} (h^+(t) - \eta h^-(t)) v(t) dt \tag{7.1}$$

where the term $\eta h^- v$ gives the braking energy regenerated by the train, such that $h^-(t) = -\min(h(t), 0)$ denotes the specific braking force (the negative part of the control) and $\eta \in [0, 1]$ is the recuperation coefficient which determines the efficiency of the regenerative braking system, since there is a limit on receptivity of the regenerative brakes [28]. In [17], a predictive fuzzy-logic controller was particularly designed for DC railway systems, where the aim was to minimize the energy demanded from the grid by maximizing receptivity. In [10], further simplifications included in the form of a level track. Finally, necessary conditions were derived by PMP application, resulting in the following optimal control strategy

$$\hat{h}(t) = \begin{cases} h_{max}(v(t)) & \text{if } \lambda(t) > v(t) \text{ (MA)} \\ h \in [0, h_{max}] & \text{if } \lambda(t) = v(t) \text{ (CR)} \\ 0 & \text{if } \eta v(t) < \lambda(t) < v(t) \text{ (C0)} \\ h \in [-h_{min}, 0] & \text{if } \lambda(t) = \eta v(t) \text{ (RB)} \\ -h_{min} & \text{if } \lambda(t) < \eta v(t) \text{ (MB)} \end{cases} \tag{7.2}$$

where RB denotes regenerative braking. This strategy considered a time domain model. Afterwards, in [48] the authors considered the EETC problem with regenerative braking with distance as the independent variable. The reformulated cost function in space domain is given by:

$$J = \min_{h} \int_0^{s_f} (h^+(s) - \eta h^-(s)) ds \tag{7.3}$$

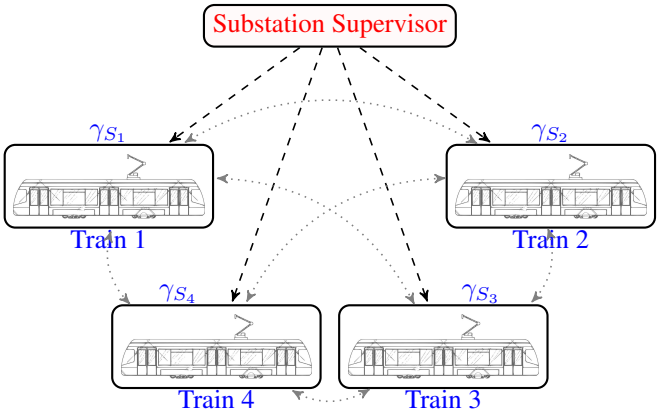

Figure 7.2: *Collaborative eco-drive architecture*

They considered variable gradient and speed limits. However, rather then the general states, time and velocity, they used time $t(s)$ and total energy $E(s) = K(s) + P(s)$ as state variables, where $K(s)$ is the kinetic energy and $P(s)$ is the potential energy at position s and formulated the optimal control problem accordingly. Finally, they derived the PMP necessary conditions and also found the optimal control structure with five regimes in space domain:

$$\hat{h}(s) = \begin{cases} h_{max}(K(s)) & \text{if } \lambda(s) > K(s) \text{ (MA)} \\ h \in [0, h_{max}] & \text{if } \lambda(s) = K(s) \text{ (CR)} \\ 0 & \text{if } \eta K(s) < \lambda(s) < K(s) \text{ (C0)} \\ h \in [-h_{min}, 0] & \text{if } \lambda(s) = \eta K(s) \text{ (RB)} \\ -h_{min} & \text{if } \lambda(s) < \eta K(s) \text{ (MB)} \end{cases} \tag{7.4}$$

Other contributions which incorporated regenerative braking into the EETC problem can be found in [3, 12, 29, 66, 68] . In this thesis, regenerative braking can be easily incorporated by modifying the cost functions in our developed strategies for the single train control presented in the previous chapters.

After discussions with our industrial partner Alstom, for the second part of this thesis, it was decided to focus on developing strategies to effectively use this regenerated energy by collaboration among trains which derive power from the same source and hence can share available regenerated energy among themselves. Besides the reduction in overall energy of

the train network, one advantage of using the available regenerative energy rather than demanding energy from the power source is the reduction of losses incurred during energy transfer from the power source to the train demanding energy for traction. Existing works mostly focus on optimizing the train timetables, so as to synchronize the acceleration and deceleration of trains as much as possible [60, 62, 67, 84].

Having in mind energy regeneration and a collaborative framework to exploit the available regeneration energy, three strategies for effective use of this regenerated energy will be presented in this and the following chapter. It is important to note here that only the trains connected to the same substation are able to share energy among themselves in any case. Consider trains operating under the same substation and capable of communicating with each other. Let us denote each train in the network with the subscript $i = 1, \ldots, \mathcal{M}$. In all the strategies presented hereafter, we assume the scenario, where the trains connected to the same substation follow the same track and run delayed in time one after the other by some seconds. Next in this chapter, we present two collaborative strategies with extensions from Chapter 4 and Chapter 6, where we introduce a supervisor (refer to Fig. 7.2 for an example), which according to a predefined state dependent triggering rule, assigns the weights of the terms constituting the cost function. The main difference between the strategies presented in this chapter and the next is that in this case, the value of the weights are always predefined while in the next chapter, a dissension strategy based adaptive law which is conceptually similar to Markov chains is used to calculate the values of the weights instantaneously. In the next section, we present an collaborative strategy based on the assumption that the supervisor has fully knowledge of the states of all the trains connected to the substation.

7.1 Adaptive RSPC Algorithm in a Networked Train Setup

Here we have extended the adaptive RSPC strategy described in Chapter 6 to include a network of trains connected to the same substation. This work has been presented in [26]. The corresponding trains models are as in (6.2) with the receding prediction horizon N_i. In the networked setup, the cost function for the ith train is given by:

$$J_{i_{\boldsymbol{\chi}_i}}(x_i, k_\tau) = \sum_{j=0}^{N_i-1} (1 - \gamma_{S_i}(k_\tau)) \ell_{i_{\sigma_i(j_i|k_i)}}(x_i(j_i|k_i), u_{i_{\sigma_i(j_i|k_i)}}(j_i|k_i)) + \gamma_{S_i}(k_\tau) F_i(x_i(N_i|k_i)) \tag{7.5}$$

with $\boldsymbol{\chi}_i = [\sigma_i(0|k_i),\, \ldots,\, \sigma_i(N_i-1|k_i)]^\top$ being the predicted switching control sequence of the ith train. The terms

$$\begin{aligned}
&\ell_{i_{\sigma_i(j_i|k_i)}}(x_i(j_i|k_i), u_{i_{\sigma_i(j_i|k_i)}}(j_i|k_i)) \\
&\qquad = \left(\frac{F_{T_i}((x_i(j_i|k_i), u_{i_{\sigma_i(j_i|k_i)}}(j_i|k_i)) - F_{R_i}(x_i(j_i|k_i))}{F_{T_{i_{\max}}}} \right)^2 \\
&F_i(x_i(N_i|k_i)) = \left(\frac{x_{i_1}(0|k_i) + T_{i_{horizon}}(k_i) - x_{i_1}(N_i|k_i)}{T_{i_{horizon}}(k_i)} \right)^2
\end{aligned} \tag{7.6}$$

Finally, for the ith train, at each step k, the applied switching strategy $\chi_i(k)$ is chosen according to the adaptive RSPC strategy in Algorithm 6.

7.1.1 Supervisor

Assume that the supervisor has full knowledge of the current train states associated with a specific substation and is capable of enforcing a triggering rule in order to assign the weights γ_{S_i} in the cost function (7.5). The aim of the proposed approach is to make the trains cooperate in order to exploit the regenerative braking energy when one or more of the trains of the network are on time and in braking operation mode. This would allow other trains to accelerate, if they need, while fulfilling the constraints.

Assume γ_{S_i}, $i = 1, \ldots, \mathcal{M}$ can take two values $\{\gamma_{S_i}^{(1)}, \gamma_{S_i}^{(2)}\}$ such that $\gamma_{S_i}^{(1)} < \gamma_{S_i}^{(2)}$. So, at the triggering instant k_τ for the ith train, the triggering rule is written as

$$\gamma_{S_j}(k_\tau) = \begin{cases} \gamma_{S_j}^{(2)} & \text{if } u_i(k_\tau) = -1 \quad \text{(Braking)} \\ \gamma_{S_j}^{(1)} & \text{otherwise} \end{cases}, \quad \forall\, j \neq i\,. \tag{7.7}$$

This means that when the ith train is in braking, the other trains can exploit its regenerative energy to accelerate if they need. This is done by increasing the weight γ_{S_j} on the time term of the cost function. Otherwise, all the trains maintain the previous value, set according to the evaluation of a Pareto graph between traction energy and journey time. For an illustrative example, Figure 7.3 shows the case with γ_{S_i} varying from $\gamma_{S_i}^{(1)} = 0.71$ and $\gamma_{S_i}^{(2)} = 0.9$, corresponding to the minimum and maximum energy consumption cases respectively, such that no handle oscillations are generated. The graph is obtained for a track of $807\,\mathrm{m}$. Table 7.1 shows the corresponding values of the ith train in terms of journey time x_{f_i}, traction energy E_{T_i} and braking energy E_{B_i}.

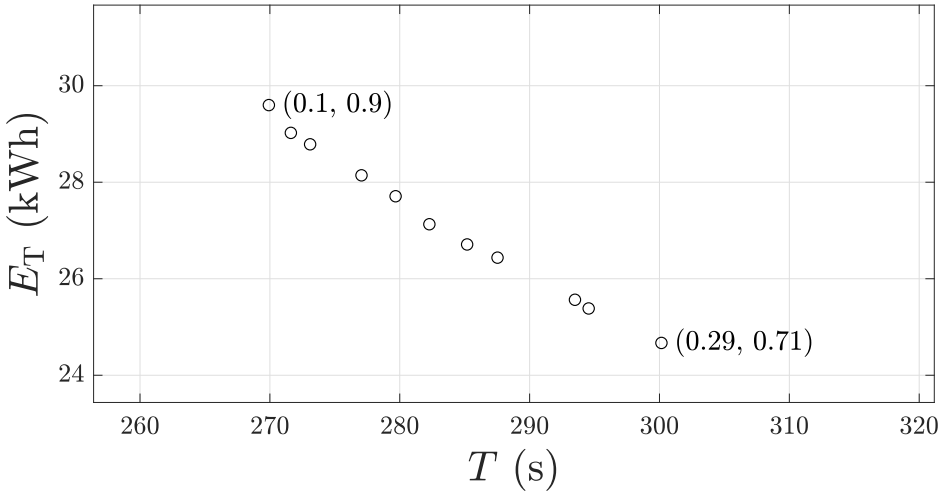

Figure 7.3: *Pareto graph between traction energy and journey time computed varying γ_{S_i} from $\gamma_{S_i}^{(1)} = 0.71$ to $\gamma_{S_i}^{(2)} = 0.9$*

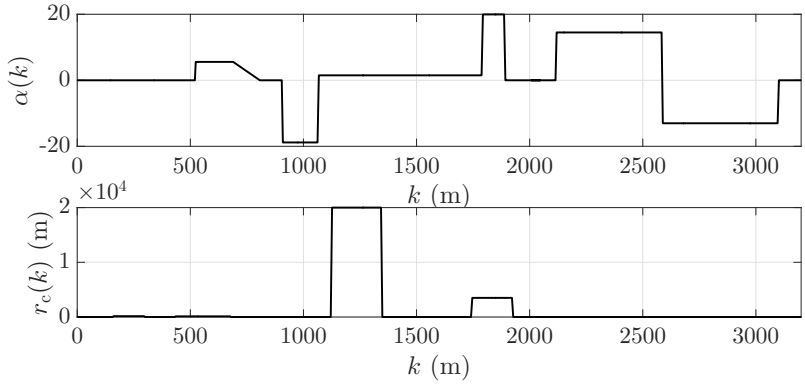

Figure 7.4: *From the top:Slope profile over the considered track: Radius of the curves of the considered track. The units are in meters.*

Table 7.1: *Values of journey time, traction and braking energy as a function of γ_{S_i}*

γ_{S_i}	x_{f_i}	E_{T_i} (kW h)	E_{B_i} (kW h)
0.71	324.8374	25.8686	-29.8699
0.75	315.7481	25.0872	-28.9236
0.83	287.5286	26.4371	-30.2063
0.87	277.0545	28.1431	-32.1269
0.9	269.921	29.5983	-33.6401

Table 7.2: *Results obtained with and without collaborative eco-drive*

	$J_{1_{\mathbf{x}_1}}$	$J_{2_{\mathbf{x}_2}}$	E_{T_1} (kW h)	E_{T_2} (kW h)	E_{B_1} (kW h)	E_{B_2} (kW h)	x_{f_1} (s)	x_{f_2} (s)
Eco-Drive	2083.2	2083.2	24.6698	24.6698	-28.1692	-28.1692	300.1505	300.1505
Co-Eco-Drive	2083.2	2037.2	24.6698	25.7221	-28.1692	-29.3333	300.1505	296.7020

Remark 7.1.1. *Note that, the triggering rule* (7.7) *is reasonable in practice since if the train j is not on time, it can exploit the energy of train i to accelerate. On the other hand, one can assume that the train j could decide not to accept the regenerative energy and maintain its current weight γ_{S_j} for the cost function.* □

7.1.2 Case Study

Here simulation results on a realistic scenario are presented. Simulations have been carried out by considering two trains. The considered track has three stops. In the considered scenario the consecutive trains run shifted in time by $60\,\mathrm{s}$. As discussed previously, assume that when the first train is approaching the stop and needs to brake thus regenerating energy available for sharing, the second delayed train, which could be either in acceleration mode or in cruising mode can benefit from this energy rather than demanding energy from the substation.

The two trains have identical parameters which are similar to the ones used in Chapter 6 (see Section 6.3 for details). Furthermore, since we are considering three stops instead of one, the considered track has curvature and slopes as illustrated in Fig. 7.4. Fig. 7.5 shows the time evolution of the velocity v_i for both the trains and the evolution of the weights γ_{S_i}, $i = 1, 2$ when the standalone eco-drive and the collaborative eco-drive (co-eco-drive) methods are applied, respectively. As expected the supervisor verifies the status of the trains. When the first train at about $80\,\mathrm{s}$ starts to brake, the second train, which is in cruise mode, decides to accelerate, by changing its weight value to 0.9, thus exploiting the braking energy of the first one. After the first stop, assuming that there are no delays, the same situation is repeated at time about $180\,\mathrm{s}$ and then at time about $300\,\mathrm{s}$. Table 7.2 shows the results obtained through the two strategies in terms of final value of the cost function $J_{i_{\mathbf{x}_i}}$, traction energy E_{T_i}, braking energy E_{B_i}, and journey time x_{f_i}. Looking at the results, we can conclude that in the case of collaboration, the value of the cost of the second train which receives the regenerated braking energy is reduced, though the traction energy associated with this train increases. This is due to the fact that the second train receives the regenerated energy from the first train and uses

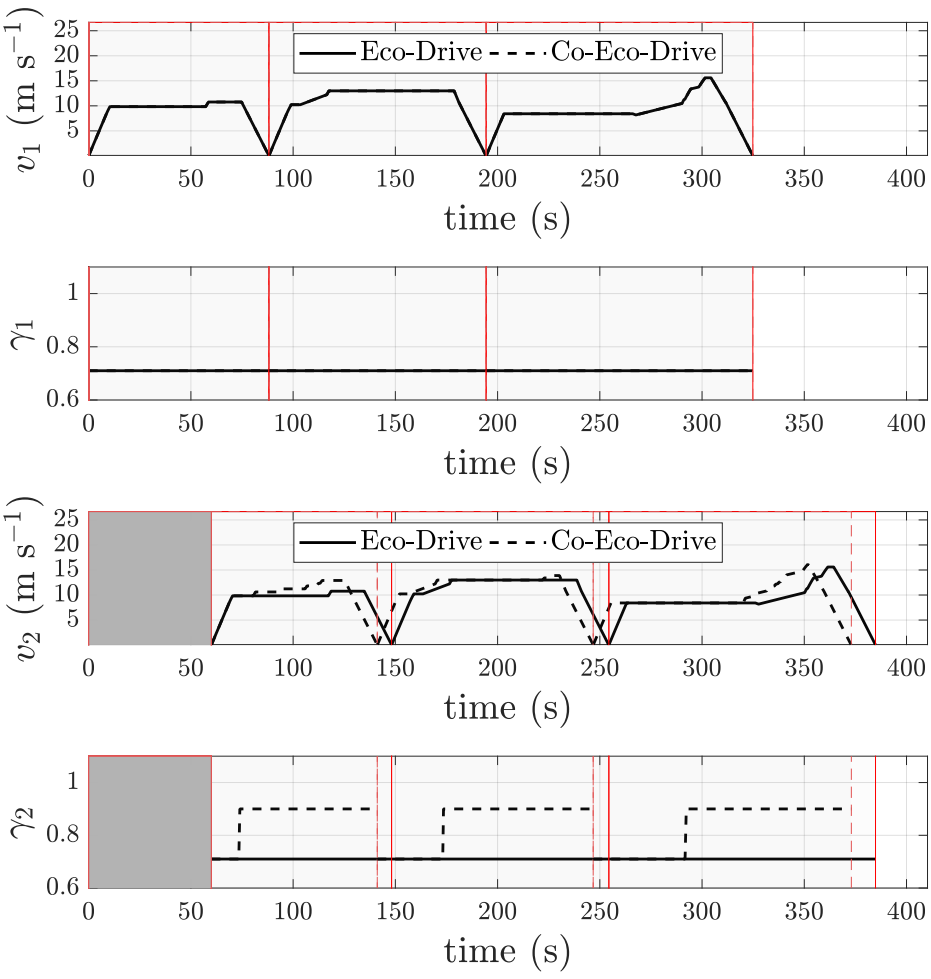

Figure 7.5: *Time evolution of the velocity profiles v_i, $i = 1, 2$ for both the considered trains and the corresponding weights γ_{S_i} of the cost function when the standalone eco-drive approach (solid black line) and the collaborative eco-drive method (dashed black line) are used*

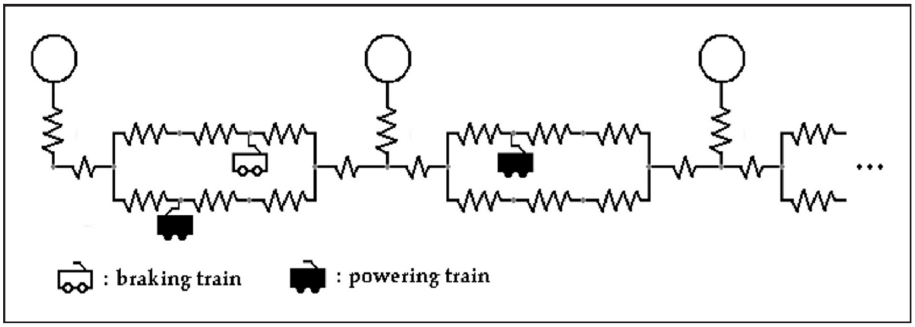

Figure 7.6: *Representational diagram of an equivalent DC electric circuit for substation model of a train network. This diagram has been borrowed from [62]*

it to accelerate and go faster. Looking at the final times, with the use of regenerated braking energy of the first train, the second train was able to arrive at the final stop faster, without asking any extra energy from the substation, which proves the advantage of using collaboration among trains as compared to no collaboration. Not only does collaboration help in saving energy directly but also prevents losses as a result of the transfer of energy from the substation to the train.

7.2 Multi-objective Relaxed SBPC Algorithm in a Networked Train Setup

For this strategy, we firstly present a simple model of the substation, which is essential to detect the regenerated energy in the substation network by detection of voltage change at the train nodes connected to the substation. In general, electrical trains can be classified as AC or DC based on their power source. In the earliest cases, electrical trains were based on DC power source, since AC was not well understood at that time, and insulation for high voltage lines (since AC systems are based on high voltage and low current) was not available. DC electric trains run at relatively low voltage (600 to 3000 volts), hence requiring very high currents in order to transmit sufficient power needed by the trains. So, they are not very feasible for the purpose of long distance trains as transferring high currents over huge distances can result in huge power losses. For the purpose of this thesis, we consider DC electric trains, which travel essentially short distances and hence current losses in the DC framework are not huge.

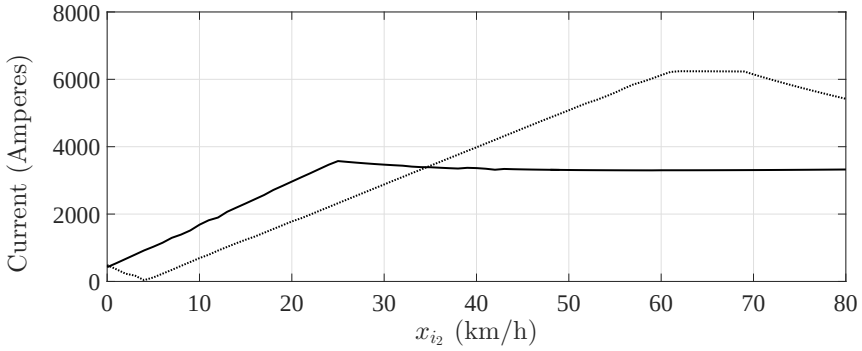

Figure 7.7: *Maximum substation traction current(solid line) and braking current (dotted) allowed for trains considered in the simulation for a source traction voltage of* 600 *volts and source braking voltage of* 685 *volts.*

7.2.1 Substation Model

Here, we introduce the electric model of the substation. In fact, as depicted in Fig. 7.6, from electrical view point one can model all track as a sequence of resistors connected to DC sources. Specifically, assume to have a resistive grid and let $V_{\rm s}$ be the substation source voltage, which is constant (for example 3000 volts in Italy), and let V_{T_i} and I_i be the train voltages in correspondence of its position and train currents, respectively. Moreover, letting $R_{\rm s}$ be the substation resistance, and $R(s_i)$ be the value of the resistance corresponding to the train position s, the algebraic model of the substation is captured by:

$$\begin{bmatrix} V_{T_1} \\ V_{T_2} \\ \vdots \\ V_{T_{\mathcal{M}}} \end{bmatrix} = \begin{bmatrix} -R_{\rm s} - R(s_1) & -R_{\rm s} & \cdots & -R_{\rm s} \\ -R_{\rm s} & -R_{\rm s} - R(s_2) & \cdots & -R_{\rm s} \\ \vdots & -R_{\rm s} & \ddots & \vdots \\ -R_{\rm s} & -R_{\rm s} & \cdots & -R_{\rm s} - R(s_{\mathcal{M}}) \end{bmatrix} \begin{bmatrix} I_1 \\ I_2 \\ \vdots \\ I_{\mathcal{M}} \end{bmatrix} + \begin{bmatrix} 1 \\ 1 \\ \vdots \\ 1 \end{bmatrix} V_{\rm s} \ . \quad (7.8)$$

The value of $R(s_i)$ considered in the simulation is 25 milli-ohms per km as provided by Alstom, while the corresponding currents as function of the train velocities are depicted in Fig. 7.7. For the ith train with $i > 1$ and the trains running consecutively delayed in time one after the other, when $V_{T_i} > V_{T_{i-1}}$, it means that regeneration is occurring. In this case, it means that the ith train behavior is that of a current generator, with current having opposite direction (see Fig. 7.1).

The strategy presented in this section is an extension of the SBPC strategy considered in Chapter 4 applied to the networked case. Now consider

the ith electric train in the network controlled by a digital control unit in discrete time, with sampling period T_{s_i}. The train control problem for the ith train has already been presented in detail in Section 4.1 of Chapter 4. For model of the ith train, refer to Eq. (4.1). In this case, since we want to use the regenerated energy available in the substation network, we will relax the terminal constraints on final space and include them as a terminal cost as in Subsection 4.3.2. In the networked case, the cost function for the ith train is given by:

$$J_i = \sum_{j_i=0}^{k_{f_i}-k_i} \ell(x_i(j_i|k_i), u_i(j_i|k_i)) + \omega_i \gamma_i \tag{7.9}$$

where

$$\begin{aligned} \ell_i(x_i(j_i|k_i), u_i(j_i|k_i)) &= \sum_{k_i=0}^{k_{f_i}} \gamma_{S_i}(I) \left| F_{T_i}(x_i(k_i), u_i(k_i)) x_{2_i}(k_i) \right| . \\ \gamma_i &= \Delta(x_i(k_{f_i}), X_{f_i}) \end{aligned} \tag{7.10}$$

where $\gamma_{S_i}(V_{T_i})$ depends on the train node voltage V_{T_i}, with $V_{T_i} = [V_{T_1},\, V_{T_2} \,\ldots\, V_{T_{\mathcal{M}}}]'$.

7.2.2 Supervisor

Now, we are in a position to exploit this signal as a triggering event to use the available regenerated energy in the network (see the control scheme in Fig. 7.2). In order to do this, we introduce the following strategy. Specifically, assuming two trains one can use a law of the following form

$$\gamma_{S_i} = \begin{cases} 1 & V_{T_i} < V_{T_{i-1}} \\ 0 & \text{otherwise} \end{cases} . \tag{7.11}$$

7.2.3 Case Study

Here simulation results on a realistic scenario are presented for Amsterdam metros. Simulations have been carried out by considering two trains. The considered track has four stops. In the considered scenario the consecutive trains run shifted in time by $120\,\mathrm{s}$. The two trains have identical parameters which are similar to the ones used in Chapter 4(see Section 4.4 for details). Furthermore, since we are considering four stops instead of one, the considered track has slopes as illustrated in Fig. 7.8.

Table 7.3: *Performances when using the proposed SBPC with (w/) and without (w/o) Collaborative strategy.*

i	Collaboration strategy	J_i [-]	E_{T_i} (KWH)
1	w/	1.1924e+10	19.9
	w/o	1.1924e+10	19.9
2	w/	1.7605e+09	23
	w/o	1.1924e+10	19.9

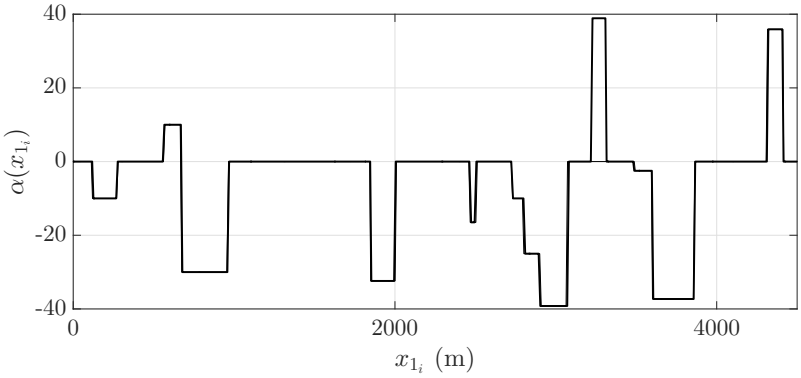

Figure 7.8: *Slope profile over the considered track. The unit is in per mille.*

Fig. 7.9 shows the evolution of the velocity x_{2_i} with respect to space for both the trains when collaboration is used. As expected, the substation verifies the status of the trains. When the first train starts to brake, the second train, decides to accelerate, by changing its weight value to 0, thus exploiting the braking energy of the first one. Table. 7.3 gives an idea of the performance, when collaboration is used as compared to no collaboration. As expected, with collaboration the cost decreases, but the traction energy of the second train which uses the regenerated energy of the first train to accelerate increases. This again shows the advantage of collaboration over no collaboration. Finally, Fig. 7.10 and Fig.7.11 show the time evolution of the velocity profile of the two trains when collaborating and their weight evolution respectively. When the first train brakes, the weight of the second train goes to zero and it starts accelerating.

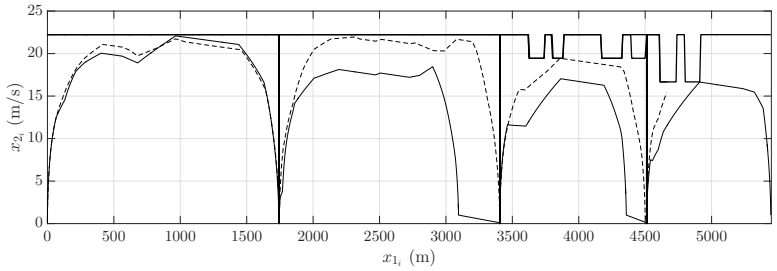

Figure 7.9: *Evolution of the velocity profiles x_{i_2}, $i = 1$ (solid line), 2 (dashed) of trains for track.*

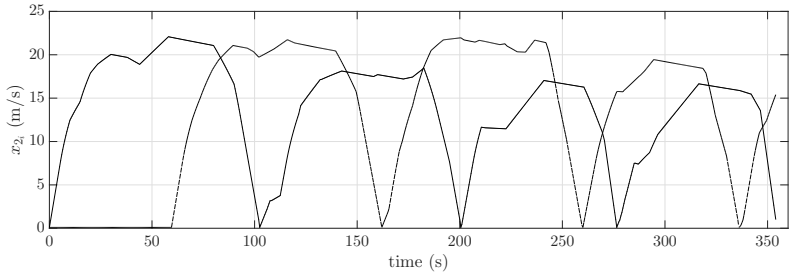

Figure 7.10: *Time evolution of the velocity profiles x_{i_2}, $i = 1$ (solid line), 2 (dashed) of trains for the entire track.*

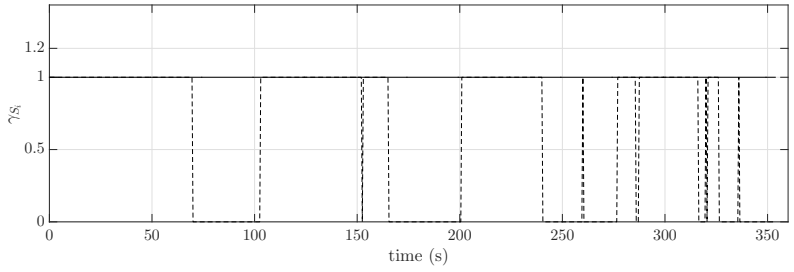

Figure 7.11: *Time evolution of the corresponding weights γ_{S_i} of the trains $i = 1$ (solid line), 2 (dashed) due to collaboration.*

CHAPTER 8

Collaborative Eco-Drive of Train Networks via Receding Horizon Switched Predictive Control and Dissension Strategy

This chapter presents another strategy for the collaboration among trains, which is based on Markov chains and has been presented in [27]. The strategy is again an extension of the adaptive RSPC strategy developed in Chapter 6 to the networked train system. In this case, an adaptive law similar to the concept of Markov chains is used in order for the trains which are connected to the same network to share the regenerated energy available in the network. A network consists of trains which are connected to the same substation and hence are able to share the regenerated energy among themselves. The main difference as compared to the adaptive RSPC strategy is that here the RSPC strategy is used with a time domain model of the train and the time samples are no longer changing but constant. Though, in time domain, there is possibility of the system dynamics in the form of slopes and curvature and also velocity limits to be overlooked, with a small enough sampling time, we can almost always make sure that it does not happen. Also, time domain modeling somehow makes it easier for the supervisor implementation in the networked case.

8.1 Switched Networked Train Control Problem

Consider a network $\mathcal{N}$ with $\mathcal{M}$ trains operating under the same substation and capable of communicating with each other. Let us denote each train in the network with the subscript $i = 1, \ldots, \mathcal{M}$. Now consider the ith electric train in the network controlled by a digital control unit in discrete time, with sampling period T_{s_i}. Let us denote with $k_i \in \mathbb{Z}$ the discrete time variable, with $x_i(k_i) = [x_{i_1}(k_i),\ x_{i_2}(k_i)]^T$ the states of the ith train, where x_{i_1} is its position and x_{i_2} its speed, and with $u_i(k_i) \in [-1, 1]$ a normalized traction force, where $u_i(k_i) = 1$ corresponds to the maximum applicable traction and $u_i(k_i) = -1$ to the maximum braking. The input u_i is the available control variable. The train has to move from one station with position $x_{i_1} = 0$ to the next one, with position $x_{i_1} = x_{f_i}$, in a prescribed time t_{f_i}. In state space modeling, the prescribed arrival position s_{f_i} (see Subsection 2.1.1) and the maximum allowed velocity limit $v_{i_{\max}}(k_i)$ (see Eq. 2.5) have been renamed as $s_{f_i} = x_{f_i}$ and $v_{i_{\max}}(k_i) = \overline{x}_{i_2}(k_i)$ to link them to the states they are representing. For a given pair of initial and final stations, the track features (slopes, curvature) are known in advance. Thus, in nominal conditions (i.e.with rated values of the train parameters, like its mass and the specifications of the powertrain and braking systems), according to Newton's laws and using the forward Euler discretization method, the equations of motion of a reasonably accurate switched model of this system read:

$$\begin{aligned} x_{i_1}(k_i+1) &= x_{i_1}(k_i) + T_{s_i} x_{i_2}(k_i) \\ x_{i_2}(k_i+1) &= x_{i_2}(k_i) + T_{s_i}\left(\frac{F_{T_i}((x_i(k_i), u_{i_{\sigma_i(k_i)}}(k_i)) - F_{B_i}(x_i(k_i), u_{i_{\sigma_i(k_i)}}(k_i)) - F_{R_i}(x_i(k_i))}{M_i}\right) \end{aligned} \tag{8.1}$$

As before, the parametric symbols have already been defined in Subsection 2.1.1 (see Tables 2.1 and 2.2 for more details). Making reference to the formulation in Eq.(6.1), since the switching signal is externally updated and is a function of space, system (8.1) is a time dependent switching system.

Remark 8.1.1. *For the ith train in the network, the model* (8.1) *has been rewritten in the form of* (6.1)*, where $\sigma_i(k_i) \in \{1, \ldots, 6\}$ is the switching signal, such that $u_{i_{\sigma_i(k_i)}}(k_i) \in \{-1,\ 0,\ 0.5,\ 0.75,\ 1,\ u_{i_{CR}}\}$ respectively, in terms of switching input handle, where $u_{i_{CR}}$ identifies the cruising mode (see Subsection 3.1.2). For example, $\sigma_i(k_i) = 1$ implies that $u_{i_1}(k_i) = -1$ is chosen to be applied to the system* (6.2) *at the sampling instant k_i.*

As already discussed in Subsection 2.1.1, besides the prescribed arrival time t_{f_i} and position x_{f_i}, there are additional state constraints that must be satisfied. These pertain to the limit on the maximum allowed velocity,

$\overline{x}_{i_2}(x_{i_1}(k_i))$, which depends on the position x_{i_1}, since a different velocity limit is imposed for safety by the regulating authority according to the track features at each position. Overall, by defining the terminal time step $k_f \doteq \lfloor t_f/T_s \rfloor$ (where $\lfloor \cdot \rfloor$ denotes the flooring operation to the closest integer), the state constraints read:

$$\begin{array}{ll} x_i(0) & = [0,\ 0]^T \\ x_i(k_{f_i}) & = [x_{f_i},\ 0]^T \\ x_{i_2}(k_i) & \geq 0,\ k_i = 0, \ldots, k_{f_i} \\ x_{i_2}(k_i) & \leq \overline{x}_{i_2}(x_{i_1}(k_i)),\ k_i = 0, \ldots, k_{f_i} \end{array} \tag{8.2}$$

The control objective is to maximize the energy efficiency of the ith train while satisfying the constraints above, which translates mathematically to minimizing the overall traction energy of the ith train given by:

$$J_i = \sum_{k_i=0}^{k_{f_i}} F_{T_i}(x_i(k_i), u_{i_{\sigma_i(k_i)}}(k_i)) x_{i_2}(k_i) \tag{8.3}$$

8.1.1 Problem Abstraction

The control problem described above for the ith train can be cast in a rather standard form:

$$\min_{\boldsymbol{\chi}_i} \sum_{k_i=0}^{k_{f_i}} \ell_{i_{\sigma_i(k_i)}}(x_i(k_i), u_{i_{\sigma_i(k_i)}}(k_i)) \tag{8.4a}$$

subject to

$$x_i(k_i+1) = f_{i_{\sigma_i(k_i)}}(x_i(k_i), u_{i_{\sigma_i(k_i)}}(k_i)) \tag{8.4b}$$

$$u_{i_{\sigma_i(k_i)}}(k_i) \in U_i,\ k_i = 0, \ldots, k_{f_i} - 1 \tag{8.4c}$$

$$x_i(k_i) \in X_i,\ k_i = 1, \ldots, k_{f_i} \tag{8.4d}$$

$$x_i(0) = x_{i_0} \tag{8.4e}$$

$$x(k_{f_i}) \in X_{f_i} \tag{8.4f}$$

where $x_i \in \mathbb{X} \subset \mathbb{R}^n$ is the system state and x_{i_0} is the initial condition. The symbol $\boldsymbol{\chi}_i = [\sigma_i(0), \ldots, \sigma_i(k_{f_i} - 1)]$ represents the vector of switching strategy to be applied to the plant. The sets $X_i \subset \mathbb{X}$ and $U_i \subset \mathbb{U}$ represent the state and input constraints (including the discrete set of allowed inputs or input modes as described above), and the set $X_{f_i} \subset \mathbb{X}$ the terminal state constraints, which include a terminal equality constraint as a special case. Furthermore, X_i is assumed to be compact, as well as the terminal constraint set X_{f_i}.

8.2 Receding Horizon Switched Predictive Control (RSPC) Approach in Time Domain

To solve (8.4) , a switched NMPC strategy with a receding horizon approach (RSPC) is adopted similar to the one in Chapter 6. The main difference with the RSPC strategy is that we are assuming constant time samples T_{s_i}, which makes it easier in the networked case for the supervisor strategy to be implemented. Also, due to the receding horizon approach explained in Subsection 8.2.1, the terminal constraint on time (see (8.2)) has been relaxed to be included as a terminal cost. Finally, in order to deal with braking dynamics which is very difficult to capture with receding horizon approach, a separate predictive braking approach in parallel is introduced.

8.2.1 Receding Horizon in a Networked Train Setup

Again consider the ith train in the network and denote its receding prediction horizon by N_i. In the networked setup, the cost function for the ith train is given by:

$$\begin{aligned} J_{i_{\boldsymbol{\chi}_i}}(x_i) = \sum_{j_i=0}^{N_i-1} \gamma_{S_i}(k_i)\ell_{i_{\sigma_i(j_i|k_i)}}(x_i(j_i|k_i), u_{i_{\sigma_i(j_i|k_i)}}(j_i|k_i)) \\ + (1-\gamma_{S_i}(k_i))F_i(x_i(N_i|k_i)) \end{aligned} \tag{8.5}$$

with $\boldsymbol{\chi}_i = [\sigma_i(0|k_i),\, \ldots,\, \sigma_i(N_i-1|k_i)]^\top$ being the predicted switching control sequence of the ith train. The terms

$$\begin{aligned} &\ell_{i_{\sigma_i(j_i|k_i)}}(x_i(j_i|k_i), u_{i_{\sigma_i(j_i|k_i)}}(j_i|k_i)) \\ &\qquad = \left(\frac{F_{T_i}((x_i(j_i|k_i), u_{i_{\sigma_i(j_i|k_i)}}(j_i|k_i)) - F_{R_i}(x_i(j_i|k_i))}{F_{T_{i_{\max}}}}\right)^2 \\ &F_i(x_i(N_i|k_i)) = \left(\frac{x_{i_1}(0|k_i) + S_{i_{horizon}}(k_i) - x_{i_1}(N_i|k_i)}{S_{i_{horizon}}(k_i)}\right)^2 \end{aligned} \tag{8.6}$$

Remark 8.2.1. *At each step k_i, the horizon distance $S_{i_{horizon}}(k_i)$ is the distance that the ith train needs to cover in that particular prediction horizon to be able to fulfill the final constraints on time, given the maximum allowed velocity limits, maximum allowed journey time, the final distance and the*

characteristics of the track. In order to compute $S_{i_{horizon}}$, a heuristic approach based on known information such as the final distance to the destination, the journey time and resistance force due to slopes and curvature is adopted.

8.2.2 RSPC Strategy

For the ith train, let us denote with $x_i(j_i|k_i)$, $j_i = 0, ..., k_{f_i} - k_i$ the state vectors predicted at space sample $k_i + j_i$ starting from the one at step k_i. At each step $k_i \in [0,\ k_{f_i} - 1]$, we formulate the following FHOCP:

$$\min_{\boldsymbol{\chi}_i(k)} \sum_{j_i=0}^{N_i-1} \ell_{i_{\sigma_i(j_i|k_i)}}(x_i(j_i|k_i), u_{i_{\sigma_i(j_i|k_i)}}(j_i|k_i)) + F_i(x_i(N_i|k_i)) \tag{8.7a}$$

subject to

$$\boldsymbol{\chi}_i(k) = [\sigma_i(0|k_i),\ \ldots,\ \sigma(N_i - 1|k_i)] \tag{8.7b}$$

$$x_i(j_i + 1|k_i) = f_{i_{\sigma_i(j_i|k_i)}}(x_i(j_i|k_i), u_{i_{\sigma_i(j_i|k_i)}}(j_i|k_i)),\ j_i = 0, \ldots, N_i - 1 \tag{8.7c}$$

$$u_{i_{\sigma_i(j_i|k_i)}}(j_i|k_i) \in U_i,\ j_i = 0, \ldots, N_i - 1 \tag{8.7d}$$

$$x_i(j_i|k_i) \in X_i,\ j_i = 1, \ldots, N_i \tag{8.7e}$$

$$x_i(0|k_i) = x_i(k_i) \tag{8.7f}$$

$$x_i(N_i|k_i) \in X_{f_i} \tag{8.7g}$$

We denote with $\boldsymbol{\chi}_i^*(k_i) = [\sigma_i^*(0|k_i),\ \ldots,\ \sigma_i^*(N_i - 1|k_i)]$ the optimal switching strategy of the ith train obtained by solving (8.7) . Moreover, we denote with $\boldsymbol{x}_i^*(k_i)$ and $\boldsymbol{u}^*_{i_{\boldsymbol{\chi}_i^*(k_i)}}(k_i)$ the corresponding predicted sequences of state and input vectors:

$$\boldsymbol{x}_i^*(k_i) = \{x_i^*(0|k_i), \ldots, x_i^*(N_i|k_i)\} \tag{8.8a}$$

$$\boldsymbol{u}^*_{i_{\boldsymbol{\chi}_i^*(k_i)}}(k_i) = \{u^*_{i_{\sigma_i^*(0|k_i)}}(0|k_i), \ldots, u^*_{i_{\sigma_i^*(N_i-1|k_i)}}(N_i - 1|k_i)\} \tag{8.8b}$$

where

$$x_i^*(0|k_i) = x_i(k_i) \tag{8.8c}$$

$$x_i^*(j_i + 1|k_i) = f_{i_{\sigma_i^*(j_i|k_i)}}(x_i^*(j_i|k_i), u^*_{i_{\sigma_i^*(j_i|k_i)}}(j_i|k_i)) \tag{8.8d}$$

The RSPC strategy is obtained by recursively solving (8.7), as described by the following pseudo-algorithm.

Algorithm 7 RSPC Strategy

1. At sampling instant k_i, measure the state $x_i(k_i)$ and solve the FHOCP (6.9). Let $\boldsymbol{\chi}_i^*(k_i)$ be the computed switching strategy solution;
2. Apply to the plant the first element of the control sequence $\boldsymbol{u}^*_{i_{\boldsymbol{\chi}_i^*(k_i)}}(k_i)$.
3. Repeat the procedure from 1) at the next sampling period.

Algorithm 7 defines the following switching strategy

$$\chi_i(k_i) = \sigma_i^*(0|k_i) \tag{8.9}$$

which in turn defines the following feedback control law:

$$u_{i_{\sigma_i(k_i)}}(k_i) = \mu_i(x_i(k_i)) = u^*_{i_{\sigma_i^*(0|k_i)}}(0|k_i), \tag{8.10}$$

and the resulting model of the closed-loop system is:

$$x_i(k_i+1) = f_{i_{\sigma_i^*(0|k_i)}}(x_i(k_i), \mu(x_i(k_i)) \tag{8.11}$$

Finally, for the ith train, at each step k, the applied switching strategy $\chi_i(k)$ is chosen according to the adaptive RSPC strategy in Algorithm 8.

8.2.3 Adaptive RSPC Strategy

At any step k_i, the braking time $T_{b_i}(k_i)$ needed for the train to stop based on the current velocity $x_{i_2}(k)$ can be calculated by the following equation with the input $u_{i_{\sigma_i(k_i)}}(k_i)) = -1$:

$$0 = x_{i_2}(k_i) + T_{b_i}(k_i)\left(\frac{-F_{B_i}(x_i(k_i), u_{i_{\sigma_i(k_i)}}(k_i)) - F_{R_i}(x_i(k_i))}{M_i}\right) \tag{8.12}$$

Also, at any step k_i, let the remaining time left for the train to reach the arrival station be denoted by $T_{p_i}(k_i)$. For a graphical representation of $T_{b_i}(k_i)$ and $T_{p_i}(k_i)$, refer to Fig. 8.1 for an example.

Finally, the resultant time $\delta T_i(k_i)$ can be calculated by

$$\delta T_i(k_i) = T_{p_i}(k_i) - T_{b_i}(k_i). \tag{8.13}$$

The adaptive RSPC strategy is obtained by the following algorithm.

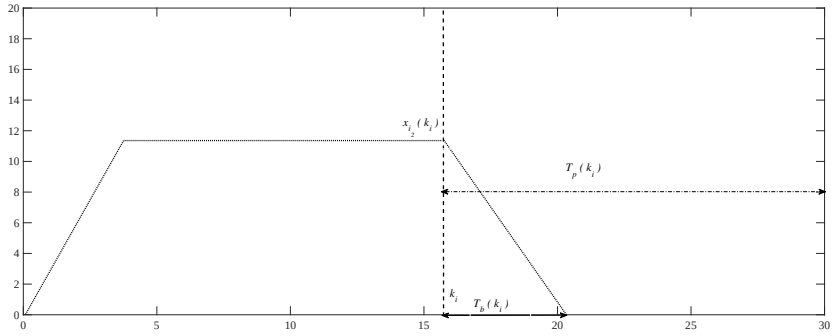

Figure 8.1: *As an example, graphical representations of the prediction times for braking, $T_{p_i}(k_i)$ and $T_{b_i}(k_i)$ are shown at the current step k_i for the ith train.*

Algorithm 8 Adaptive RSPC Algorithm

if $\delta T_i(k_i) > 0$ **then**
  $\chi_i(k) = \sigma_i^*(0|k_i)$
else if $\delta T_i(k_i) = 0$ **then**
  $\chi_i(k_i) = \sigma_i(k_i) = 1, i.e.\ \ u_{i_1}(k_i) = -1.$
end if

8.3 Dissension Strategy

The aim of the proposed dissension strategy is to make the trains of the network cooperate in order to exploit the regenerative braking energy when one or more of the trains are in braking operation mode. When braking is detected in any of the trains, the non-braking trains are allowed to accelerate if they need, of course without constraint violation on the maximum allowed velocity limits. The main idea underlying this strategy is to induce this behavior though the tuning of the weights γ_{S_i} associated with each train i in the RSPC cost function (8.5) by the application of the dissension strategy. The proposed control scheme is reported in Fig. 8.2.

Hereafter we assume that the state of the network is detected by a supervisor or each train i has full knowledge of the actual state of the other ones. The network $\mathcal{N}$ can be described through a directed graph $\mathcal{G} = (\mathcal{N}, \mathcal{E})$, where $\mathcal{N} = \{1, \ldots, \mathcal{M}\}$ is the set of nodes (trains), $\mathcal{E} \subseteq \mathcal{N} \times \mathcal{N}$ are the edges associated to communication links such that (t_t, t_r) belongs to $\mathcal{E}$, if and only if the train t_t transmits information to train t_r and the ith train can be considered as ith agent of the network. Moreover, let $\mathcal{N}_{\mathrm{r}} = \{t_r \in \mathcal{N} : (t_t, t_r) \in \mathcal{E}\}$ be the set of receiving neighbors of agent i, while

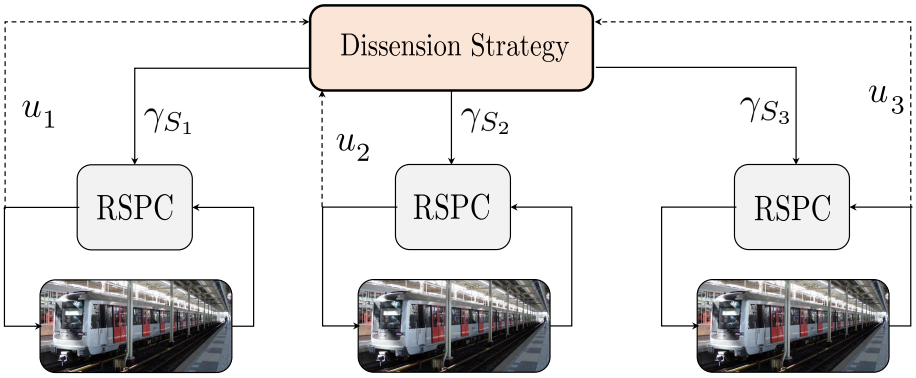

Figure 8.2: *Collaborative eco-drive using dissension strategy architecture.*

$\mathcal{N}_{\mathrm{t}} = \{t_t \in \mathcal{N} \,:\, (t_r,\, t_t) \in \mathcal{E}\}$ be the set of transmitting neighbors of agent i. Moreover, the communication graph is symmetric and complete, i.e., $\mathcal{N}_{\mathrm{t}} = \mathcal{N}_{\mathrm{r}} = \mathcal{N}$ and $\mathcal{N}_i = \mathcal{N} \setminus i$, respectively. The notation $\mathcal{S}$ represents the number of states of each agent such that $p = 1, \ldots, \mathcal{S}$. For our case, consider that each train $i \in \mathcal{N}$ of the substation can assume two possible states, i.e., $\mathcal{S} = 2$:

1. *State 1:* indicates the braking (B) operation mode;
2. *State 2:* all the other possible modes: Acceleration (AC), Cruising (CR), Coasting (CO).

For the sake of clarity, the continuous-time domain is considered. Having in mind a dissension behavior of the trains in the network, for the ith train in the network, we define the following adaptive law in order to determine the weights γ_{S_i} in (8.5), i.e.,

$$\dot{q}_i = \left(Q_i^T + \mathcal{A}_i^T\right) q_i \tag{8.14}$$

where $q_i = [\gamma_{S_i},\, 1 - \gamma_{S_i}]^T$. The matrices Q_i and $\mathcal{A}_i$ are Metzler matrices. Matrix Q_i satisfies the property $\mathbf{1}^T Q_i = 0$, while the matrix $\mathcal{A}_i$ represents the interaction dynamics of the agent i with the neighboring agents, such that

$$a_{lm_i}(t) = \frac{\lambda_p}{\mathcal{M} - 1} \sum_{\kappa \in \mathcal{N}_i} \mathcal{I}_\kappa \tag{8.15}$$

$$\mathcal{I}_\kappa = \begin{cases} 1 & p = 1, \quad \text{(i.e., B)} \\ 0 & \text{otherwise} \end{cases} \tag{8.16}$$

with λ_p being the influence strength intensity, while $\mathcal{I}_\kappa$ being an indicator function equal to one when the κth train is braking, zero otherwise and

$$a_{ll_i}(t) = -\sum_{m=1,\, m\neq l}^{\mathcal{S}} a_{lm_i}(t) \tag{8.17}$$

Now, consider the overall network $\mathcal{N}$. Let $\Sigma(t) \in \mathcal{S}^{\mathcal{M}}$ be the state of the network and $q(t) = \otimes_{i=1}^{\mathcal{M}} q_i(t)$ denote the distribution of $\Sigma(t)$. The entries of $q(t)$ represent the condition at time t of a given configuration of the train states in the network. The dynamics of $q(t)$ obeys the differential equation

$$\dot{q}(t) = Q_0^T q(t) \tag{8.18}$$

with

$$Q_0 = \sum_{i=1}^{\mathcal{M}} I_{\mathcal{S}^{i-1}} \otimes Q_i \otimes I_{\mathcal{S}^{\mathcal{M}-i}} \ . \tag{8.19}$$

Given the interaction model (8.14) of the ith train, the whole dynamics of the network is given by

$$\dot{q}(t) = (Q_0^T + A_0^T) q(t) \tag{8.20}$$

Model (8.20) describes the desired dissension behavior. That is, the transition rate to state 2 (AC, CR, CO) undergoes an increase which is proportional to the number of neighbors that are in state 1 (B). Since $\lambda_2 = 0$, trains cannot brake if the other ones are accelerating. Moreover, simultaneous state jumps are not allowed.

Remark 8.3.1. *Note that, in principle the case $\lambda_2 > 0$ could be possible. In fact, if for some reason, the authority decided to force some delayed trains to accelerate, it could exploit also the regenerative energy of trains which are on time and accelerating, making them brake. Hence, with $\lambda_2 > 0$, it is possible for the transition rate to state 1 (B) to undergo an increase which is proportional to the number of neighbors that are in state 2 (i.e., AC, CR, CO).*

Remark 8.3.2. *Note that the proposed adaptive strategy resembles a consensus algorithm characterized by time-homogeneous Markov stochastic processes with infinitesimal generator $Q_i \in \mathbb{R}^{2\times 2}$, the entries q_{lm_i} of which represent the transition rates between $\mathcal{S}^{\mathcal{M}}$ states $\mathcal{P}_i(t)$, with $\mathcal{P}_i(t) \in \mathcal{S}$ and $\mathcal{S} = \{1,\, 2\}$. By analogy, the weight γ_{S_i} are the probability of being in state 1 (i.e., in braking mode) at time t. Precisely, one would have that*

$$\gamma_{S_i} = \mathbb{P}\left\{\mathcal{P}_i(t) = 1\right\} \ . \tag{8.21}$$

Analogously, the probability distribution would obey the differential equation (8.14) *with entries of the Metzler matrix* $\mathcal{A}_i$ *such that*

$$a_{lm_i}(t) = \frac{\lambda_p}{\mathcal{M}-1} \sum_{\kappa \in \mathcal{N}_i} \mathcal{I}_{\mathcal{P}_\kappa(t)} \tag{8.22}$$

$$\mathcal{I}_{\mathcal{P}_\kappa(t)} = \begin{cases} 1 & \mathcal{P}_\kappa(t) = 1 \\ 0 & \textit{otherwise} \end{cases} \tag{8.23}$$

with $\lambda_1 > 0$ *and* $\lambda_2 = 0$*. In this case, the model describes a dissension behavior, that is the transition rate to state* m *undergo an increase which is proportional to the number of neighbors that share opinion* l*.*

8.4 Case Study

Consider a substation with three trains ($\mathcal{M} = 3$). The matrix A_0 for this network topology is as follows:

$$\left[\begin{array}{cccc:cccc} -3\lambda_1 & \lambda_1 & \lambda_1 & 0 & \lambda_1 & 0 & 0 & 0 \\ 0 & -\lambda_1 & 0 & \frac{\lambda_1}{2} & 0 & \frac{\lambda_1}{2} & 0 & 0 \\ 0 & 0 & -\lambda_1 & \frac{\lambda_1}{2} & 0 & 0 & \frac{\lambda_1}{2} & 0 \\ 0 & 0 & 0 & -\lambda_1 & 0 & 0 & 0 & \lambda_1 \\ \hdashline 0 & 0 & 0 & 0 & -\lambda_1 & \frac{\lambda_1}{2} & \frac{\lambda_1}{2} & 0 \\ 0 & 0 & 0 & 0 & 0 & -\lambda_1 & \lambda_1 & 0 \\ 0 & 0 & 0 & 0 & 0 & 0 & -\lambda_1 & \lambda_1 \\ 0 & 0 & 0 & 0 & 0 & 0 & 0 & 0 \end{array}\right].$$

Note that, for instance the first row represents the transition starting from $\Sigma(t) = [1\,1\,1]^T$, that is when all the trains are in braking and only one train at that time is allowed to accelerate if the others are braking. Conversely, the last row is zero because it corresponds to transitions starting from $\Sigma(t) = [2\,2\,2]^T$, that is they are in acceleration, cruising or coasting mode. Analogously, the bottom left 4×4 block is also zero.

The trains used in the simulations have exactly the same parameters, which are similar to the train used in the simulations of Chapter 6. Simulations have been carried out by considering three trains ($N = 3$), with the total track having 20 stops. The route has a total length of $22.4\,\mathrm{km}$. The parameters of the entire track, which are curve radius and slopes are shown in Fig. 8.3. Furthermore, in the considered scenario the consecutive trains run shifted in time by $48\,\mathrm{s}$ and $80\,\mathrm{s}$, respectively with respect to the first one. The sampling time is $T_\mathrm{s} = 0.4\,\mathrm{s}$ and the initial weights for each train are

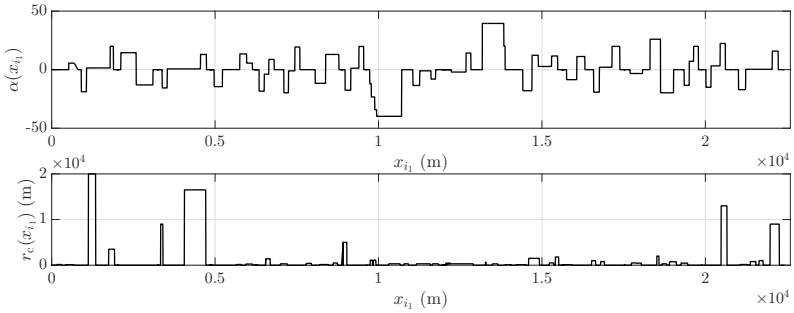

Figure 8.3: *From the top:slope profile of the considered track in per mille with respect to distance* x_{i_1}, $i = 1, 2, 3$*; radius of curve of the considered track in meters with respect to distance* x_{i_1}, $i = 1, 2, 3$*;*

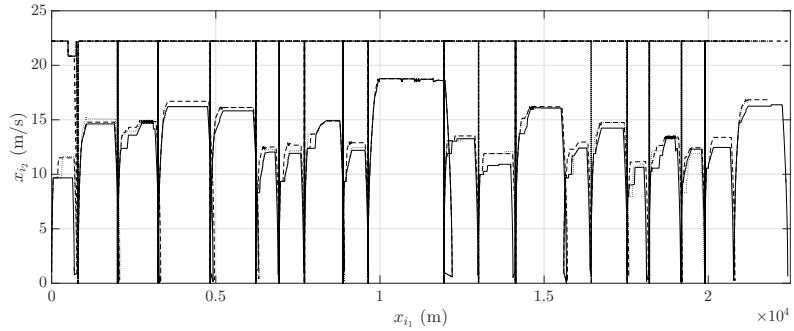

Figure 8.4: *Evolution of the velocity profiles* x_{i_2}, $i = 1$ *(solid line),* 2 *(dashed),* 3 *(dotted) of trains for the entire track.*

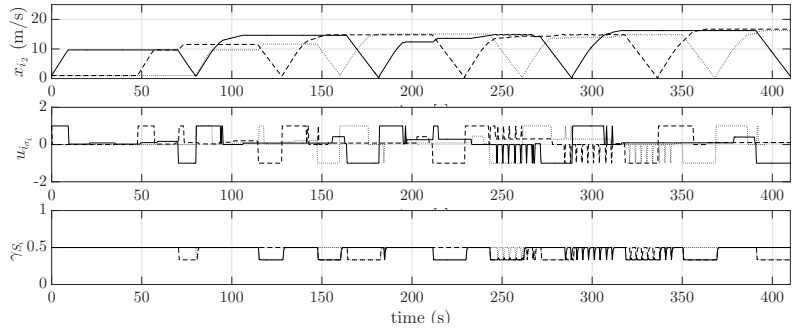

Figure 8.5: *From the top: time evolution of the velocity profiles* $x_{i_2}, i = 1$ *(solid line),* 2 *(dashed),* 3 *(dotted) of trains over time; time evolution of the handle* u_i, $i = 1$ *(solid line),* 2 *(dashed),* 3 *(dotted); time evolution of the weights* γ_{S_i}, $i = 1$ *(solid line),* 2 *(dashed),* 3 *(dotted) of the cost function* (8.5)*.*

Table 8.1: *Performances when using the proposed RSPC with (w/) and without (w/o) Dissension strategy.*

i	Dissension strategy	J_i [-]	E_{T_i} (KWH)	E_{B_i} (KWH)
1	w/	50572	545.46	401.54
	w/o	50610	511.29	372.22
2	w/	37455	581.82	415.13
	w/o	44886	503.58	349.26
3	w/	43126	557.93	397.42
	w/o	47971	500.09	349.26

chosen as $\gamma_{S_i} = 0.5$ being the first entry of the Frobenius left eigenvector associated with Q_i ($i = 1, 2, 3$).

Fig. 8.4 shows the evolution of the train speed over all the track. It can be observed that the velocity limits are always fulfilled and sometimes trains behave in different way depending on the weights γ_{S_i} used in the cost function. More specifically, the effect of the Dissension strategy can be better appreciated in Fig. 8.5, where for the sake of clarity only the first four stops ($5\,\mathrm{km}$) are illustrated. Fig. 8.5, in fact, reports the time evolution of the velocity x_{i_2} for all the trains, the corresponding inputs $u_{i_{\sigma_i}}$ and weights γ_{S_i}, $i = 1,\ 2,\ 3$. As expected, after $48\,\mathrm{s}$ the second train (dashed line) starts to run and analogously the third train (dotted line) after $80\,\mathrm{s}$. While initially all the profiles are identical, the effect of Dissension strategy is visible at $70.8\,\mathrm{s}$ when the second train is induced to accelerate by virtue of the braking energy provided by the first train (solid line). The same situation occurs at the time instant $115.2\,\mathrm{s}$ when the second train starts to brake and the third one accelerates. At the time $214\,\mathrm{s}$ the first train instead accelerates thanks to the braking energy provided by the second one. In correspondence of these events the values of γ_{S_i} of the braking trains decrease from 0.5 to 0.3. Note also that γ_{S_i} is reset equal to 0.5 after each stop. Numerical results for the performances in terms of value of the cost function (J_i), traction energy (E_{T_i}) and braking energy (E_{B_i}), both expressed in KWH, are reported in Table 8.1. It can be observed that the values of the cost function are reduced for all the trains when the proposed RSPC with Dissension strategy is adopted. As a consequence of this mechanism, the traction energy of all the trains is higher with respect to the case without collaboration. This is because the braking energy shared among the trains is exploited. On the other hand, higher braking energy is required. Then, by virtue of this strategy, trains do not need to require energy from the grid, thus avoiding possible losses and achieving a better grid utilization.

8.5 Conclusion

This chapter considered the problem of energy efficient train operation with eco-drive in a collaborative way. To address this problem, an optimal control solution to predict the velocity profile of a train by using switching RSPC algorithm in a collaborative fashion was proposed. For the purpose, a Dissension strategy was introduced to manage all the trains governed by the same substation and tune the RSPC law in order to use the braking energy, while taking into account constraints on velocity and journey times. Results show that the proposed RSPC is able to minimize the traction energy, which depends on the input handle and on the characteristics of the track while fulfilling all the constraints. Moreover, the Dissension strategy allows trains to effectively use the regenerated energy which is available in the substation when braking occurs.

CHAPTER 9

Conclusions

This thesis explored the problem of energy efficient control of railways. The main goal was to develop driving styles which are energy efficient and environment friendly. Moving from the current state of art, two main research directions were explored. The first research direction was associated with a single train control problem, where the control problem was to find the best driving strategy for the train to go from one stop to another, given an optimal timetable. As mentioned, EETC strategies can be either fully automated (ATO) or serve as an advisory system to the driver (DAS) for the purpose of assisting drivers in following an energy efficient driving style. For this purpose, three control strategies using Model Predictive Control (MPC) were presented. In the first two strategies, shrinking horizon techniques were combined with input parametrization approaches to reduce the computational burden of the control problem and to realize the nonlinear integer programming control problem which arises in the DAS scenario, while the third strategy was based on switching MPC with receding horizon. All the strategies were tested on the official simulation tool CITHEL of our industrial partner Alstom, and the obtained results in comparison with the existing techniques were proven to be more energy efficient.

The second research direction, which falls under the paradigm of col-

laborative eco-drive control strategies, involved multiple trains belonging to a substation network. The main aim was to use the energy regenerated by the braking trains through collaboration among the trains connected and active in the network. In this case, three strategies to decide the collaborative law were presented along with the extensions from the single train control strategies presented in the first part of the thesis. For the design of collaborative laws, techniques such as manual supervision, substation modeling and dissension based adaptive laws with concept similar to Markov chains were used. The strategies were validated with simulation examples. Finally, comparisons of energy efficiency with and without collaboration were presented in each case, which showed the advantage of using the developed collaborated laws as compared to no collaboration.

Bibliography

[1] UIC (2012). Moving towards sustainable mobility, paris, france.

[2] National Geographic (2018). Causes and effects of climate change.

[3] Amie Albrecht, Phil Howlett, Peter Pudney, Xuan Vu, and Peng Zhou. The key principles of optimal train controlpart 1: Formulation of the model, strategies of optimal type, evolutionary lines, location of optimal switching points. *Transportation Research Part B: Methodological*, 94:482–508, 2016.

[4] Amie Albrecht, Phil Howlett, Peter Pudney, Xuan Vu, Peng Zhou, and Dewang Chen. Using maximum power to save energy. In *Intelligent Transportation Systems (ITSC), 2014 IEEE 17th International Conference on*, pages 1205–1208. IEEE, 2014.

[5] Amie Albrecht, Phil Howlett, Peter Pudney, Xuan Vu, Peng Zhou, et al. The two train separation problem on level track. 2013.

[6] Amie Albrecht, Phil Howlett, Peter Pudney, Xuan Vu, Peng Zhou, et al. Using timing windows to allow energy-efficient recovery from delays. In *10th World Congress on Rail Research*, 2013.

[7] Amie R Albrecht, Phil G Howlett, Peter J Pudney, and Xuan Vu. Energy-efficient train control: from local convexity to global optimization and uniqueness. *Automatica*, 49(10):3072–3078, 2013.

[8] Thomas Albrecht and Steffen Oettich. A new integrated approach to dynamic schedule synchronization and energy-saving train control. *WIT Transactions on The Built Environment*, 61, 2002.

[9] Szilárd Aradi, Tamas Becsi, and Péter Gáspár. A predictive optimization method for energy-optimal speed profile generation for trains. In *Computational Intelligence and Informatics (CINTI), 2013 IEEE 14th International Symposium on*, pages 135–139. IEEE, 2013.

[10] IA Asnis, AV Dmitruk, and NP Osmolovskii. Solution of the problem of the energetically optimal control of the motion of a train by the maximum principle. *USSR Computational Mathematics and Mathematical Physics*, 25(6):37–44, 1985.

[11] Yun Bai, Tin Kin Ho, Baohua Mao, Yong Ding, and Shaokuan Chen. Energy-efficient locomotive operation for chinese mainline railways by fuzzy predictive control. *IEEE Transactions on Intelligent Transportation Systems*, 15(3):938–948, 2014.

[12] LA Baranov, IS Meleshin, et al. Optimal control of a subway train with regard to the criteria of minimum energy consumption. *Russian Electrical Engineering*, 82(8):405, 2011.

[13] BR Benjamin, AM Long, IP Milroy, RL Payne, PJ Pudney, et al. Control of railway vehicles for energy conservation and improved timekeeping. In *Conference on Railway Engineering 1987: Preprints of Papers*, page 41. Institution of Engineers, Australia, 1987.

[14] VF. Borrelli, A. Bemporad, and M. Morari. *Predictive Control for Linear and Hybrid Systems*. Cambridge University Press, 2017.

[15] Raphael Cagienard, Pascal Grieder, Eric C Kerrigan, and Manfred Morari. Move blocking strategies in receding horizon control. *Journal of Process Control*, 17(6):563–570, 2007.

[16] Danilo Caporale, Patrizio Colaneri, and Alessandro Astolfi. Adaptive nonlinear control of braking in railway vehicles. In *Decision and Control (CDC), 2013 IEEE 52nd Annual Conference on*, pages 6892–6897. IEEE, 2013.

[17] CS Chang, YH Phoa, W Wang, and BS Thia. Economy/regularity fuzzy-logic control of dc railway systems using event-driven approach. *IEE Proceedings-Electric Power Applications*, 143(1):9–17, 1996.

[18] Patrizio Colaneri, Jose C. Geromel, and Alessandro Astolfi. Stabilization of continous-time switiched nonlinear systems. *Systems and Control Letters*, 57(1):95–103, 2008.

[19] Patrizio Colaneri and Riccardo Scattolini. Robust model predictive control of discrete-time switched systems. *IFAC Proceedings Volumes*, 40(14):208–212, 2007.

[20] William J Davis. *The tractive resistance of electric locomotives and cars*. General Electric, 1926.

[21] Bart De Schutter, T Van den Boom, and A Hegyi. Model predictive control approach for recovery from delays in railway systems. *Transportation Research Record: Journal of the Transportation Research Board*, (1793):15–20, 2002.

[22] Luigi Del Re, Frank Allgöwer, Luigi Glielmo, Carlos Guardiola, and Ilya Kolmanovsky. *Automotive model predictive control: models, methods and applications*, volume 402. Springer, 2010.

[23] L. Fagiano and A.R. Teel. Generalized terminal state constraint for model predictive control. *Automatica*, 49(5):2622–2631, 2013.

[24] H. Farooqi, L. Fagiano, and P. Colaneri. Efficient train operation via shrinking horizon parametrized predictive control. In *Proceedings of the 6th IFAC Conference on Nonlinear Model Predictive Control*, Madison, WI, USA, 2018.

[25] H. Farooqi, L. Fagiano, and P. Colaneri. Shrinking horizon move-blocking predictive control with application to efficient train operation. *Submitted to Automatica*, 2018.

[26] H. Farooqi, G. P. Incremona, and P. Colaneri. Collaborative eco-drive of railway vehicles via switched nonlinear model predictive control. In *Proceedings of the 18th IFAC Conference on Technology Culture and International Stability*, Baku, Azerbaijan, 2018.

[27] H. Farooqi, G. P. Incremona, and P. Colaneri. Railway collaborative ecodrive via dissension based switching nonlinear model predictive control. *Submitted to European Control Journal*, 2018.

[28] James B Forsythe. Light rail/rapid transit: new approaches for the evaluation of energy savings, part ii-on the receptivity of a transit system. *IEEE Transactions on Industry Applications*, (5):665–678, 1980.

[29] Rüdiger Franke, Peter Terwiesch, and Markus Meyer. An algorithm for the optimal control of the driving of trains. In *Decision and Control, 2000. Proceedings of the 39th IEEE Conference on*, volume 3, pages 2123–2128. IEEE, 2000.

[30] Yang Gang and Liu Mingguang. Nmpc applied to operation of high-speed train. In *Computer Science and Network Technology (ICCSNT), 2012 2nd International Conference on*, pages 1005–1008. IEEE, 2012.

[31] Jose C. Geromel and Patrizio Colaneri. Stability and stabilization of continous-time switiched systems. *Society for Industrial and Applied Mathematics*, 45(5):1915–1930, 2006.

[32] Jose C. Geromel and Patrizio Colaneri. Stability and stabilization of discrete-time switiched systems. *International Journal of Control*, 79(7):719–728, 2006.

[33] Nima Ghaviha, Javier Campillo, Markus Bohlin, and Erik Dahlquist. Review of application of energy storage devices in railway transportation. *Energy Procedia*, 105:4561–4568, 2017.

[34] MATTEO GIUGNO. Ecodrive: speed tuning for energy saving in railway vehicles. 2014.

[35] Ravi Gondhalekar and Jun-ichi Imura. Recursive feasibility guarantees in move-blocking MPC. In *46th IEEE Conference on Decision and Control*, pages 1374–1379, 2007.

[36] Ravi Gondhalekar and Jun-ichi Imura. Strong feasibility in input-move-blocking model predictive control. *IFAC Proceedings Volumes*, 40(12):816–821, 2007.

[37] Ravi Gondhalekar and Jun-ichi Imura. Least-restrictive move-blocking model predictive control. *Automatica*, 46(7):1234–1240, 2010.

[38] Ravi Gondhalekar, Jun-ichi Imura, and Kenji Kashima. Controlled invariant feasibility - a general approach to enforcing strong feasibility in MPC applied to move-blocking. *Automatica*, 45(12):2869–2875, 2009.

[39] G. C. Goodwin, M. M. Seron, and J. A. De Don. *Constrained control and estimation: an optimisation approach*. Springer, London, 2005.

[40] E Greenberg. An activists journey to raise awareness about electromagnetic pollution, 19 (4). 56-65. *Explore Publication*, 2010.

[41] Qing Gu, Tao Tang, Fang Cao, and Yong-duan Song. Energy-efficient train operation in urban rail transit using real-time traffic information. *IEEE Transactions on Intelligent Transportation Systems*, 15(3):1216–1233, 2014.

[42] Izumi Hasegawa, Seigo Uchida, et al. Braking systems. *Japan Railway and Transport Review*, 20:52–59, 1999.

[43] PG Howlett, IP Milroy, and PJ Pudney. Energy-efficient train control. *Control Engineering Practice*, 2(2):193–200, 1994.

[44] Phil Howlett. An optimal strategy for the control of a train. *The ANZIAM Journal*, 31(4):454–471, 1990.

[45] Phil G Howlett, Peter J Pudney, and Xuan Vu. Local energy minimization in optimal train control. *Automatica*, 45(11):2692–2698, 2009.

[46] Shiuh-Jer Huang and Shang-Lin Her. Fuzzy control of automatic train operation system. *International Journal of Modelling and Simulation*, 17(2):143–150, 1997.

[47] Kunihiko Ichikawa. Application of optimization theory for bounded state variable problems to the operation of train. *Bulletin of JSME*, 11(47):857–865, 1968.

[48] Eugene Khmelnitsky. On an optimal control problem of train operation. *IEEE transactions on automatic control*, 45(7):1257–1266, 2000.

[49] L.Grune and J.Pannek. *Nonlinear Model Predictive Control*. Springer, London, 2011.

[50] Shengbo Eben Li, Zhenzhong Jia, Keqiang Li, and Bo Cheng. Fast online computation of a model predictive controller and its application to fuel economy–oriented adaptive cruise control. *IEEE Transactions on Intelligent Transportation Systems*, 16(3):1199–1209, 2015.

[51] Zhong-Qi Li, Hui Yang, Kun-Peng Zhang, and Ya-Ting FU. Distributed model predictive control based on multi-agent model for electric multiple units. *Acta Automatica Sinica*, 40(11):581–586, 2014.

[52] Rongfang Rachel Liu and Iakov M Golovitcher. Energy-efficient operation of rail vehicles. *Transportation Research Part A: Policy and Practice*, 37(10):917–932, 2003.

[53] Xiaojuan Lu, Qi Guo, Haiying Dong, and Baofeng MA. The research and application of nmpc in automatic train operation, 2015.

[54] J.M. Maciejowski. *Predictive Control with Constraints*. Prentice Hall, 2000.

[55] D.Q. Mayne. Model predictive control: Recent developments and future promise. *Automatica*, 50:2967–2986, 2014.

[56] Prashant Mhaskar, Nael H El-Farra, and Panagiotis D Christofides. Predictive control of switched nonlinear systems with scheduled mode transitions. *IEEE Transactions on Automatic Control*, 50(11):1670–1680, 2005.

[57] Ian P Milroy. *Aspects of automatic train control*. PhD thesis, © Ian Peter Milroy, 1980.

[58] Matthias A Müller and Frank Allgöwer. Improving performance in model predictive control: Switching cost functionals under average dwell-time. *Automatica*, 48(2):402–409, 2012.

[59] Matthias A Müller, Pascal Martius, and Frank Allgöwer. Model predictive control of switched nonlinear systems under average dwell-time. *Journal of Process Control*, 22(9):1702–1710, 2012.

[60] A Nasri, M Fekri Moghadam, and H Mokhtari. Timetable optimization for maximum usage of regenerative energy of braking in electrical railway systems. In *Power Electronics Electrical Drives Automation and Motion (SPEEDAM), 2010 International Symposium on*, pages 1218–1221. IEEE, 2010.

[61] Hrvoje Novak, Vinko Lešić, and Mario Vašak. Hierarchical coordination of trains and traction substation storages for energy cost optimization. In *Intelligent Transportation Systems (ITSC), 2017 IEEE 20th International Conference on*, pages 1–6. IEEE, 2017.

[62] Maite Peña-Alcaraz, Antonio Fernández, Asuncion Paloma Cucala, Andres Ramos, and Ramon R Pecharromán. Optimal underground timetable design based on power flow for maximizing the use of

regenerative-braking energy. *Proceedings of the Institution of Mechanical Engineers, Part F: Journal of Rail and Rapid Transit*, 226(4):397–408, 2012.

[63] Lev Semenovich Pontryagin. *Mathematical theory of optimal processes*. Routledge, 2018.

[64] Peter Pudney and Phil Howlett. Optimal driving strategies for a train journey with speed limits. *The ANZIAM Journal*, 36(1):38–49, 1994.

[65] S.J. Qin and T.A. Badgwell. A survey of industrial model predictive control technology. *Control Engineering Practice*, 11:733–764, 2003.

[66] Jianwei Qu, Xiaoyun Feng, and Qingyuan Wang. Real-time trajectory planning for rail transit train considering regenerative energy. In *Intelligent Transportation Systems (ITSC), 2014 IEEE 17th International Conference on*, pages 2738–2742. IEEE, 2014.

[67] Andrés Ramos, María Teresa Pena, Antonio Fernández, and Paloma Cucala. Mathematical programming approach to underground timetabling problem for maximizing time synchronization. *Dirección y Organización*, (35):88–95, 2008.

[68] E Rodrigo, S Tapia, JM Mera, and M Soler. Optimizing electric rail energy consumption using the lagrange multiplier technique. *Journal of Transportation Engineering*, 139(3):321–329, 2013.

[69] Gerben M Scheepmaker. *Running time supplements in railway timetables: Energy efficient operation versus robustness*. PhD thesis, MSc Thesis), NS Reizigers/Delft University of Technology (TU Delft), Utrecht, the Netherlands, 2013.

[70] Gerben M Scheepmaker and Rob MP Goverde. The interplay between energy-efficient train control and scheduled running time supplements. *Journal of Rail Transport Planning & Management*, 5(4):225–239, 2015.

[71] Gerben M Scheepmaker, Rob MP Goverde, and Leo G Kroon. Review of energy-efficient train control and timetabling. *European Journal of Operational Research*, 257(2):355–376, 2017.

[72] Rohan C Shekhar and Jan M Maciejowski. Robust variable horizon mpc with move blocking. *Systems & Control Letters*, 61(4):587–594, 2012.

[73] Yongduan Song and Wenting Song. A novel dual speed-curve optimization based approach for energy-saving operation of high-speed trains. *IEEE Transactions on Intelligent Transportation Systems*, 17(6):1564–1575, 2016.

[74] Horst Strobel, Peter Horn, and Manfred Kosemund. Contribution to optimum computer-aided control of train operation. In *Proceedings of the 2nd IFAC/IFIP/IFORS symposium on traffic control and transportation systems*, 1974.

[75] Shuai Su, Xiang Li, Tao Tang, and Ziyou Gao. A subway train timetable optimization approach based on energy-efficient operation strategy. *IEEE Transactions on Intelligent Transportation Systems*, 14(2):883–893, 2013.

[76] Shuai Su, Tao Tang, Xiang Li, and Ziyou Gao. Optimization of multitrain operations in a subway system. *ieee transactions on intelligent transportation systems*, 15(2):673–684, 2014.

[77] G Valencia-Palomo, JA Rossiter, CN Jones, Ravi Gondhalekar, and B Khan. Alternative parameterisations for predictive control: How and why? In *American Control Conference (ACC), 2011*, pages 5175–5180, 2011.

[78] LAM Van Dongen and JH Schuit. Energy-efficient driving patterns in electric railway traction. In *Main Line Railway Electrification, 1989., International Conference on*, pages 154–158. IET, 1989.

[79] Xuan Vu. *Analysis of necessary conditions for the optimal control of a train*. PhD thesis, University of South Australia Australia, 2006.

[80] Pengling Wang and Rob MP Goverde. Multiple-phase train trajectory optimization with signalling and operational constraints. *Transportation Research Part C: Emerging Technologies*, 69:255–275, 2016.

[81] Zhihui Wang, Yonghua Zhou, and Deng Liu. Models and algorithms of conflict detection and scheduling optimization for high-speed train operations based on mpc. *Journal of Control Science and Engineering*, 2018, 2018.

[82] Xihui Yan, Baigen Cai, Bin Ning, and Wei ShangGuan. Online distributed cooperative model predictive control of energy-saving trajectory planning for multiple high-speed train movements. *Transportation Research Part C: Emerging Technologies*, 69:60–78, 2016.

[83] Hui Yang, Ya-Ting Fu, Kun-Peng Zhang, and Zhong-Qi Li. Speed tracking control using an anfis model for high-speed electric multiple unit. *Control Engineering Practice*, 23:57–65, 2014.

[84] Xin Yang, Anthony Chen, Xiang Li, Bin Ning, and Tao Tang. An energy-efficient scheduling approach to improve the utilization of regenerative energy for metro systems. *Transportation Research Part C: Emerging Technologies*, 57:13–29, 2015.

[85] Mingzhao Yu and Lorenz T Biegler. A stable and robust NMPC strategy with reduced models and nonuniform grids. *IFAC-PapersOnLine*, 49(7):31–36, 2016.

[86] Lixian Zhang, Songlin Zhuang, and Richard D Braatz. Switched model predictive control of switched linear systems: feasibility, stability and robustness. *Automatica*, 67:8–21, 2016.

[87] Yonghua Zhou and Xin Tao. Robust safety monitoring and synergistic operation planning between time-and energy-efficient movements of high-speed trains based on mpc. *IEEE Access*, 6:17377–17390, 2018.

[88] Yonghua Zhou, Xun Yang, and Chao Mi. Model predictive control for high-speed train with automatic trajectory configuration and tractive force optimization. *CMES Comput. Model. Eng. Sci*, 90(6):415–437, 2013.

Publications

The list of publications by Hafsa Farooqi is hereafter reported.

Journal Papers

- H. FAROOQI, L. FAGIANO AND P. COLANERI, "Shrinking Horizon Move-blocking Predictive Control with Application to Efficient Train Operation", *Automatica*, SECOND REVIEW RUN.
- H. FAROOQI, G. P. INCREMONA AND P. COLANERI, "Railway Collaborative Ecodrive via Dissension Based Switching Nonlinear Model Predictive Control", *European Journal of Control*, FIRST REVIEW RUN.

Conference Papers

- HAFSA FAROOQI, G. P. INCREMONA AND P. COLANERI, "Collaborative Eco-Drive of Railway Vehicles Via Switched Nonlinear Model Predictive Control ", *Proc. 18th IFAC Conference on International Stability, Technology and Culture*, Baku, Azerbaijan, Sep. 2018.
- HAFSA FAROOQI, L. FAGIANO AND P. COLANERI, "Efficient Train Operation via Shrinking Horizon Parametrized Predictive Control ", *Proc. 6th IFAC Conference on Nonlinear Model Predictive Control*, Madison, WI, USA, Aug. 2018.